AN ABSTRACT OF THE DISSERTATION OF

Hong Ji for the degree of Doctor of Philosophy in Chemistry presented on July 24, 2007.
Title: Development of Fragmentation Techniques in Mass Spectrometry For Biological Applications

Abstract approved: _____
Douglas Barofsky

In this dissertation, I present the work of developing more efficient and economical techniques for fragmenting large bio-molecules, and ultimately making mass spectrometry a more powerful tool in proteomics, DNA sequencing, and other areas of biomolecular analysis.

Aiming at lowering the installation and operating cost, and delivering electron capture dissociation (ECD) technique to general users for the study of proteomics, I present the results of developing ECD on a triple-quadrupole mass spectrometer in the second chapter of this thesis. With a cross-flow configuration design, I demonstrate that zero-energy electrons (i.e. electron with energies on order of 1/2kT) can be transmitted into the reaction volume of the ECD chamber in numbers sufficient to produce detectable resonance electron capture (REC) reactions while maintaining ion transmission at a high enough level to perform cross-beam experiments. With a parallel-flow configuration design, on the other hand, I obtained the ECD spectrum of a peptide called substance P and demonstrate that the cross section for ECD can be increased by increasing both the interaction time and effective volume for interaction.

I also demonstrate that with further improvements, in particular increasing the magnetic field strength it should be possible to turn ECD into a high-throughput tool for applications in proteomics.

In chapter three I present the results of the first observation ever of the charge remote fragmentation (CRF) of a series of long-chain saturated and monounsaturated fatty acid anions during fast atom bombardment (FAB) of analyte-matrix mixture without collisional activation. I demonstrate that the process is efficient enough to allow recording of collision induced dissociation (CID) and metastable ion decomposition MS/MS spectra of any charge-remote $[M\text{-}H_2\text{-}(CH_2)_n]^-$ fragments as well as of spectra of neutral losses. These new results indicate that a multi-step radical mechanism is involved in CRF ion formation. The first step of the process appears to be accompanied by hydrogen elimination that occurs randomly throughout the molecule. The primary fragment radical ions formed can decompose further with the formation of the next generation of CRF ions.

In the last chapter I present our new discovery that FAB mass spectrometry in the negative ion mode can be used to unambiguously distinguish between *cis*- and *trans*- isomers of monounsaturated fatty acids by the relative strengths of two signals in the mass spectrum. I show the results of six fatty acids and demonstrate that under normal FAB ionization/desorption conditions, the deprotonated molecules $[M\text{-}H]^-$ of fatty acids undergo CRF. A characteristic fragmentation pattern of two intense clusters of mass peaks with three weak intervening peak-clusters can be used in each case to

identify the position of the double bond. I also discuss the possibility of REC occurring during the FAB process.

Development of Fragmentation Techniques in Mass Spectrometry For Biological Applications

by
Hong Ji

A DISSERTATION

submitted to

Oregon State University

in partial fulfillment of
the requirements for the
degree of

Doctor of Philosophy

Presented July 24, 2007
Commencement June 2008

Doctor of Philosophy dissertation of Hong Ji presented on July 24, 2007

APPROVED:

Major Professor, representing Chemistry

Chair of the Department of Chemistry

Dean of the Graduate School

I understand that my dissertation will become part of the permanent collection of Oregon State University Libraries. My signature below authorizes release of my dissertation to any reader upon request.

Hong Ji, Author

ACKNOWLEDGEMENTS

Although this thesis is the direct product of the time I spent in graduate school at Oregon State University, it is also the fruit of the many years that proceeded. It is therefore to all the people who guided and influenced me since the beginning that I owe thanks here. However, since there are so many, only a few can be given the individual mention that they all deserve.

First and foremost I have my graduate advisor, Professor Douglas Barofsky, to thank above all other mentors for his guidance, occasional parenting, and making this all possible. It is immeasurable how much I have benefited from his deep insights, optimistic attitude and strong faith in science.

I would extend my appreciation to my colleagues for providing a stimulating and a fun environment in which to learn and grow. I am especially grateful to Dr. Valery Voinov for sharing his invaluable experience in the Mass Spec with me; thank him for all those in-depth and fruitful discussions. Jeff Morré and Dr. Yury Vasil'ev are all great partners to work with. Also, I want to thank Ted Hinke for sharing so many smart ideas with me.

I would like to express my appreciation to my doctoral committee members: Dr. Deinzer, Dr. Evans, Dr. Kong and Dr. Jovanovic. Thank them for sharing their knowledge, for taking the time to guide me through my dissertation.

Finally, I would thank my dear husband Yonggang. Without your support and understanding, I won't be able to come all the way. You help me regain my confidence when I take a fall; you share the joy with me when I succeed. Most importantly, you are always there for me, and being aware of this gives me all the courage I need to explore the world…..

TABLE OF CONTENTS

TABLE OF CONTENTS (Continued)

LIST OF FIGURES

LIST OF FIGURES (Continued)

LIST OF TABLES

1. Introduction

In the past few decades, the mass spectrometry community has witnessed its interests shift from small volatile molecules to large biologically important molecules. The change in focus revolved heavily around two key technical problems. The first was how to bring thermally unstable bio-polymers into the vacuum intact. The second was how to partially and selectively break the gas phase target molecules into sequence-revealing fragments, which could then be identified in a tandem way. The first problem was solved by the development of novel techniques such as electrospray ionization (ESI) and Matrix assisted laser desorption ionization (MALDI) in 1988.[1] Since then the majority of efforts in the field focused on solving the second technical problem. A popular choice for solving this problem has been collision induced dissociation (CID). In many cases, tandem mass spectrometry (MS/MS) coupled with CID has succeeded in resolving the sequences or structures of large biomolecules. However CID has its own drawbacks. In peptide sequencing, CID produces incomplete primary structural information and it promotes fragmentation of post-translational modifications,[2] which makes it ill suited for locating these important biochemical features. New light was shed on this problem by Zubarev et al. in 1998 with the observation of electron capture dissociation (ECD) of peptides in a Fourier transform ion cyclotron resonance (FT-ICR) cell.[3] Compared to CID, this new technique has many unique properties. First, it produces c and z ions in polypeptides.[4] Second, it

seldom cleaves the chemical bonds of post-translation modifications. Instead it prefers cleaving disulfide bonds, which eliminates additional preparative steps before sample analysis.5 Very recently, it has also been found that it can reduce or eliminate scrambling in H/D experiments on proteins. Furthermore, ECD makes it possible to distinguish between the isomeric leucine and isoleucine.[6] Although encouraging, performance of ECD in a FT-ICR mass spectrometer is too expensive and difficult, which has been a factor in limiting its application primarily to fundamental research. The work presented in this thesis has been directed toward developing more efficient and economical techniques for fragmenting large bio-molecules with ECD, and ultimately for making mass spectrometry a more powerful tool in proteomics, DNA sequencing, and other areas of biomolecular analysis.

This chapter will provide a brief overview of electron capture dissociation, currently one of the potentially most powerful methods in proteomics, and charge-remote fragmentation, a well-known process induced by collisional activation.

1.1. Electron Capture Dissociation

Electron capture dissociation is a new MS/MS technique that is particularly well suited for the analysis of posttranslational modifications as well as disulfide bonds in polypeptides.[6] Since it gives more abundant backbone cleavages than conventional MS/MS techniques, ECD can also be useful in de novo protein sequencing.[7] Here a brief overview of ECD is given, including the concept of electron capture dissociation, a historic background of the ECD method, and current experimental efforts.

1.1.1. Concept

An electron in the vicinity of a cation will experience a Columbic attraction toward the latter. This can result in the capture of the electron by the cation. The fate of the species after the capture is determined by competition among several possible channels. These competitive pathways mainly come from the fact that the system has to dissipate the excess energy to stabilize itself. According to Bardsley and Biondi, this process has to finish within a very short time (less than 10 fs).[8] Vibrational relaxation normally takes place in a few tenths of picoseconds to a few picoseconds. Radiative relaxation by emitting photons typically proceeds at an even slower rate (more than nanoseconds). These channels are obviously too slow for energy dissipation. Prompt dissociation (typically 10^{-16} – 10^{-15} s) is, therefore, the only winning channel that stabilizes species in such electron capture processes.

Since dissociation takes place so fast, in most cases, electron capture and bond cleavage appear to be one concerted process. It must be noted that even in the case that the electron is captured first in a high Rydberg state of the cation (which has a relatively long lifetime), the final bond-cleavage still proceeds faster than all other possible channels. It is not easy to predict the fragmentation products of these effectively non-ergodic processes.[9]

A general opinion is that ECD can only be implemented on a Fourier transform ion cyclotron resonance (FT-ICR) mass spectrometer.[10] Although fragmentation in an electron capture process takes place very fast, a relatively long interaction time (milliseconds) usually is required to compensate for the small cross section for a collision between an ion and an electron. The strong magnetic and weak electrostatic fields presented in a FT-ICR cell trap the ions inside the cell without changing significantly the kinetic energy of the electrons; this situation permits long interaction times (minutes) and energy-resolved measurements. The residence time of ions in many other types of mass spectrometers, including time-of-flight and quadrupole instruments, is normally much smaller than this and thus renders difficulties for implementing ECD in these instruments. In addition, high efficiency of ECD requires electrons to have energies smaller than 1 eV,[11] a requirement that is extremely difficult to fulfill in quadrupole ion traps and other RF-devices.

1.1.2. Historic Background

The first ECD experiments were performed with low-energy electrons produced by UV laser irradiation of the surrounding walls and electrodes. Later, Zubarev, Kelleher, and McLafferty replaced the laser with a filament-based electron source.3 These electron sources, however, have some major drawbacks. The major one is that cross section of the electron beam is much narrower than that of the ion cloud.12 Significantly reduces the reaction volume. If the diameter of the electron beam could be increased to the same order as that of the ion cloud, the reaction volume could be much greater and the rate of interaction would then depend mainly on the electron density.13 In this case, the trapped cations would interact more efficiently with electrons. Furthermore after the trapped cation dissociates, charged fragments are likely to be trapped as well, which in turn largely increases the collection efficiency of fragmentation reactions. For these considerations, indirectly heated cathodes were introduced recently to replace previously used electron sources. The much higher efficiency of the new source reduced the required interaction time from seconds to milliseconds.[12,13] Such short times rendered on-line use of HPLC in combination with ECD possible.[14,15] This breakthrough highly pushed the development in traditional proteomics studies.

It is worth noting that most of the literature published so far on ECD has focused on proof-of-principle type of studies, or instrumental issues. Reports on its applications to study biologically relevant systems have been rare. McLafferty and co-workers pioneered the research in this direction. Recently, they characterized deviations in protein sequences from those predicted by DNA analysis.[16] Fenselau and colleagues recently characterized biomarkers from spores of Bacillus cereus T with ECD.[17] Costello and co-workers, on the other hand, characterized a proline-rich protein PRP-3 with ECD and CID.[18]

1.1.3. New efforts on experimental approaches

As has been mentioned above, ECD was and is still mainly performed in FT-ICR mass spectrometers. Although powerful in terms of sensitivity, resolution and mass accuracy, FT-ICR is very expensive. It is also very difficult to operate and maintain. In addition, because of the limited capability to handle the amount of samples, it is not suitable for the high throughput analyses required in proteomics studies. In order to overcome these obstacles, new efforts have been made in finding other less expensive options. In the following, two new methods will be briefly discussed.

As small systems without superconducting magnets, radio frequency (RF) traps have for sometime now been proposed for performing ECD. Achieveng ECD in RF traps is, however, technically very challenging.[19] The difficulty comes from the fact that the presence of a RF voltage, with an amplitude of hundreds of volts, will either rapidly accelerate the electrons above the energy range useful for electron capture (< 10 eV) or repel them from interacting with trapped ions. In an effort by Vachet et al., the authors injected electrons into a three-dimensional radio frequency-quadrupole (RFQ) ion trap, or Paul trap. In this experiment, however, ECD was not observed. The authors owed the failure to the fact that the electrons were energized, or heated, by the RF field.[20] Recently, in a simulation by Ivonin and Zubarev, the authors showed the feasibility of ECD using a Paul trap with a weak magnetic field.[21] At the same time, Baba et al. proposed a three-dimensional static electromagnetic trap (Penning trap) for ECD. The test, however, showed no success.[22]

In 2004 and 2005, exciting results came out from two parallel studies by Baba et al.[23] and by Silivra et al.[24] In the study of Baba et al., the authors reported on the first evidence of electron capture dissociation (ECD) in a radio frequency ion trap. In this study, a linear RF ion trap was used as the ECD cell for ion confinement. It consisted of a two-dimensional radio frequency electric field in the radial direction, and a static electric field in the axial direction. In the experiment,

electrons were injected along the axial direction, where the RF field is zero. By doing this, perturbation of electrons by the ion trap RF field, or RF heating was minimized. Another unique design of the trap was the use of a magnetic field applied parallel to the axial direction to confine electrons along that direction. This magnetic field (~ 0.1 T) was believed to be able to obtain high transmission efficiency of electrons and to reduce heating of electrons by the ion trap RF field. Using this ECD cell, the authors successfully cleaved substance P peptide ions, $[\text{substance P}]^{2+}$ and obtained a c and z fragment-ion spectrum. The authors claimed that the ECD in the RF trap proceeded in largely the same manner as in a FT-ICR instrument, since the ECD fragment pattern obtained was similar to an ECD fragmentation obtained by FT-ICR.

In the study of Silivra et al., the authors used a modified Bruker Esquire LC instrument.[24] Inside the ring electrode (RE), the authors installed a set of permanent magnets to create a magnetic field parallel to the main instrumental axis. They also placed another two sets of magnets on the end cap electrodes to reduce magnetic field inhomogeneity. The field strength in the trap varied along the main axis from ~ 250 G near end caps to ~ 400 G in the center. Such a field was believed to be sufficient to magnetize electrons but would not affect the motion of ions with $m/z > 100$. The authors called the new technique magnetized electrons, in-phase injection (MEPhI). Before analyzing polypeptide ions, the authors

characterize the MEPhI technique with theoretical simulations and experiments with SF_6 molecule. The simulations confirmed the principle of electron trapping. In the simulation, the authors showed that the extended trapping times for electrons were achieved by the combination of magnetic field confinement in the radial direction and electric field trapping in the axial direction, which is similar to ion trapping in the Penning trap of an FT-ICR instrument. After characterization, the authors investigated di-cations of Substance P. According to the authors, the data quality is at least as good as in the experiments with a linear ion trap described in the paper of Baba et al.

Although encouraging, the designs by Silivra et al. and Baba et al. each have significant technical drawbacks. One of these drawbacks is that trapped electrons seem to be too hot for the analysis of labile modifications. Another drawback is that the ECD efficiency is too low for high-sensitivity analytical applications. i.e. Baba et al. estimated that 95% of emitted electrons are lost from the dispenser cathode, and transmission efficiency of the ions from the ion source into the ECD cell was only 0.25%.23 Future efforts are thus necessary in turning this method into sophisticated high throughput analytical tool in proteomics research.

1.2. Charge-remote fragmentation

Since one of the major components of this thesis is focused on the studying of charge-remote metastable ion fragmentation of free fatty acids under FAB MS, a brief review of this field will be given in this section, including the concept of CRF, a short historic account, general experimental approaches, proposed mechanisms and its applications.

1.2.1. Concept

Charge-remote fragmentation (CRF) has been defined as a class of gas-phase reaction that is generally used to describe decompositions of ions occurring physically remote from the charge site.[25] The name came from the fact that this type of reaction is independent of the charge site. Numerous studies have shown that there appears to be no important interaction between reaction sites and the charge sites. As a consequence, CRF has been considered to be similar to gas-phase thermolysis.[26] For example, under high energy collision activation (CA), charge-remote fragmentations always take place along a fatty-acid chain no matter how the fatty acid is charged, specifically, the precursor ion can be $[M - H + 2Met]^+$ (Met = alkali metal ions),[27] $[M + Met - H]^+$ (Met = alkaline earth metal ions),[28] $[M - H]^-$,[29] or the $[M + H]^+$ of a suitably derivatized acid.[30,31]

One of the key factors that determine the competition between a charge-remote fragmentation and a charge-driven reaction is the position of the charge on a molecular chain. In order to observe a charge-remote fragmentation as the predominant reaction channel, the charge has to be fixed. In most cases, the charge has to be fixed at one end of the molecular chain. In cases where the charge is not fixed, charge-driven reactions take place. This will lead to the generation of a mixture of product-ions and results in spectra that are too complicated to interpret. For example, reaction of the $[M - H + 2Li]^+$ species of fatty acids induced by CA results in exclusively product ions from charge remote fragmentation. This is owing to the fact that the two lithium ions are tightly bound to the carboxylate. In comparison, $[M + H]^+$ of the same fatty acid does not undergo charge-remote fragmentation. This is because the initial reaction is H_2O loss from the precursor, which causes the charge to migrate onto the alkyl chain and produce charge-driven processes instead.[27]

Some general trends for charge-remote fragmentation are: High-energy CA always favors the reaction; ions with long alkyl chains and a fixed charge always undergo charge-remote fragmentations, given that sufficient energy is deposited into them. These facts indicate that the ionization method is not critical for charge-remote fragmentations. Nevertheless fast atom bombardment (FAB) has been the most frequently used ionization method to generate precursor ions for

charge remote fragmentations. In general, electron ionization (EI), chemical ionization (CI), field desorption (FD), electrospray ionization, and matrix-assisted laser desorption/ionization can also be utilized.

1.2.2. Historic background

Before the 80s, the information provided by the field of mass spectrometry was dominated by radical cations that were produced by electron ionization, while little was known about the fragmentation of closed-shell ions. The exceptions were a few studies of ions produced by chemical ionization. For example, the identification and location of functional groups in fatty acids, surfactants, steroids, complex lipids, and related materials had been a long-standing problem.[32] Studying of charge-remote fragmentation was intriguing because of the prospect of gaining new structural information on these important molecules that had been difficult to study by traditional mass spectrometry methods.

The name charge-remote fragmentation was coined by Gross et al. in 1983 after the authors observed such a reaction in a study of unsaturated fatty acids.[33] In fact, the phenomenon had been reported in the literature before, but the reaction had not been systematically studied simply because there was no means of introducing closed-shell ions of nonvolatile materials into the gas phase back in

that time. The discovery of fast atom bombardment in 1981 by Barber and co-workers dramatically changed the world of mass spectrometry and also opened up this field.[34] FAB has been introducing nonvolatile and biologically interesting molecules into the gas phase as a relatively simple and routine method. Although FAB was associated with little fragmentation and high chemical noise in the beginning, MS/MS methods soon solved these problems by inducing additional fragmentation and removing most of the chemical noise. Since then, the study of charge-remote fragmentation started to flourish.

1.2.3. Experimental approaches

Many experimental approaches have been applied to the study of charge-remote fragmentation. Here only some key factors will be summarized. One common requirement is that collisional activation is required after precursor ions are selected. This makes a multi-mass analyzer a key component for most experimental approaches.

FAB is the most used ionization method to produce molecular ions of fatty acids. Triple sector and four sector instruments have both been utilized as the mass analyzer with FAB. Generally speaking, using a triple sector as the mass analyzer, in which an electric sector is the second mass analyzer after the collision cell,

limits the mass resolving power to only 100-200.33 In order to achieve a mass resolving power good enough to separate a doublet peak at m/z 200-300, a four sector instrument has to be applied.

The electrospray ionization (ESI) method has also been applied to study charge-remote fragmentation. Since it also produces molecular ions almost exclusively, coupling with a triple quadrupole mass analyzer is also necessary. However, the collision energy for this approach is much lower than that used in a typical FAB/sector instrument. In general, the collision energy for the former setting is lower than 200 eV, while the collision energy for the latter setting is 3 ~ 8 keV, depending on different types of instruments.

1.2.4. Mechanisms been proposed

To date, various mechanisms of charge-remote fragmentation have been proposed. Many research groups have successfully used these proposed mechanisms to explain their observations in the elucidation of structures of a variety of synthetic and natural compounds. However, there still exists some controversy about the energetics and mechanisms in the explanations of charge-remote fragmentation.

1.2.4.1. 1,4-elimination

The 1,4-elimination mechanism was the first proposal by Jensen, Tomer and Gross to explain charge-remote fragmentation.[35] The proposal was based on a homologous series of saturated fatty acid anions ranging in chain length from 5 to 18 carbons. This mechanism involves a 1,4-loss of H_2 to give a terminally unsaturated fatty acid carboxylate and a 1-alkene. (see Scheme 1)

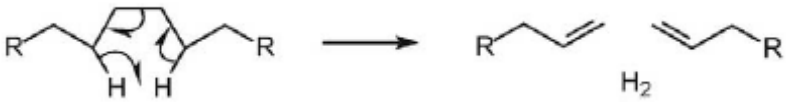

Scheme 1. 1,4-hydrogen elimination proposed for the charge remote fragmentation of aliphatic chains.

The authors proposed this mechanism based on the following three considerations. First, the reaction does not depend on the nature of the charge. The charge site can contain a positive or negative charge. It can be a carboxylate, a sulfate, sulfonate, a metal-cationized fatty acid or alcohol, an ammonium or phosphonium ion, or the macrocyclic ring of a porphyrin. This wide variety of charge carriers and charge states is evidence that charge is not important in the charge remote reactions. This conclusion is supported by observations that steroids charged at the end of the molecule undergo decompositions at a remote site where

interaction with the charge site is not possible. More evidence comes from a recent study on a steroid linked with an oxofatty acid in such a way that charge and reaction sites cannot interact.[36] The compound undergoes charge-remote fragmentations that are almost identical to those of the oxofatty acid itself.

The second consideration based on which the 1,4-hydrogen elimination that was proposed is that the fragments formed by reactions along an alkyl chain are a series of homologous C*n*H2*n*. If formation of alkanes accompanied the rearrangement, the two sets of ionic products for cleavages along an alkyl chain would depend on the direction of the hydrogen transfer. One set would be saturated or contain alkyl groups; the other would be unsaturated and contain alkenyl groups. The formation of only unsaturated ionic product is consistent with a 1,4-H_2 elimination.

The third consideration that leads to the 1,4-H_2 elimination comes from the results of deuterium labeling, although these results are not affirmative proof that the process is a 1,4-H_2 elimination.

An important feature of the 1,4-H_2 elimination is that the energy required for the reaction should be low, owing to the fact that the mechanism incorporates both bond breaking and bond making. To verify this, Jeanette Adams and Gross

performed a series of experiments to measure the energy required for the charge-remote cleavages along an alkyl chain of a fatty alcohol.[37] In those studies, the fatty alcohols were desorbed as $[M + Met]^+$, where Met was Li, Na, K, Rb, or Cs. The affinities of the alcohol for these alkali metal ions could be approximately estimated. The authors found that $[M + Cs]^+$ fragmented exclusively by releasing Cs^+; whereas in cases of $[M + Na]^+$ and $[M + K]^+$, charge-remote decompositions compete with the release of the metal ion itself. These observations, together with the known metal ion affinities of simple alcohols led to an estimate of the energy required for charge-remote cleavage of a C–C bond of between 1.3 and 1.9 eV. The authors concluded that this value, which is approximately one half a C–C bond energy, is consistent with the 1,4-elimination reaction. For the transition structure, the bond would be approximately half broken. This would be followed by bond-making in concert with bond-breaking. Furthermore, the transition structure involves six electrons, which makes it aromatic-like. This stabilization effect lets the reaction happen at energies that would be less than those required to cleave a C–C or C–H bond to give an intermediate free radical.

Strong support for the 1,4-H_2 elimination was also provided by the identification of the neutral products formed in the charge-remote fragmentation along an alkyl chain. Indeed, Chrys Wesdemiotis and co-worker have characterized the neutral products by neutral fragment-reionization mass spectrometry.[38] They

found that the neutral products are alkenes and not alkyl radicals or alkanes. This finding is consistent with the proposed 1,4-elimination process.

1.2.4.2. Homolytic carbon–carbon bond cleavage and carbon-hydrogen bond cleavage with the formation of radicals

The 1,4-elimination mechanism was first challenged by Wysocki and Ross, who proposed a two-step process in which the first step was a hemolytic cleavage of a C–C bond.[39] Another radical mechanism was proposed by Claeys and co-workers in a series of recent papers.[40] The authors observed that the $[M + Li]^+$ ions of fatty-acid esters fragment upon high-energy CA to give one series of closed-shell ions by losses of C_nH_{2n+2} and another of open-shell ions by losses of C_nH_{2n+1}. The authors also observed abundant molecular hydrogen loss from $[M + H]^+$ and $[M + Met]^+$ (Met = Na or Li) ions of saturated fatty-acid esters. Information from CA of $[M + Met - H_2]^+$ ions of a saturated fatty-acid ester leads to the conclusion that the H_2 loss occurs randomly along the fatty-acid chain, producing a mixture of monounsaturated fatty-acid ester ions. From these observations, the authors proposed that in the charge-remote fragmentation a C–H bond cleavage is the dominant step. Both C–H and C–C cleavages place a radical site on the alkyl chain as a distonic ion. This mechanism explains the formation of simple-cleavage products that are occasionally seen. The even-electron ions, which

are most common in charge-remote fragmentation, are then explained to be triggered by the radical site. The authors attributed the fact that both odd and even-electron ions are formed to interactions between the reaction center and the charge site, particularly when the charge is provided by an alkali-metal ion.

In addition, isotope effects have also been observed to accompany the decomposition of deuterium-labeled $[M + Li]^+$ ions of fatty acid esters. The study found that the ions formed by reactions that involve C-D cleavages are less abundant than those that involve the corresponding C-H cleavages. For example, ions formed by C2-C3 and C5-C6 cleavages from the $[M + Li]^+$ ion of n-butyl 4,4-d_2-heptadecanoate are less abundant than those formed by the corresponding cleavages from the unlabeled species. The difference suggests that the rate-determining step is C-H cleavages.

Later, Denekamp et al. found an unusual isotope effect of cleavage along an alkyl chain in another study.41 For three alkyl cations (n-hexadecylpyridinium, hexadecyltriphenylphosphonium, and n-hexadecyltriethyl-ammonium), the authors observed that when the product contains $–CD=CH_2$, a small isotope effect (~ 1.3) remained for cleavage along the alkyl chain that contained $-CD_2$. The authors believe that this “one-way isotope effect” is inconsistent with the pericyclic

mechanism, and interpret it as an evidence for a C-H bond cleavage as the rate-determining step.

1.2.4.3. Comparison of the 1,4-elimination and the radical mechanism

The 1,4-elimination mechanism suggests that two C-H bonds and one C-C bond break almost simultaneously. The diradical mechanism, on the other hand, prefers that the C-H bond cleavage is the first step of the decomposition. But both mechanisms postulate that the rate-determining step involves a C-C bond breakage.

The 1,4-elimination mechanism is supported by molecular orbital calculations because it has a lower activation energy than that of homolytic cleavage.[42] However formation of some product ions, as pointed out even by Gross et al., cannot be explained by the mechanism.[43] An example is the formation of the product ion by the loss of CH_4. Product ions that are radical cations or anions formed near the positive or negative charge should be formed by homolytic cleavages since they are open-shell species. The homolytic-cleavage mechanism, however, also has its own limitations. This mostly comes from the high activation energy along the reaction path. In addition, if the reaction is a two-step process and the formation of the two diradicals generated by homolytic C-C bond cleavage is the rate-determining step, then an isotope-effect should not

exist. In other words, the isotope-effect should pertain to the 1,4-elimination mechanism, and the difference should reflect whether the H atom is transferred toward or away from the double bond.

In the studies on fatty-acid esters cationized with Na^+ or Li^+ of Claeys et al., the authors also observed a facile loss of H_2 that occurs randomly along the fatty-acid chain, producing a mixture of monounsaturated fatty ester ions.[40] Later, Gross et al. interpreted this easy loss of H_2 to occur by hydrogen radical removal. This phenomenon may to some extent support the argument that charge-remote reactions start with C–H cleavage. Claeys and co-workers also find isotope effects that are consistent with rate-determining C–H cleavage.40 The 1,4-H_2 elimination, however, also involves C–H bond breaking in its transition structure and should show a kinetic isotope effect.

Gross et al. pointed out that there might be a problem with the interpretation in Denekamp et al.'s study as well.43 They think that the departing neutral could be initially a radical, which is known to be an alkene.[21] Gross et al. further pointed out that the initially formed charged product, based on the mechanism where C-H bond cleavage occurs, would be a distonic ion that would fragment by loss of a second H atom. The more likely reaction of a distonic product, then, would be a radical-triggered loss of ethene.

Using neutralization-reionization mass spectrometry (NRMS), Cordero and Wesdemiotis studied the charge-remote fragmentation of fatty-acid ions by analyzing the neutral products.44 Their results showed that the neutral products are not alkyl radicals or alkanes, but alkenes. This observation excluded any 1,2-alkane eliminations. Although the experimental data are in agreement with the concerted 1,4-elimination mechanism, the results do not necessarily exclude the diradical mechanism because the two radicals may exist only as intermediates. In other words, the initial radicals may have converted to terminal alkenes by losses of hydrogen atoms before the reionization step. Ultimately, the neutrals and the ions formed by the two mechanisms are the same.

1.2.4.4. charge-assisted process

In order to explain the ions found in the high-energy CID spectra of various fatty acid types and several features of the spectra that were difficult to explain earlier, an alternative fragmentation mechanism, based on a charge-associated process has been recently suggested by Harvey.[45]

The new mechanism is termed charge-assisted process. As an additional mechanism to the charge-remote process, it can account for ions of the [M - C_nH_{2n+2}] series found in the positive and negative, high-energy CID spectra of fatty

acids and related compounds when ionized as closed-shell ($[M - H]^-$ or $[M + X]^+$) species. The new mechanism is based on the same process commonly invoked to account for similar ions in the electron-impact spectra of derivatized fatty acids. For those compounds the positive charge on the derivative abstracts a hydrogen atom from various positions of the alkyl chain to leave a radical that initiates a radical-induced cleavage of the chain. In the new mechanism, the authors proposed that in the high energy CID spectra of closed-shell ions, similar hydrogen migrations occur but unpairing of electrons is avoided by charge transfer to the alkyl chain. This charge then initiates a concerted cleavage of the chain to give an allylic carbonium (positive ion spectrum) or carbanion (negative ion spectrum). According to the authors, the new mechanism avoids the need to involve radicals or loss of hydrogen atoms from even-electron (closed shell) ions and provides a driving force for the reaction, namely, the formation of ions with a stabilized charge. An extension of the mechanism is also proposed to account for the formation of odd-electron ions from these compounds. The authors pointed out, however, that the charge-assisted mechanism does not rule out the occurrence of other mechanisms that have been accepted for many years. It only provides an alternative process that can account for some spectral features which were hard to explain with previously proposed mechanisms.

It must be noted that the involvement of the charge in such reactions has suggested by Wysocki and Ross in one of the early studies.[46] Furthermore, Contado et al. also noted that, for unsaturated fatty acids containing the double bond towards the middle of the chain, charge-remote fragmentations involving allylic bond fission should be equally probable on either side of the double bond.[47] Since such behavior is not seen, the charge should have some influence on the fragmentation. In a study by Antoine and Adams, the authors found that the fragmentation spectra of $[M - H + 2Cat]^+$, where Cat is an alkali metal, depended on the nature of the alkali metal.[48] This observation also suggests charge involvement. Similar phenomena have also been documented by other researchers.[40]

In fact, owing to the flexibility of hydrocarbon chains, the interaction between the reaction sites and charge sites is inevitable in most long-chain systems, especially when the reactions take place near the charge. It has been found that some product ions formed by cleavages near the charge are stabilized by charge. For example, the unusual radical anion of m/z 86, which is formed from CA of fatty-acid $[M - H]^-$ ions, is obviously stabilized enhanced by the formation of a six-membered ring structure through an interaction between the charge and the radical.[35] There are other processes whereby the breakage of bonds remote to a charge site is accompanied by bond cleavage at the charge site. In the study of

decompositions of long-chain quaternary ammonium ions, Tuinman, Cook and Magid discovered a series of reactions that they termed “mixed-site fragmentation reactions”.[49] This phenomenon has been further investigated by Bambagiotti-Alberti et al.,[50] Whalen et al.,[51] and Seto et al.[52] In these studies, although ions from mixed-site fragmentation reactions are generally less abundant than those from charge-remote fragmentation, one of C=C breakage is produced with high abundance. This result suggests that the two radicals interact to form a double bond, generating a stable structure with a six-membered ring. The facility of the reaction could suggest that the radicals are bypassed in a concerted process. By using MS/MS/MS, the authors determined that the structures of ions from charge-remote and mixed-site fragmentations are indeed different. Another example of the competition between charge-remote and charge-driven processes is provided by a study on fragmentations of the non-8-enoate anion.[53] Under collisional activation, the anion loses C_3H_6, C_4H_8, and C_6H_{12}. The authors proved by isotope labeling (^2H and ^{13}C) and NRMS that the loss of C_3H_6 is caused by a charge-driven process, whereas the losses of C_4H_8 and C_6H_{12} come from charge-remote fragmentation.

1.2.4.5. From the energetic point of view

The existence of the abovementioned controversies among various proposed mechanisms renders a closer look at the energetic of these reactions very necessary.

Busch and coworkers has studied the energetics of charge-remote fragmentation using carbocyanine dyes as molecular probes.[54,55] These compounds all contain two long alkyl chains and a resonance-stabilized charge site. Their results show the existence of two distinct charge-remote processes, depending on the energy supplied to the precursor ion. Under the condition of low-energy CA, the precursor ion loses the entire first alkyl chain followed by charge remote fragmentation along the second alkyl chain. The authors found that the relative abundances of ions produced by charge-remote fragmentation can be controlled by varying collision energy. Simply, the higher the collision energy, the more abundant the product ions. When sufficient collision energy is supplied, product ions from charge-remote fragmentation on the first alkyl chain show up and become dominant. The authors concluded that the charge-remote fragmentation on the second chain is a low-energy process, whereas that on the first chain is a high-energy one.[55]

Cheng, Pittenauer and Gross observed an energy dependency that may be contradictory to previous observations.[56] In their experiment, the $[M + Na]^+$ ions of

triacylglycerols with lower internal energy, which are produced by ESI, undergo high-energy, homolytic cleavages to generate ions by losing C_nH_{2n+1} fragments. The ions with higher internal energy, which are produced by FAB, however, react through the low-energy 1,4-H_2 elimination process to generate ions with C_nH_{2n+2} losses. Based on the internal energy distribution, ρ(E), of the precursor ions the authors suggested the following explanation: after collisional activation, a small portion of the relatively "cold" ESI-produced precursor ions are promoted to the "long-tail" high-energy region. This will allow both simple cleavages and rearrangements to take place, with the former dominant. In contrast, the ions produced by FAB initially contain higher internal energy. Collisional activation thus pushes a larger fraction in the distribution into the region where rearrangement takes place. Although the long-tail region is still populated by collisional activation, the fraction of ions with internal energies in the high-energy tail is small. This will lead to fewer product ions formed by simple cleavage. Alternatively, based on Claeys and coworkers' mechanism, the reactions of the ions produced by FAB start with the higher energy C-H homolytic cleavage, and those of ESI-produced ions are initiated by the lower energy C-C cleavages. That the pericyclic reaction is a higher energy process than that initiated by a hemolytic C=C or C=H bond cleavage is not likely.

Voinov and Claeys showed additional evidence in favor of a rate-determining C-H cleavage for reactions along a saturated alkyl chain.[58] In their study, the authors produced an $[M - H]^-$ of a fatty acid by resonant electron capture (7.2 eV). This fatty acid had been modified in a way that the H had been abstracted from the alkyl chain. Surprisingly, these species give a charge-remote pattern that is standard for fatty acids. According to the quasi-equilibrium theory of mass spectrometry, the internal excitation with a energy of 7.2 eV is not enough to promote charge-remote fragmentation, if the energy is delocalized prior to fragmentation. The authors thus concluded that charge-remote fragmentation is "non-ergodic", indicating that high-energy processes can occur by the deposition of energy at localized sites. Interestingly, they also found that at lower capture energies, the dominant fragmentation was loss of radicals. This is in good agreement with the study by Cheng, Pittenauer and Gross.[56]

1.2.5. Applications of CRF

Charge-remote fragmentation has been applied in the structural determination of various synthetic and natural long-chain and poly-ring molecules. In this section, the application of CRF will be briefly summarized.

1.2.5.1. Fatty Acids, lipids and their derivatives

This is the most studied category of compound by charge-remote fragmentation since the latter's discovery. Under CA, the structural information that can be obtained from the studies of fatty acids using CRF by comparing peak patterns of corresponding ions include locations of double bond, alkyl, hydroxyl, epoxy, and cyclopropane/cyclopropene substitutions on fatty-acid chains.[33, 29, 57, 59, 26 27, 28, 60, 61, 62] In addition, structures of alkylamines, fatty alcohols, and fatty-acid esters, and related materials have also been well studied.[63, 40(a), 64, 65, 66, 67]

Useful structural information can also be obtained under low-energy CA condition using CRF. This application was initiated by Whalen, Grossert and Boyd, who observed that ions of charge remote fragmentation could be initiated in quadrupole collision cells.[68] Later, Hsu and Turk assigned locations of double-bond in an alkenyl chain with a triple-stage quadrupole instrument.[69] Low energy CA can be even more useful when the elucidation of only the functional groups in fatty acids is sought. Wheelan, Zirrolli and Murphy investigated the decomposition of an important lipid mediator, LTB4, and its metabolites, by ESI with low-energy CA.[70] Although the structures of LTB4 and its metabolites are complicated, structural information from their study revealed the nature of the

alkyl chain, including the number and locations of double bonds and hydroxyl groups.

The combination of using CRF to identify fragments and chromatographic separation method makes it even a more powerful tool in identifying fatty acids in mixtures obtained from biological systems. Using this method Couderc studied pentafuorobenzyl-ester derivatives of a fatty-acid mixture obtained from Mycobacterium fallax and M. aurum by concatenating GC/MS/MS with electron-capture ionization.[71] The authors well separated the mixtures and obtained detailed structural information on each fatty-acid chain, including carbon numbers, degree of unsaturation, and locations of double bonds, alkyl branches, and cyclopropane rings by charge-remote fragmentation. The authors believed that this approach can be used to characterize structures of fatty-acid mixtures at the nanogram level.

Phospholipids are important lipid in bacterial, plant, and animal membrane. Using charge-remote fragmentations the structural determination of phospholipids was first introduced by Gross and co-workers.[72,73,74] These investigations clearly revealed the structures of two acyl groups and their ester linkages on the glycerol backbone. This efficient method was further developed by Huang, Gage and Sweeley.[75] Later, Kim, Yoo and Kim suggested investigating fragmentations of

$[M + Na]^+$, $[M – H + 2Na]^+$, and $[M + Na - 2H]^-$ ions of phospholipid molecules by FAB-MS/MS.[76] This method extended the application of CRF to the determination of structures of phospholipids isolated from biological systems. Using this method, the same group has also investigated sulfoquinovosyl, monogalactosyl, and digalactosyl diacylglycerols, agroup of Glycolipids that are found at high abundance in the photosynthetic membrane in plants, algae, and bacteria.[77] In fact, similar studies of looking at fragmentations of $[M + Na]^+$, $[M + K]^+$, or $[M - H]^-$ ions of phospholipids were also reported .[78,79] Right after these studies, Turk and coworkers investigated fragmentations of lithiated adducts of phospholipids using electrospray and low-energy CA, and achieved the determination of structures of phospholipids mixtures.[80,81,82]

1.2.5.2. Steroids

Studying the structures of steroid-ring containing compounds by charge-remote fragmentation was first reported in the 80s.[83,84,85] Structural information of the ring systems obtained from these studies include positions of unsaturation, hydroxy, or keto groups.[86,87,88,89,90] In addition, Stroobant et al. created a strategy that they analyzed both charge-driven and charge-remote fragmentations together with isotope-labeling technique.[91] In the investigation of

14 tauroconjugated bile acids by FAB-MS/MS, the authors not only elucidated the ring structure but also the chain strcture.

Claeys et al. employed a similar strategy in their study of four aglycons, tomatidine, demissidine, solanidine, and solasodine, by using high and low-energy CA.[40(b)] The authors also investigated the glycosidic complex of these molecules (a-tomatine, a-chaconine, and a-soanine). These investigations led to structural information of the carbohydrate sequence, linkage sites, and structural features of the rings in the aglycone moiety.

1.2.5.3. Other important biomolecules

CRF has indeed been applied in structural determination of so many other biological important systems. Siegel and coworkers applied this technique to the structural elucidation of polyether antibiotics.[92,93] Naoki, Murata and Yasumoto,[94] Havlicek, Ryska and Pospisil[95] successfully used tandem mass spectrometry to characterize the structures of natural polycyclic ethers. Kim et al. then studied nigericin, abierixin, and O-demethylabierixin by FAB-MS/MS.[96] The same method has also been used by Van Breemen et al. to determine the structures of the anti-parasitic pentamidine and its metabolites.[97] CA of proton or metal ion-charged peptides can also generate ions from charge-remote fragmentation and

can provide some structural information.[98,99,100,101,102,103] Furthermore, by analyzing charge-remote fragmentation caused by CA of $[M - H]^-$, $[M + H]^+$, and $[M + Met]^+$, Ann and Adams has completely determined the structures of ceramides.[104,105] Hsu and Turk characterized structures of sphingomyelin by ESI-MS, using low energy CA.[106] Structures of some other systems that have been characterized by charge-remote fragmentation include polyaminetoxins,[107,108,109] bis-tetrahydrofuran acetogenins,[110,111] pheromones,[112] liposidomycins,[113] arsenosugars,[114] antioxidants,[115] α-tocopherol and β-carotene and their oxidation products[115] and polyhdroxybis(tetrahydrofuran) acetogenins.[111]

.

1.3. This thesis

The second chapter of this thesis focuses on the new development of ECD on a triple-quadrupole mass spectrometer. The ultimate goal is to lower the installation and operating cost, and deliver this technique to general users for the study of proteomics. In this endeavor, a triple quadrupole (Q-q-Q) mass spectrometer was modified into a quadrupole-electron capture dissociation-quadrupole (Q-ECD-Q) mass spectrometer. A unique feature of this new design is a collimated longitudinal magnetic field produced by a solenoid that slightly concentrates electrons along the axis without disturbing the ions. An ECD

spectrum of substance P was successfully recorded using this new technique. Comparison of this new method with previous approaches using RF-traps is made.

The third and the fourth chapter will focus on the study of charge-remote fragmentation (CRF). Chapter three provides the results and discussion of the first observation ever of the CRF of a series of long-chain saturated and monounsaturated fatty acid anions during fast atom bombardment (FAB) of the analyte-matrix mixture without collisional activation. It is shown that the process is efficient enough to allow recording of collision induced dissociation (CID) and metastable ion decomposition MS/MS spectra of any charge-remote fragments $[M\text{-}H_2\text{-}(CH_2)_n]^-$ as well as of spectra of neutral losses. The results obtained contradict the generally accepted theory that CRF results exclusively in terminally unsaturated carboxylate anions. The new results indicate that a multi-step radical mechanism is involved in CRF ion formation. The first step of the process appears to be accompanied by hydrogen elimination that occurs randomly throughout the molecule. The primary fragment radical ions formed can decompose further with the formation of the next generation of CRF ions.

The fourth chapter concentrates on the discovery that FAB mass spectrometry in the negative ion mode can be used to unambiguously distinguish between *cis*- and *trans*- isomers of monounsaturated fatty acids by the relative

signal strengths of an intense doublet. Six fatty acids were chosen for the investigation. The results show that under normal FAB ionization/desorption conditions, the deprotonated molecules $[M-H]^-$ of fatty acids undergo CRF. A characteristic fragmentation pattern of two intense peak-clusters with three weak intervening peak-clusters are used in each case to identify the position of the double bond. The possibility of resonance electron capture (REC) occurring during the FAB process is also be discussed.

1.4. References

1. (a) Meng, C. K., Mann, M., and Fenn, J. B. *Z. Phys. D* **1988**, 10, 361. (b) Wong, S. F., Meng, C. K., and Fenn, J. B. *J. Phys. Chem.* **1988**, 92, 546. (c) Fenn, J. B.; Mann, M.; Meng, C. K.; Wong, S. F.; Whitehouse, C. M. *Science* **1989**, *246*, 64. (d) Karas, M.; Hillenkamp, F. *Anal Chem* **1988**, *60*, 2299–2301.

2. (a) Kelleher, N. L., Zubarev, R. A., Bush, K., Furie, B., Furie, B. C., McLafferty, F. W., and Walsh, C. T. *Anal. Chem.* **1999** *71*, 4250-4253. (b) Mirgorodskaya, E., Roepstorff, P., and Zubarev, R.A. *Anal. Chem.* **1999** *71*, 4431-4436. (c) Mann, M. and Jensen O.N. *Nature Biotechnology* **2003**, *21*, 255-261.

3. Zubarev, R. A., Kelleher, N. L., McLafferty, F. W. *J. Am. Chem. Soc.* **1998**, *120*, 3265.

4. Roman A.; Zubarev, R. A. *Mass Spectrom. Rev.* **2003**, *22*, 57**.**

5. Zubarev, R. A., Kruger, N. A., Fridriksson, E. K., Lewis, M. A., Horn, D. M., Carpenter, B. K., and McLafferty, F. W. *J. Am. Chem. Soc.* **1999**, *121*, 2857.

6. Kjeldsen, F.; Haselmann, K. F.; Budnik, B. A.; Sorensen, E. S.; Zubarev, R. A. *Anal. Chem.* **2003,** *75*, 2355–2361.

7. Horn, D. M.; Zubarev, R. A.; McLafferty, F. W. *Proc. Natl. Acad. Sci. U.S.A.* **2000,** *97,* 10313–10317.

8. Bardsley, J. N., Biondi, M. A. Advances in atomic and molecular physics. In: Bates DR, editors. New York: Academic Press. **1970**, pp 1–57.

9. Andersen, L. H., Heber, O., Kella, D., Pedersen, H. B., Vejby-Christensen, L., Zajfman, D. *Phys. Rev. Lett.* **1996**, *77*, 4891–4894.

10. Marshall, A.G., Hendrickson, C.L., Jackson, G.S. *Mass. Spectrom. Rev.* **1998**, *17*, 1–35.

11. Zubarev, R.A., Horn, D.M., Fridriksson, E.K., Kelleher, N.L., Kruger, N.A., Lewis, M.A., Carpenter, B.K., McLafferty, F. W. *Anal. Chem.* **2000**, *72*, 563-573.

12. Haselmann, K.F., Budnik, B.A., Olsen, J.V., Nielsen, M.L., Reis, C.A., Clausen, H., Johnson, A.H., Zubarev, R.A. *Anal. Chem.* **2001**, *73*, 2998–3005.

13. Tsybin, Y.O., Hakansson, P., Budnik, B.A., Haselmann, K.F., Kjeldsen, F., Gorshkov, M., Zubarev, R.A. *Rapid Commun. Mass Spectrom.* **2001**, *15*, 1849–1854.

14. Davidson, W., Frego, L. *Rapid Commun. Mass Spectrom.* **2002**, *16*, 993–998.

15. Palmblad, M., Tsybin, Y.O., Ramstrom, M., Bergquist, J., Hakansson, P. *Rapid Commun. Mass Spectrom.* **2002**, *16*, 988–992.

16. Ge, Y., Lawhorn, B.G., ElNaggar, M., Strauss, E., Park, J.H., Begley, T.P., McLafferty, F.W. *J. Am. Chem. Soc.* **2002**,*124*, 672–678.

17. Demirev, P.A., Ramirez, J., Fenselau, C. *Anal. Chem.* **2001**, 73, 5725–5731.

18. Leymarie, N., Berg, E.A., McComb, M.E., O'Connor, P.B., Grogan, J., Oppenheim FG, Costello CE. *Anal. Chem.* **2002**, *74*, 4124–4132.

19. Zubarev, R. A. *Curr. Opin. Biotechnol.* **2004**, *15*, 12-16.

20. Vachet, R. W.; Clark, S. D.; Glish, G. L. Proceedings of the 43rd ASMS Conference on Mass Spectrometry and Allied Topics, 1995; p 1111.

21. Ivonin, I.; Zubarev, R. A. Proceedings of the 51st ASMS Conference on Mass Spectrometry and Allied Topics, 2003; ThPE057.

22. Baba, T.; Black, D. M.; Glish, G. L. Proceedings of the 51st ASMS Conference on Mass Spectrometry and Allied Topics, 2003; ThPJ1 165.

23. Baba, T., Hashimoto Y., Hasegawa H., Hirabayashi A., and Waki I. *Anal. Chem.* **2004**, *76*, 4263.

24. Silivra, O. A., Kjeldsen F., Ivonin I. A., and Zubarev R. A., *J. Am. Soc. Mass Spectrom.* **2005**, *16*, 22–27.

25. (a) Adams J. *Mass spectrom. Rev.* **1990**, 9, 141. (b) Gross M. L. *Int. J Mass Spectrom. Ion Processes* **1992**, 118/119, 137. (c) Adams J. Songer M. J.

Trends Anal. Chem.**1993**, 12, 28. (d) Cheng C.; Gross M. L. *Mass spectrom. Rev.* **2000**, 19, 398.

26. Adams, J.; Gross, M. L. *J. Am. Chem. Soc.* **1989**, *111*, 435.

27. Adams, J.; Gross, M.L., *Anal. Chem.* **1987**, *59*, 1576.

28. Davoli, E.; Gross, M.L. *J. Am. Soc. Mass. Spectrom.* **1990**, *1*, 320-324.

29. Tomer, K.B.; Jensen, N.J.; Gross, M.L. *Anal. Chem.* **1986**, *58*, 2429-2433.

30. Deterding, L.J.; Gross, M.L. *Anal. Chim. Acta.* **1987**, *200*, 431-445.

31. Deterding, L.J.; Gross, M.L. *Org. Mass Spectrom.* **1988**, *23*, 169-177.

32. Specialist Periodical Reports: Mass Spectrometry, Williams, D. H., Ed.; Chemical Society: London, **1971;** Vol. l, pp **144-146** and references therein.

33. Tomer K.B.; Crow, F.W.; Gross, M.L. *J. Am. Chem. Soc.* **1983**, *105*, 5487.

34. Barber, M.; Bordoli, R.S.; Sedwick, R.D.; Tyler, A.N. *J. Chem. Soc., Chem. Commun.* 1981, 325.

35. Jensen, N.J.; Tomer, K.B.; Gross, M.L. *J. Am. Chem. Soc.* **1985**,*107*, 1863.

36. Cheng, C.; Gross, M.L. *J. Am. Soc. Mass Spectrom.* **1998**, *9*, 620.

37. Adams, J.; Gross, M.L. *J. Am. Chem. Soc.* **1986**, *108*, 6915.

38. Cordero, M.M.; Wesdemiotis, C. *Anal. Chem.* **1994**, *66*, 861.

39. Wysocki, V.H.; Ross, M.M.; *Int. J. Mass Spectrom. Ion Processes* **1991**, *104*, 179.

40. (a) Claeys, M.; Van den Heuvel, H. *Biol. Mass Spectrom.* **1994**, *23*, 20. (b) Claeys, M.; Nizigiyimana, L.; Van den Heuvel, H.; Derrick, P.J. *Rapid Commun. Mass Spectrom.* **1996**, *10*, 770. (c) Claeys, M.; Van den Heuvel, H.; Chen, S.; Derrick, P.J.; Mellon, F.A.; Price, K.R. *J. Am. Soc. Mass Spectrom.* **1996**, *7*, 173. (d) Nizigiyimana, L.; Van Den Heuvel, H.; Claeys, M. *J. Mass Spectrom.* **1997**, *32*, 277. (e) Claeys, M.; Nizigiyimana, L.; Van Den Heuvel, H.; Vedernikova, I.; Haemers, A. *J. Mass Spectrom.* **1998**, *33*,

631. (f) Huysmans, L.; Nizigiyimana, L.; Van den Heuvel, H., Claeys, M. *Int. J. Mass Spectrom.* **1999**, *188*, 39.

41. Denekamp, C.; Van den Heuvel, H., Voinov, V.G.; Claeys, M.; Seto, C.; Grossert, J.S.; Waddell, D.S.; Curtis, J.M.; Boyd, R.K. *Rapid Commun Mass Spectrom* **2000**, *14*, 1035 -1043.

42. Siegel, M.M.; Colthup, N.B. *Appl. Spectrosc.* **1988**, *42*, 1214-1221.

43. Cheng C.; Gross, M. L. *Mass Spectrometry Reviews*, **2000**, *19*, 398-420.

44. Cordero, M.M.; Wesdemiotis, C. *Anal. Chem.* **1994**, *66*, 861-886.

45. Harvey, D. J. *J. Am. Soc. Mass Spectrom.* **2005**, *16*, 280–290.

46. Wysocki, V.H.; Ross, M.M. *Int. J. Mass Spectrom. Ion Processes* **1991**, *104*, 179-211.

47. Contado, M.J.; Adams, J.; Jensen, N.J.; Gross, M.L. *J. Am. Soc. Mass Spectrom.* **1991**, *2*, 180-183.

48. Antoine, M.; Adams, J. Implication of the charge site in charge-remote fragmentations. *J. Am. Soc. Mass Spectrom.* **1992,** *3*, 776–778.

49. Tuinman, A.A.; Cook, K.D.; Magid, L.J. *J. Am. Soc. Mass Spectrom.* **1990**, *1*, 85-91.

50. Bambagiotti-Alberti, M.; Coran, S.A.; Benvenuti, F.; LoNostro, P.; Catinella, S.; Favretto, D.; Traldi, P. *J. Mass Spectrom.* **1995**, *30*, 1742-1746.

51. Whalen, K.; Grossert, J.S.; Curtis, J.M.; Boyd, R.K. *Int. J. Mass Spectrom. Ion Processes* **1997**, *160*, 223-240.

52. Seto, C.; Grossert, J.S.; Vaddell, D.S.; Curtis, J.M.; Boyd, R.K. *Int. J. Mass Spectrom.* **1999**, *188*, 27-38.

53. Dua, S.; Bowie, J.H.; Cerda, B.A.; Wesdemiotis, C.; Raffery, M.J.; Kelly, J.F.; Taylor, M.S.; Blanksby, S.J.; Buntine, M.A. *J. Chem. Soc. Perkin Trans.* **1997**, *2*, 695-702.

54. Carlson, R.E.; Busch, K.L. *Org. Mass Spectrom.* **1994**, *29*, 632-640.

55. Melnyk, M.C.; Carlson, R.E.; Busch, K.L.; Schey, K.L.; Bartlett, M.G. *J. Mass Spectrom.* **1998**, *33*, 75-84.

56. Cheng, C.; Pittenauer, E.; Gross, M.L. *J. Am. Soc. Mass Spectrom.* **1998**, *9*, 840-844.

57. Jensen, N.J.; Tomer, K.B.; Gross, M.L. *Anal. Chem.* **1985**, *57*, 2018-2021.

58. Voinov, V.G.; Claeys, M. *Int. J. Mass Spectrom.* **2000**, *198*, 23-32.

59. Adams, J.; Gross, M. L. *J. Am. Chem. Soc.* **1986**, *108*, 6915-6921.

60. Crockett, J.S.; Gross, M.L.; Christie, W.W.; Holman, R.T. *J. Am. Soc. Mass Spectrom.* **1990**, *1*, 183-190.

61. Bernstrom, K.; Kayganich, K.; Murphy, R.C. *Anal. Biochem.* **1991**, *198*, 203-211.

62. Wheelan, P.; Zirrolli, J.A.; Murphy, R.C. *Biol. Mass Spectrom.* **1993**, *22*, 465-473.

63. Shimomura, O.; Takai, Y.; Yamada, H.; Ishikawa, T.; Sawada, M.; Takahashi, S.; Goto, K.; Kinoshita, T. *J. Mass Spectrom. Soc. Jpn.* **1993**, *41*, 159-163.

64. Calas, M.; Cordina, G.; Gilles, I.; Aubagnac, J.L. *J. Mass Spectrom.* **1997**, *32*, 147-151.

65. Li, X.; Zhang, R.; Guo, X.; Liu, S. *Fenxi Ceshi Xuebao* **1997**, *16*, 10-16.

66. Suma, K.; Raju, N.P.; Vairamani, M. *Rapid Commun. Mass Spectrom.* **1997**, *11*, 1939-1944.

67. Li, Z.L.; Liu, S.Y. *Youji Huaxue* **1998**, *18*, 57-61.

68. Whalen, K.; Grossert, J.S.; Boyd, R.K. *Rapid Commun. Mass Spectrom.* **1995**, *9*, 1366-1375.

69. Hsu, F-F.; Turk, J. *J. Am. Soc. Mass Spectrom.* **1999**, *10*, 600-612.

70. Wheelan, P.; Zirrolli, J.A.; Murphy, R.C. *J. Am. Soc. Mass Spectrom.* **1996**, *7*, 129-139.

71. Couderc, F. *Lipids* **1995**, *30*, 691-699.

72. Jensen, N.J.; Tomer, K.B.; Gross, M.L. *Lipids* **1986**, *21*, 580-588.

73. Jensen, N.J.; Tomer, K.B.; Gross, M.L. *Lipids* **1987**, *22*, 480-489.

74. Jensen, N.J.; Gross, M.L. *Mass Spectrom. Rev.* **1988**, *7*, 41-69.

75. Huang, Z.H.; Gage, D.A.; Sweeley, C.C. *J. Am. Soc. Mass Spectrom.* **1992**, *3*, 71-78.

76. Kim, Y.H.; Yoo, J.S.; Kim, M.S. *Bull. Korean Chem. Soc.* **1997**, *18*, 874-880.

77. Kim, Y.H.; Yoo, J.S.; Kim, M.S. *J. Mass Spectrom.* **1997**, *32*, 968-977.

78. Nagaki, H.; Kitaoka, M.; Rick, P.D.; Kinoshita, T. *Nippon. Iyo. Masu. Supekutoru Gakkai Koenshu* **1992** *17*, 183-186.

79. Takayama, M. *J. Mass Spectrom. Soc. Jpn.* **1995**, *43*, 177-178.

80. Hsu, F-F.; Bohrer, A.; Turk, J. *J. Am. Soc. Mass Spectrom.* **1998**, *9*, 516-526.

81. Ramandham, S.; Hsu, F-F.; Bohrer, A.; Nowatzke, W.; Ma, Z.; Turk, J. *Biochemistry* **1998**, *37*, 4553-4567.

82. Hsu, F-F.; Turk, J. *J. Mass Spectrom.* **2000**, *35*, 596-606.

83. Liehr, J.G.; Kingston, E.E.; Beynon, J.H. *Biomed. Mass Spectrom.* **1985**, *12*, 95-99.

84. Tomer K.B.; Crow, F.W.; Gross, M.L.; Whitney, J. *Biomed. Environ. Mass Spectrom.* **1986**, *13*, 265-272.

85. Tomer K.B.; Gross, M.L. *Biomed. Environ. Mass Spectrom.* **1988**, *15*, 89-98.

86. Griffiths, W.J.; Zhang, J.; SjoÈvall, J. *Rapid Commun. Mass Spectrom.* **1993**, *7*, 235-240.

87. Griffiths, W.J.; Zhang, J.; SjoÈvall, J. *Rapid Commun. Mass Spectrom.* **1994**, *8*, 227-236.

88. Marschall, H-U.; Griffiths, W.J.; Zhang, J.; Wietholtz, H.; Matern, H.; Matern, S.; SjoÈvall, J. *J. Lipids Res.* **1994**, *35*, 1599-1610.

89. Rossi, S-A.; Johnson, J.V.; Yost, R.A. *Biol. Mass Spectrom.* **1994**, *23*, 131-139.

90. Ikeda, M.; Fujita, T.; Naoki, H.; Naya, Y.; Mamiya, Y.; Kamba, M.; Sonobe, H. *Rapid Commun. Mass Spectrom.* **1995**, *9*, 1480-1483.

91. Stroobant, V.; De Hoffmann, E.; Libert, R.; Van Hoof, F. *J. Am. Soc. Mass Spectrom.* **1995**, *6*, 588-596.

92. Chang, T.T.; Tsou, H.R.; Siegel, M.M. *Anal. Chem.* **1987**, *59*, 614-617.

93. Siegel, M.M.; McGahren, W.J.; Tomer, K.B.; Chang, T.T. *Biomed. Environ. Mass Spectrom.* **1987**, *14*, 29-38.

94. Naoki, H.; Murata, M.; Yasumoto, T. *Rapid Commun. Mass Spectrom.* **1993**, *7*, 179-182.

95. Havlicek, V.; Ryska, M.; Pospisil, S. *J. Mass Spectrom.* **1995**, *30*, 1089-1094.

96. Kim, Y.H.; Yoo, J.S.; Lee, C.H.; Goo, Y.M.; Kim, M.S. *J. Mass Spectrom.* **1996**, *31*, 855-860.

97. Van Breemen, R.B.; Jiang, O.; Tidwell, R.R.; Hall, J.E.; Brewer, T.G. *J. Mass Spectrom.* **1995**, *30*, 549-556.

98. Johnson, R.S.; Martin, S.A.; Biemann, K.; Stults, J.T.; Watson, J.T. *Anal. Chem.* **1987**, *59*, 2621-2625.

99. Johnson, R.S.; Martin, S.A.; Biemann, K. *Int. J. Mass Spectrom. Ion Proc.* **1988**, *86*, 137-154.

100. Ishidawa, K.; Nishimura, T.; Koga, Y.; Niwa, Y. *Rapid Commun. Mass Spectrom.* **1994**, *8*, 933-938.

101. Summerfield, S.G.; Dale, V.C.M.; Despeyroux, D.D.; Jennings, K.R. *Eur. Mass Spectrom.* **1995**, *1*, 183-194.

102. Boutin, J.A.; Hennig, P.; Lambert, P-H.; Bertin, S.; Petit, L.; Mahieu, J-P.; Serkiz, B.; Volland, J-P.; Fauchere, J-L. *Anal. Biochem.* **1996**, *234*, 126-141.

103. Heerma, W.; Versluis, C.; de Koster, C.G.; Kruijtzerm J.A.W.; Zigrovic, I.; Liskamp, R.M. *Rapid Commun. Mass Spectrom.* **1996**, *10*, 459-464.

104. Ann, Q.; Adams, J. *J. Am. Soc. Mass Spectrom.* **1992**, *3*, 260-263.

105. Ann Q, Adams J. *Anal. Biochem.* **1993**, *65*, 7-13.

106. Hsu, F-F.; Turk, J. *J. Am. Soc. Mass Spectrom.* **2000**, *11*, 437-449.

107. Palma MS, Itagaki Y, Fujita T, Naoki H, Nakajima T. 1998 Toxicon 36:485-493.

108. Itagaki, Y.; Naoki, H.; Fujita, T.; Hisada, M.; Nakajima, T. *Yakugaku Zasshi* **1997**, *117*, 715-728.

109. Fujita, T.; Itagaki, Y.; Naoki, H.; Nakajima, T.; Hagiwara, K. *Rapid Commun. Mass Spectrom.* **1995**, *9*, 365-371.

110. Queiroz, E.F.; Roblot, F.; Laprevote, O.; Serani, L.; Cave, A. *J. Nat. Prod.* **1997**, *60*, 760-765.

111. Hirayama, K.; Akashi, S.; Yuji, R.; Niitsu, U. *Org. Mass Spectrom.* **1993**, *28*, 1516-1524.

112. Domon, B.; Muelle,r D.R.; Richter, W.J. *Org. Mass Spectrom.* **1992**, *27*, 1276-1283.

113. Ubukata, M.; Kimura, K.; Isono, K.; Nelso, C.C.; Gregson, J.M.; McCloskey, J.A. *J. Org. Chem.* **1992**, *57*, 6392-6403.

114. Pergantis, S.A.; Francesconi, K.A.; Goessler, W.; Thomas-Oates, J.E. *Anal. Chem.* **1997**, *69*, 4931-4937.

115. McClure, T.D.; Liebler, D.C. *J. Mass Spectrom.* **1995**, *30*, 1480-1488.

2. ECD in a Linear RF-Field

Hong Ji,[𝄞] Jeff Morré,[𝄞] Valery G. Voinov,[𝄢] Max L. Deinzer,[𝄞] and Douglas F. Barofsky[𝄞]*

[𝄞]Department of Chemistry, Oregon State University, Corvallis, Oregon 97331

[𝄢]Pacific Institute of Bioorganic Chemistry, Vladivostok, 690022, Russia

Analytical Chemistry, **2007**, to be submitted.
American Chemical Society
Columbus, OH 43210, USA

* Corresponding author, email: doug.barofsky@oregonstate.edu, fax: 541-737-2062

2. ECD in a Linear RF-Field

2.1. Abstract

ECD, one of the most powerful means used to induce fragmentation in mass spectrometry for proteomics applications, have been largely limited from becoming a practical and high-throughput tool, due to the intrinsic instrumental limitations of FT ICR. The current study is aimed at finding an alternative way in lowering the operational cost and demonstrating the feasibility of performing analytically practical levels of ECD in a linear RF-field. Two designs are discussed. With a cross-flow configuration, it is demonstrated that zero-energy electrons can be transmitted into the reaction volume of the ECD chamber in numbers sufficient to produce detectable resonance electron capture reactions while maintaining ion transmission at a high enough level to perform cross-beam experiments. With a parallel-flow configuration, it is shown that the cross section for ECD can be increased by increasing both the interaction time and effective volume for interaction. Using this design, an intense ECD spectrum of substance P has been obtained. With this design it should be possible to tune the average kinetic energy of the electrons with a narrow distribution. This result opens the door to the possibility of using electron energy to achieve selectivity in fragmentation. With further improvements, in particular increasing the magnetic field strength by about an order of magnitude, it should be possible to turn ECD into a high-throughput tool for applications in proteomics.

2.2. Introduction

In the last two decades, mass spectrometry has risen to prominence as an analytical tool in the life sciences and in particular for characterizing the structure and function of proteins. However, limited by the advancement of the techniques for dissembling proteins, the nascent science of proteomics currently taps only a small fraction of the information that can potentially be revealed by mass spectrometry.

Currently, the most common means used to induce fragmentation in a mass spectrometer is forcing precursor ions to collide with inert gas atoms. This technique, which is known as collision induced dissociation (CID), is a powerful tool for acquiring amino acid sequence data from peptides that can be used to identify proteins and sites of modification on proteins. While practical and robust, CID techniques do have shortcomings. First of all, the amino acid residues of a protein can fragment at several different positions. Too frequently, CID either fails to sufficiently fragment peptides or it fragments peptides into too many pieces. Insufficient fragmentation generally leaves gaps in the sequence-data, while the excessive fragmentation frequently prevents post-translational modifications of proteins from being properly identified. In fact, the post-translational modifications regulate the function of many proteins and are crucial for understanding pathophysiological processes.[1,2,3] Furthermore, during data acquisition, the intensities of fragment peaks can vary from almost background level to that of the most intense signal in the

spectrum. As a consequence, the interpretation of CID mass spectra is a much more tedious process than the acquisition of them.

Recently, electron-capture dissociation (ECD) has been shown to be an exceedingly effective means for causing ESI produced precursor-ions to fragment.[4,5,6,7,8,9] With this method, radical site dissociation products of a multiply charged cation are induced by allowing it to capture an electron. The products of ECD must be ions so that their mass to charge (m/z) ratios can be identified by a mass analyzer; therefore, only multiply charged cations, which yield cationic products on reduction, can serve as precursors. ECD produces odd-electron, radical driven fragmentation of the same type generated by electron impact mass spectrometry; as such, this fragmentation is different and often complementary to that produced by CID and other slow, even-electron fragmentation methods.[8,9] ECD occurs almost exclusively at only one type of bond in the backbone of a peptide, specifically, between the backbone amide and the alpha carbon to form C-type and $Z^{\bullet}$-type ions. The cleavage sites show very little selectivity for particular amino acids; two exceptions are disulphide bonds (where the affinity for radicals is high) and proline (which is cyclic around the amide-alpha carbon and therefore requires that two bonds be broke).[10] Labile post-translational modifications, e.g., phosphorylation, o-glycosylation, and n-glycosylation, remain attached to the backbone during ECD tandem mass spectrometric (MS/MS) experiments allowing determination of the site and identity of post-translational modifications.[1 2 3] Finally, ECD occurs at more

backbone sites than does CID, leaving far fewer gaps in the sequence-data than CID. As a consequence of all of these characteristics, ECD spectra are generally easier to interpret than CID spectra.

Despite its manifold advantages, ECD MS/MS can for the present only be performed on Fourier transform ion cyclotron resonance (FT-ICR) mass spectrometers. This significantly limits the opportunity for application of the technique. While FT-ICR instruments are arguably the most powerful (in terms of sensitivity, resolution, and mass accuracy) mass spectrometers in existence, they are also the most expensive to purchase and the most difficult and expensive to operate. In Several ways they are less well suited to the high throughput analyses generally required in proteomics studies than other less expensive technologies. Furthermore, the means by which ECD FT-ICR analyses are conducted place fundamental and practical limits on many applications. The methods used to produce low-energy electrons and expose precursor-ions to them permit only crude control over electron energy and ionization efficiency. Experiments can be difficult to conduct and reproduce. Results are spectacular when they are obtained, but that occurrence cannot be reliably predicted.

In order to overcome these obstacles, some efforts have been initiated to find other instrumental platforms for ECD.[11,12 13] In 2004 and 2005, encouraging results emerged from parallel studies by Baba et al.[14] and by Silivra et al.[15] In the study by

Baba et al., the first evidence for ECD in a radio frequency (RF) ion trap was reported.[14] Specifically, a linear RF ion trap was used as the ECD cell for ion confinement. It consists of a two-dimensional radio frequency electric field in the radial plane, and a static electric field in the axial direction. A quadrupole deflector was used to inject electrons along the axial direction where the RF field was zero. With this configuration, perturbation of electrons by the ion trap RF field, or RF heating was avoided. Another unique feature of the trap was a magnetic field (~0.01T) applied parallel to the quadrupole axis to confine electron motion primarily to that direction, and thereby increase transmission efficiency of the electrons. Using this ECD cell, the authors successfully cleaved doubly charged substance P ions, $[M + 2H]^{2+}$ to produce the c and z fragment ions which are characteristic of ECD. The authors claimed that ECD in the RF trap proceeded in largely the same manner as in FT-ICR since the fragment pattern generated in the former was similar to that generated by FTICR.

In the study of Silivra et al., the authors used a modified Bruker Esquire LC instrument.[15] Inside the ring electrode (RE), the authors installed a set of permanent magnets to create magnetic field parallel to the main instrumental axis. They also placed another two sets of magnets on the end cap electrodes to reduce the magnetic field inhomogeneity. The field strength in the trap varied along the main axis from ~ 250 G near end caps to ~ 400 G in the center. Such a field was believed to be sufficient to magnetize electrons but not affect the motion of ions with $m/z > 100$. The authors called the new technique magnetized electrons, in-phase injection (MEPhI).

Before analyzing polypeptide ions, the authors characterize the MEPhI technique with theoretical simulations and experiments with SF_6 molecules. The simulations supported the principle of electron trapping. In the simulation, the authors showed that the extended trapping times for electrons were achieved by the combination of magnetic field confinement in the radial plane and electric field trapping in the axial direction, which is similar to ion trapping in the Penning trap of an FTICR instrument. Experimentally, an ECD-spectrum of the dications of Substance P was produced. According to the authors, the data quality is at least as good as in the experiments with a linear ion trap described in the paper of Baba et al.

Although encouraging, both of the preceding studies have drawbacks in their designs that make it unlikely to find application in proteomics. Specifically, the ECD efficiency with these experimental settings was too low for high-sensitivity analytical applications. i.e. the spectrum presented by Baba et al. was a summation of 6000 ECD scans.[14] Furthermore, neither of the methods makes it possible to control the energy of the electrons precisely. In the case of the linear RF trap, there is little potential for combination with HPLC because the duration of electron injection in one ECD sequence was 80ms. In the case of the 3D trap, the need to inject electrons during a particular short phase of the RF cycle fundamentally limits the sensitivity of the device to level that exceed the practical requirement of proteomics.

In this paper we demonstrate a way to adapt ECD to a triple-quadruple mass spectrometer, a less expensive but more easily operated form of mass spectrometer, and thereby, make ECD tandem mass spectrometry widely available for the analysis of peptides and proteins.

2.3. Instrument design and experimental approach

A Finnigan triple quadrupole instrument TSQ 700 was chosen to be the platform since its quadrupole mass analyzers are mounted on an easily accessible optical bench. The original configuration of the instrument was a quadrupole-octupole-quadrupole (Q-q-Q) analyzer coupled with an electrospray ionization (ESI) ion source. The two quadrupoles could be operated as mass analyzing, ion transmission, or ion selection devices. The octupole in RF-only mode was used as a transmission device or, when needed, as a collision cell. The focus of the present work was on converting the latter device into an ECD cell.

2.3.1. ESI condition

Figure 2.1. shows the ESI configuration of the TSQ 700. A skimmer and several pumping stages are used to achieve a suitable vacuum pressure in the main manifold. In order to obtain the best signal intensity, the following parameters were

tested and optimized: the distance between the end of the ESI capillary and the entrance of the heated capillary; the flow rate; and the spray voltage for electrospray.

In this study, three peptides, reserpine (mainly used for tuning the instrument), neurotensin, and substance P (mainly used for testing the ECD condition) were used for testing the instrumental modification. Various solvent systems were tested for both peptides. The ECD spectra of neurotensin and substance P with and without the presence of electrons were compared.

2.3.2. ECD chamber

In this study, two ECD chamber configurations, namely cross-flow and parallel-flow were tested and compared.

2.3.2.1. Cross-flow configuration

In this configuration, the octupole of the original instrument was replaced by a crossed flow ECD reaction chamber (Figure 2.2). The ECD chamber contains entrances for electrons and precursor ions respectively as well as corresponding exits. (Figure 2.3) In order to maximize electron/ion interactions, the two channels were designed so both axes were within the same plane and were orthogonal to each other. The diameter of the ion-entrance ranged from 3mm to 10mm, depending on the type of filament (see below) used. The thickness of the chamber along the ion-axis

determined the number of lenses that could be placed at the entrance and exit of the ion channel. Two permanent magnets were mounted to the chamber to produce a magnetic field parallel to the electron-axis.

In order to increase the density of the low energy electrons and thereby optimize the opportunity for interaction between electrons and ions, various kinds of filaments were tested and compared. Specifically, wires made of different materials with various diameters and cross sections. (~ 3 - 4mm long) were spot welded onto a filament holder (JEOL). The filament was positioned above and perpendicular to the ion path. A collector with a diameter slightly larger than the inside diameter of the electron exit was located 10mm away from the filament. A sensitive current meter (μA) was connected to the collector, and the current was measured with the potential difference between the cathode and the collector set at two values (10V and 70 V).

To obtain more emission current, a barium tungsten dispenser cathode (STD 134, HeatWave Labs, Inc.) was tested. Although this kind of cathode has high emission current and large surface area, a strong electric potential is required to pull the electrons away from the surface of the cathode to prevent space charging. For this purpose, two grids were placed between the filament and collector. The first grid was placed 1mm away from the cathode, which was set at a potential about 200 V more positive relatively to the filament in order to pull electrons away from the surface of the cathode and avoid space charging. The second grid was placed 1mm away from the first grid. It was set at the chamber potential, which was slightly more positive

than the filament potential in order to decelerate the electrons accelerated by the first grid. As a result, the energy of the electrons entering the chamber was determined by the potential difference between the filament and the chamber. In this case, the ID of the ECD cell was about 10mm. Two extra lenses, one at the entrance and one at the exit, were used for ion focusing.

A thoria-coated Iridium disc cathode (ES-509, Kimball Physics, Wilton, New Hampshire 03086-9742 USA) was also tested in this study for generating low energy electrons. The design of the ECD chamber was similar to the one with the dispenser cathode, except that the volume of the ECD cell was reduced. In this case, the ID of the ion channel was decreased to 3mm (Figure 2.4). The existence of zero energy electrons was tested by monitoring the formation of Cl^- (m/z = 35, 37) from CCl_4 and SF_6^- (m/z = 146) from SF_6.

2.3.2.2 Parallel-flow configuration

In this configuration, the original collision cell, which is a RF-only octupole, was encased in a solenoid and used as an ECD cell (Figure 2.5). A rhenium-tungsten ring (2mm in diameter) was used as the filament. The filament was placed between the first quadrupole and the octupole. The axis of the ring was adjusted to overlap with the ion path. To get the best ion transmission, three lenses were placed at the ion entrance side of the cathode. The lens closest to the cathode (pushing lens) was also tuned to push the electron beam towards the octupole. Two more lenses (pulling lens)

were placed at the exit of the chamber. They were tuned for optimum electron emission and transmission without disturbing the ion transmission. The whole octupole was encased in a solenoid which produces a linear magnetic field along the octupole's axis. The strength of the magnetic field was adjusted so that it could be used to guide and confine the electrons into the octupole while leaving the ions undisturbed. Another small solenoid was added to extend the magnetic field beyond the location of the cathode. A permanent magnet with a hole in the center to allow ions transmission was attached to the pushing lens so that the magnetic field lines extended even further (Figure 2.6) to guarantee that the cathode sat in the linear part of the magnetic field.

The energy of the electrons entering the octupole was determined by the difference between the filament and octupole potentials. In detail, the octupole potential was initially set at a reasonable value to maintain efficient ion transmission. The potential of the filament was then tuned to obtain electron energy less than 1 eV. The strength of the magnetic field as well as the potentials of the pushing and pulling lenses were tuned to simultaneously maintain both the ion and the electron transmissions at the highest possible levels and to maintain the filament emission current at the highest possible level. A typical filament emission current was less than 1 μ A.

To observe the electrons transmission efficiency through octupole, Q3 was operated in the negative ion RF-only mode (transmission mode). To observe the ion

transmission efficiency, Q3 was operated in the positive mode (mass analyzing mode). The effects of both magnetic field strength and octupole RF potential on the electrons' and ions' transmission efficiencies through octupole were examined.

To obtain the ECD spectrum of substance P, Q3 was operated in the positive ion mode. Spectra with and without the electron beam were recorded and compared without changing the other experimental conditions. The magnetic field strength was set at about 50G.

2.4. Results and discussion

2.4.1. ESI condition

ESI was selected as the ionization method for two principle reasons. First, ESI can produce multiply charged cations or anions of intact biopolymers. This is critical for ECD since only multiply charged ions can capture an electron to produce in the unstable excited states that can lead to further dissociation. Second, ESI is generally compatible with eluents (e.g. methanol, acetonitrile, and water) commonly used in liquid chromatography (LC) with close flow rates. This feature makes it possible to pair LC separation with ECD mass spectrometry.

Three key parameters were optimized and correlated: the distance between the end of the ESI capillary and the entrance of the heated capillary; the flow rate of the

ESI solution; and the spray voltage. In the whole study, the distance between the end of the ESI capillary and the end of the heated capillary was normally set to about 1cm. At this distance and a flow rate of 0.08 mL/hr, the spray voltage had to be set to 5kV. When lowering the flow rate to 0.03~0.04 mL/hr, the spray voltage had to be decreased to 4kV. This is due to the fact that, for higher flow rates, the force from the electrical field is often not strong enough to nebulize the liquid flow without causing electrical discharge.[16] It was also found that, in order to obtain stable and sensitive ESI signal, the ESI capillary had to be extended 0.5mm out of the metal tip.

For Reserpine, the optimum solvent was found to be 50 : 50 methanol : H_2O with 1% acetic acid added. A concentration of 5 μg/10 mL gave the best signal intensity. For substance P, the optimum solvent was found to be 50 : 50 methanol : H_2O. A concentration of 10 μM was selected.

2.4.2. ECD chamber

2.4.2.1. Chamber material

Various materials for making the ECD chamber were screened. When emitting electrons, the surface temperature of the filament can reach ~ 2000 C^o. This high temperature eliminates use of aluminum, copper, and even stainless steel. These metals tend to sublimate and later deposit onto surrounding cool surfaces; a phenomenon that causes unwanted short circuiting.

Although expensive and difficult to machine, molybdenum has the lowest heating expansion of any commercially used metal and the a highest melting point of (2623°C) among all the the metals tested.[17] It is an ideal material to be used to overcome the abovementioned problems. In our design, a tube made of molybdenum is covered by the main body of the chamber made of stainless steel. This assures that the hot filament is fully shielded while keeping the whole design at a reasonable cost.

2.4.2.2. Cross flow configuration

The first configuration of the ECD chamber was based on the idea that ECD could happen when the ions pre-selected by the first quadrupole were crossed by low energy electron beam with enough electron density. This was thought to be the simplest and least expensive way to attempt electron capture dissociation of multiply charged positive ions in a non-FT ICR instrument. In this configuration the low-energy electron source were arranged so that the precursor ions flow along one direction into the reaction chamber while the electrons flow into the chamber along a path that is transverse to the ions' axis.

2.4.2.2.1. Wire and ribbon filament

Various materials and shapes for the filaments were tested and the results are listed in Table 2.1. Rhenium ribbon produced the highest emission current and had a large surface area; consequently, it was chosen as the filament for the attempting

ECD. When the electron energy was tuned close to zero, the emission current of the rhenium ribbon was less than 1 μ A and was almost undetectable with the current meter. Furthermore, with this configuration, only the electrons emitted from the area right above the ion path had any possibility of interacting with the ions (Figure 2.7). These electrons were only small portion of the whole emission current. Consequently, the probability of the interaction between the electrons and the ions was low. Filaments with emission surfaces that matched the ion beam size and high emission current/area were needed.

2.4.2.2.2. Barium Tungsten Dispenser Cathode with support legs

Using the Barium Tungsten dispenser cathode turned out to be also unsuccessful. Based on the technical data sheet of the product, if was estimated that, with the extraction grid placed about 1mm in front of a cathode with a diameter of 0.134", the emission current of the cathode should be close to 270 mA. However, in our study the current measured at the collector never exceed 5mA. This is less than 2% of the calculated value. There might be two root causes that lead to this problem. First, due to the use of ESI as the ion source, the vacuum condition (10^{-5} torr) did not meet the requirement of the cathode (10^{-7} torr). Second, the proximity of the extraction grid at 200V limited the number of electrons that could reach the collector. The detection of a leakage current on this grid, which was only 1 mm away from the cathode, confirmed that the grid absorbed the majority of the electrons.

2.4.2.2.3. Thoria-coated Iridium disc cathode

In addition to its capability for providing high emission current (10mA), a thoria-coated iridium disc cathode was chosen for testing based on four additional considerations. First, operation of this indirectly heated iridium cathode is not restricted to high vacuum conditions. For example, even at 10^{-4} torr, the cathode can still provide stable and uniform electron emission. This is ideally suited for our instrument design since the vacuum under the working condition (with ESI) is normally at $1.2*10^{-5}$ torr. Second, the disc has a diameter about 2mm which means the emission current/area is larger. Third, it has a long life time since iridium is a noble metal and is resistant to oxidation and other forms of chemical attack. Fourth and final, the heating wire of the cathode is mounted on a molybdenum pin that will not sublimate during the operation.

In order to increase the efficiency for interaction between electrons and ions in our cell to a level where we might observe ECD, it was necessary to find conditions that increase the population of low-energy electrons in the cell without interrupting the transmission of ions from the first mass analyzer (MS_1) to the second mass analyzer (MS_2). The transmission of low-energy electrons is exceedingly difficult to control; even the slightest stray electric or magnetic field will affect their motion. The magnetic field lines that run between the cathode and the collector serve to collimate the electrons; nevertheless, at kinetic energies close to zero, the electron current at the collector was below the detection limit of our apparatus. To ensure the

existence of electrons with energy close to zero electron volts, the ECD cell was tuned to transmit ions while exploiting resonance electron capture (REC) ionization reactions that occur at electron energies close to 0 eV. Specifically, when the gaseous sample of CCl_4 and SF_6 mixture was introduced into the instrument, the zero-energy resonances, i.e. both the formation of Cl^- (m/z = 35, 37) from CCl_4 and SF_6^- (m/z = 146) from SF_6, were monitored with Q3. The appearance of the Cl^- ions and the SF_6^- ions in the spectrum (Figure 2.8) indicated that with correct tuning, zero-energy electrons can be transmitted into the reaction volume of our chamber without disturbing the ions' transmission. The high abundances of the Cl^- and SF_6^- ions also indicate that the number of the zero-energy electrons must be sufficient to produce detectable REC ions.

Neurotensin (M_r = 1,669 Da) was used as the test compound for the initial ECD experiments with crossed ion and electron beams. This peptide was chosen as a model because, under ESI, it yields highly abundant doubly and triply charged ions (*m/z* = 835.5 and *m/z* = 557.3 respectively) that should readily capture zero-energy electrons. The spectrum of neurotensin obtained in the absence of low-energy electrons, in fact, changes when the doubly and triply charged precursors are exposed to a cross beam of low-energy electrons (Figure 2.9). In particular after exposure to low-energy electrons, a significant number of new ion signals appear at *m/z*-values greater than that of the doubly charged neurotensin (*m/z* = 835.5) suggesting that singly charged fragments are being produced by ECD.

As a negative consequence of the modifications made on the TSQ700, it was not possible to produce MS/MS spectra on this instrument and, by this means, interpret the neurotensin spectra. This is so, in part, because the TSQ700's first quadrupole (MS_1) can only function as an ion transmitter when the instrument is set to operate in the MS/MS mode (thereby preventing selection of a single precursor ion from the unduly complex spectrum) and, in part, because there was too much fluctuation in the ion signals.

Although the results were promising, these experiments revealed the difficulty in controlling the zero-energy electrons in the cross-flow configuration. In order for the cross-flow chamber to be practicable, it would be necessary to devise means for increasing the population of low-energy electrons in the ECD chamber and for more precisely controlling the energy of the low-energy electron beam. These tasks were deemed too difficult to pursue on the TSQ700.

2.4.2.3. parallel-flow configuration

In order to overcome the short interaction time frame and consequently increase the efficiency of the interaction between the low energy electrons and the ions, a parallel-flow ECD chamber was built and tested. In this design, continuous streams of low energy electrons and precursor ions were successfully introduced into a RF-only octupole simultaneously. A magnetic field generated by a solenoid was

used to collimate the electrons along the axis of the octupole without disturbing the ions transition. The spiral movement of electrons around the magnetic field lines has the added benefit of lengthening the path of the electrons through the octupole and, thereby, increasing the interaction time between the electrons and the ions.

2.4.2.3.1. The effect of the CRFP parameter of octupole on the transmission efficiency of both electrons and ions

The basic operation of an octupole's RF potential on ions passing through it can be illustrated by using a stability diagram (Figure 2.10). In this diagram the area within the triangular region corresponds to pairs of DC and RF voltages that provide stable ion-trajectories for a range of m/z-values; the area outside the triangular region corresponds to DC/RF-settings that produce unstable trajectories. When the octupole is operated in a mass analyzing mode, the RF and DC voltages are scanned simultaneously while keep their ratio constant; this mode is illustrated by the red-scan line in Figure 2.10. When operating in a transmission-only mode, the DC voltage is set at zero so that the scan line has a slope equal to zero (red dotted line in Figure 2.10).

Since in the TSQ 700 mass spectrometer, the RF voltage setting is controlled by tuning a parameter designated as CRFP, the value of this parameter affects both the electrons and the ions simultaneously. It was necessary to examine the effects of changing CRFP value on both the electrons and the ions transmission efficiencies

individually. In the transmission-only mode, the octupole's efficiency at low-mass is set by its geometry, construction, and operating frequency. The transmission efficiency of the TSQ700's octupole at its low-mass cut-off was observed as a function of CRFP value by operating Q3 in the spectrometer in the positive ion mode. As the CRFP value increased at the devices operating frequency, the low mass cut off of the ion transmission increased as is typical for a multipole transmission device (Figure 2.11). The effect of the CRFP setting on the electrons' transmission was observed by operating Q1 in the spectrometer in the negative ion mode. For a given magnetic field, increasing the CRFP value decreased the transmission of the electrons (Figure 2.11). By exercising considerable care, it was possible to tune the TSQ700 so that appreciable numbers of both the doubly charged ions of substance P (M_r = 1347.63 Da) and electrons passed through the octupole simultaneously.

2.4.2.3.2. ECD spectrum of substance P

Although it was only possible to achieve a small overlap in the electron and ion populations in the octupole (Figure 2.11), this conjunction was sufficient to achieve ECD. Spectra of substance P without (Figure 2.12) and with (Figure 2.13) electrons present in the quadrupole were recorded with Q3 in the TSQ700 operating in the positive ion scan mode. Both spectra exhibit signals corresponding to the doubly charged molecular ion (protonated at m/z 674.8 and sodiated at m/z 685.8) of substance P as base peaks, but the singly charged molecular ion of substance P and the backbone cleavage ions C6, C7, C8, C9, and C10 were only recorded (Figure 2.13)

when low energy electrons coexisted with ions in the octupole. The spectrum shown in Figure 2.13, which would qualify for practical proteomics analysis, is the average of 50 single scans (3 s/scan); however, single scan spectra (not shown) displayed the same structural information contained in the averaged spectrum, albeit with diminished S/N. This is strong evidence that ECD was taking place efficiently in the non-FT-ICR cell despite the less than optimum reaction conditions.

The production of sodiated substance P presumably originates from the ESI solvent. Since no acid was added to the spray-solvent, the formation of sodiated substance P ions in the solution and, consequently, their appearance in the gas phase would have been favored. The presence of a strong signal for $[M+H+Na]^+$ or any C-type fragments containing sodium (Figure 2.13) is noteworthy. Since the electron affinity of sodium is larger than that of hydrogen, one would expect the presence of sodiated molecular ions to increase the probability of electron capture. This seems to be supported by the strong signal in the ECD spectrum corresponding to $[M+H+Na]^+$. The absence of sodiated fragment ions, however, suggests that this latter species does not fragment appreciably and that, therefore, all of the C-type fragments in the spectrum are products of $[M+2H]^+$, whose signal is less abundant. This curious observation warrants further investigation.

2.4.2.3.3. The effect of magnetic field strength on electrons transmission

In addition to carefully tuning the RF potential, two other approaches were used to increase the electron density in the octupole. First, electrons were focused into a small volume along the axis of the octupole with the aid of focusing lenses. Such focusing reduces electron-loss because the RF field's affect on the electrons is very limited in the center of the octupole to create a nearly RF-field-free region in which the electrons do not gain energy. Second, the electron trajectories were sequestered along the magnetic field lines after entering the RF field free region. This capture by the magnetic field reduces the probability of the electrons colliding with the octupole's rods. As illustrated in Figure 2.14, it should be possible to substantially increase the efficiency of the ECD reaction by increasing the strength of the magnetic field. Limits imposed by the geometry and size of the optical train in the TSQ700, however, prevented taking advantage of this possibility. A platform with room for a significantly more powerful solenoid is therefore needed for further investigation of ECD in a linear, parallel-flow RF-cell.

2.5. Concluding remarks

Intrinsic technical limitations of FT ICR, i.e. ion-number and electron-number densities restricted by space charge and the inability to control electron energy, have prevented ECD from becoming a practical and high-throughput tool in proteomics applications. The current study was aimed at demonstrating the feasibility of performing analytically practical levels of ECD in a linear RF-chamber.

Two designs were tested. With a cross-flow configuration, it was demonstrated that zero-energy electrons can be transmitted into the reaction volume of the ECD chamber in numbers sufficient to produce detectable resonance electron capture reactions while maintaining ion transmission at a high enough level to perform cross-beam experiments. Using neurotensin as the test compound, experiments with crossed ion and low-energy electron beams produced a significant number of new ion signals at *m/z*-values greater than that of the doubly charged neurotensin suggesting that singly charged fragments had been produced by ECD.

With a parallel-flow configuration, the cross section for ECD was successfully increased by increasing both the interaction time and effective volume for interaction. Using this design, an intense, i.e. analytically useful, ECD spectrum of substance P has been obtained. In principle, this device should make it possible to tune the average kinetic energy of the electrons while maintaining a narrow distribution of energies about this average. This opens the door to the possibility of using electron energy to achieve selectivity in fragmentation. With further improvements, in particular increasing the magnetic field strength by about an order of magnitude (i.e. from ~ 0.05 T to ~ 0.5 T), it should be possible to turn ECD into a high-throughput tool for applications in proteomics.

2.6. Acknowledgement

The research reported in this paper was supported directly by a grant from the W.M. Keck Foundation and indirectly by an Environmental Health Sciences Center Grant (ES00210) from the National Institute of Environmental Health Science.

2.7. References

1. Kelleher, N. L., Zubarev, R. A., Bush, K., Furie, B., Furie, B. C., McLafferty, F. W., and Walsh, C. T. *Anal. Chem.* **1999** *71*, 4250-4253.

2. Mirgorodskaya, E., Roepstorff, P., and Zubarev, R.A. *Anal. Chem.* **1999** *71*, 4431-4436.

3. Mann, M. and Jensen O.N. *Nature Biotechnology* **2003**, *21*, 255-261.

4. Zubarev, R. A., Kelleher, N. L., McLafferty, F. W. *J. Am. Chem. Soc.* **1998**, *120*, 3265.

5. Axelsson, J., Palmblad, M., Håkansson, K., and Håkansson, P. *Rapid Commun. Mass Spectrom.* **1999**, *13*, 474-477.

6. McLafferty, F.W., Fridriksson, E.K., Horn, D.M., Lewis, M.A., and Zubarev, R.A. *Science* **1999**, *284*, 1289-1290.

7. Zubarev, R.A., Horn, D.M., Fridriksson, E.K., Kelleher, N.L., Kruger, N.A., Lewis, M.A., Carpenter, B.K., and McLafferty, F.W. *Anal. Chem.* **2000**, *72*, 563-573.

8. Zubarev, R.A., Haselmann, K.F., Budnik, B., Kjeldsen, F., and Jensen, F. (). *Eur. J. Mass Spectrom.* **2002**, *8*, 337-349.

9. Roman A. Zubarev, R.A. *Mass Spectrom. Rev.* **2003**, *22***,** 57-77**.**

10. Zubarev, R.A., Kruger, N.A., Fridriksson, E.K., Lewis, M.A., Horn, D.M., Carpenter, B.K., and McLafferty, F.W. *J. Am. Chem. Soc.* **1999**, *121*, 2857-2862.

11. Vachet, R. W.; Clark, S. D.; Glish, G. L. Proceedings of the 43rd ASMS Conference on Mass Spectrometry and Allied Topics, 1995; p 1111.

12. Ivonin, I.; Zubarev, R. A. Proceedings of the 51st ASMS Conference on Mass Spectrometry and Allied Topics, 2003; ThPE057.

13. Baba, T.; Black, D. M.; Glish, G. L. Proceedings of the 51st ASMS Conference on Mass Spectrometry and Allied Topics, 2003; ThPJ1 165.

14. Baba, T.; Hashimoto, Y.; Hasegawa, H.; Hirabayashi, A.; Waki, Izumi. *Anal. Chem.* **2004**, *76*, 4263-4266.

15. Silivra, O. A.; Kjeldsen, F.; Ivonin, I. A.; Zubarev, R. A. *J. Am. Soc. Mass Spectrom.* **2005**, *16*, 22–27.

16. Ikonomou, M. G., Blades, A. T. and Kebarle, P., *J. Am. Soc. Mass Spectrom.* **1991**, *2*, 497.

17. Emsley, J. *Nature's Building Blocks* Oxford: Oxford University Press, **2001**, 262-266. 0-19-850341-5.

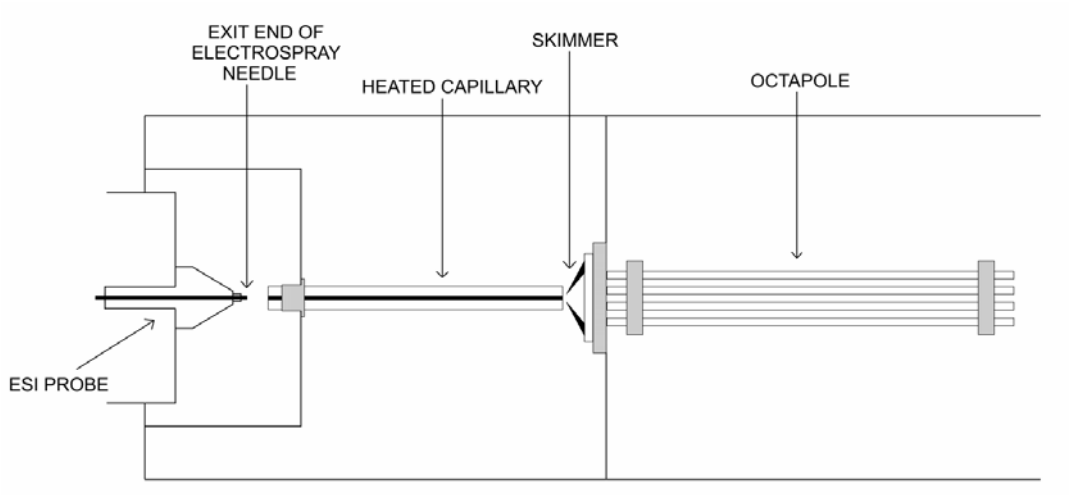

Figure 2.1 ESI configuration of TSQ 700.

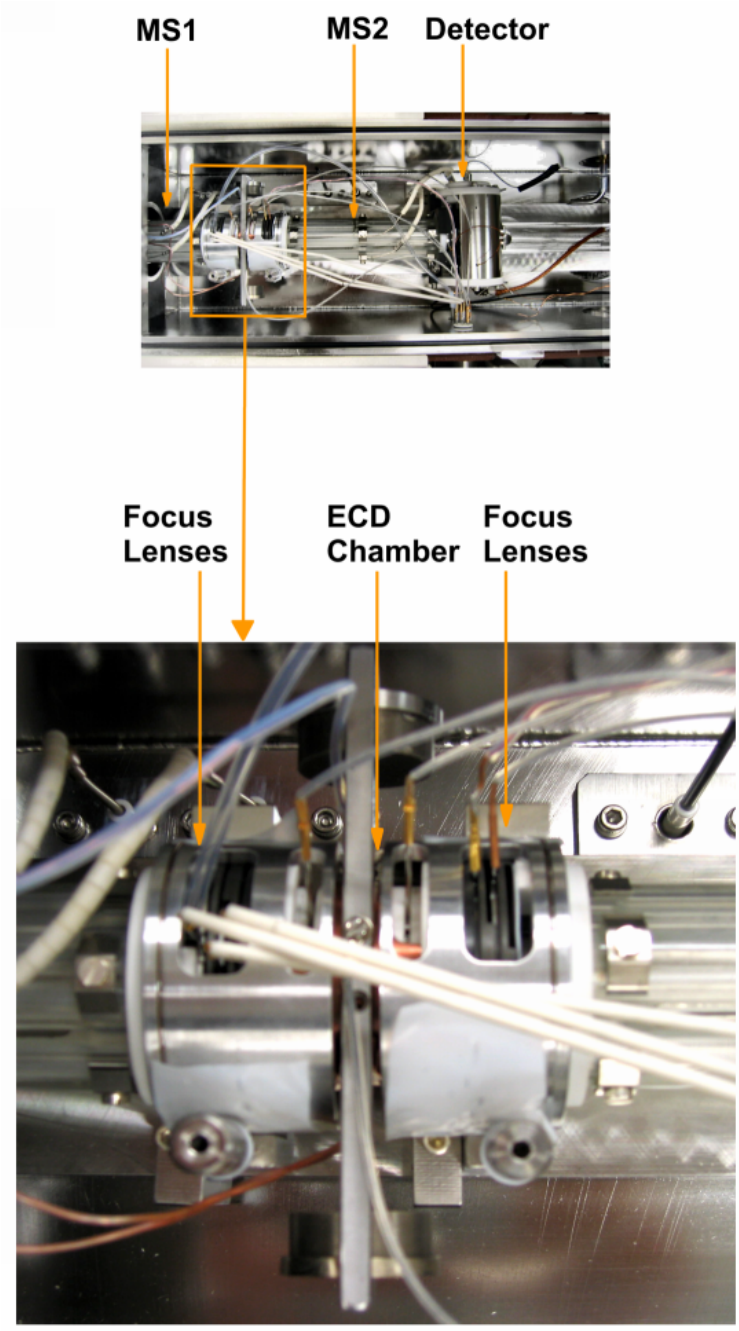

Figure 2.2 Picture of the ECD chamber in cross-flow configuration.

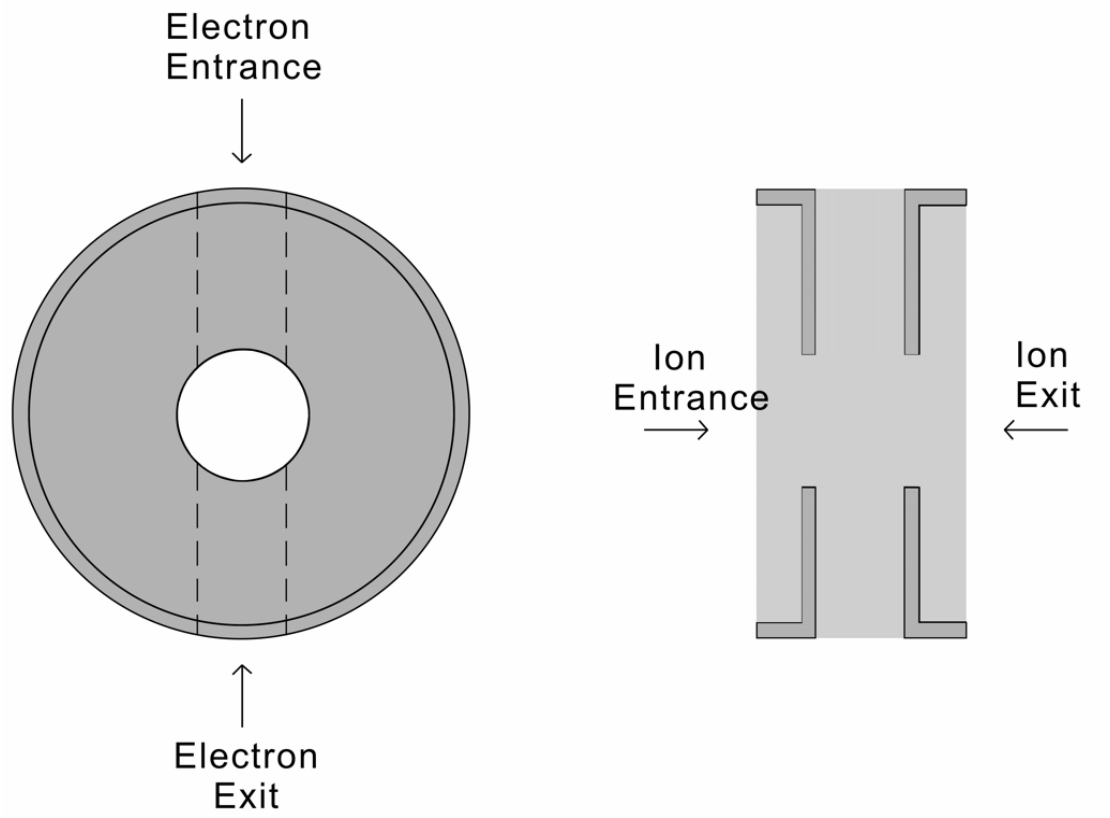

Figure 2.3 Front view and center cut view of the ECD chamber in general form.

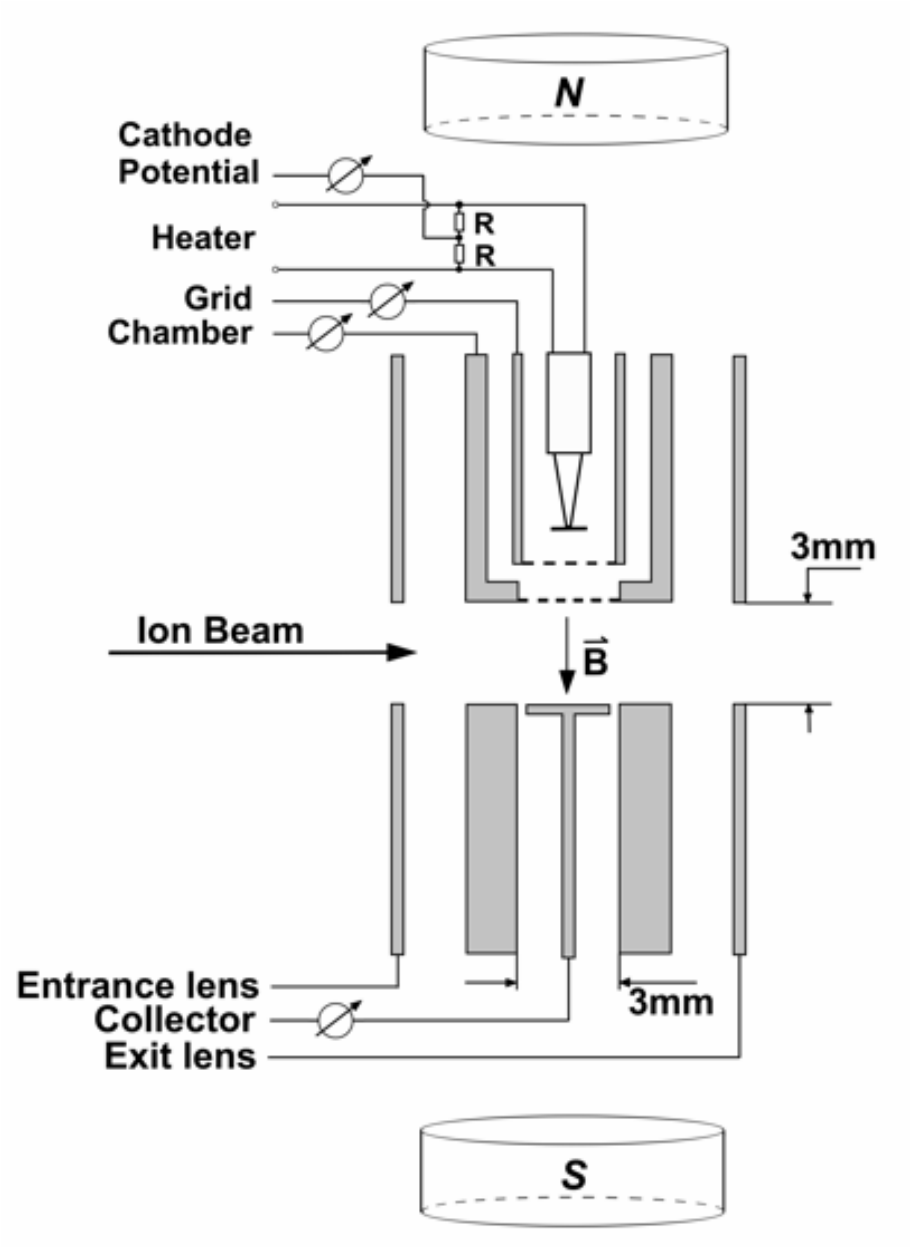

Figure 2.4 Scheme of a cross-flow configuration chamber with a thoria-coated Iridium disc cathode.

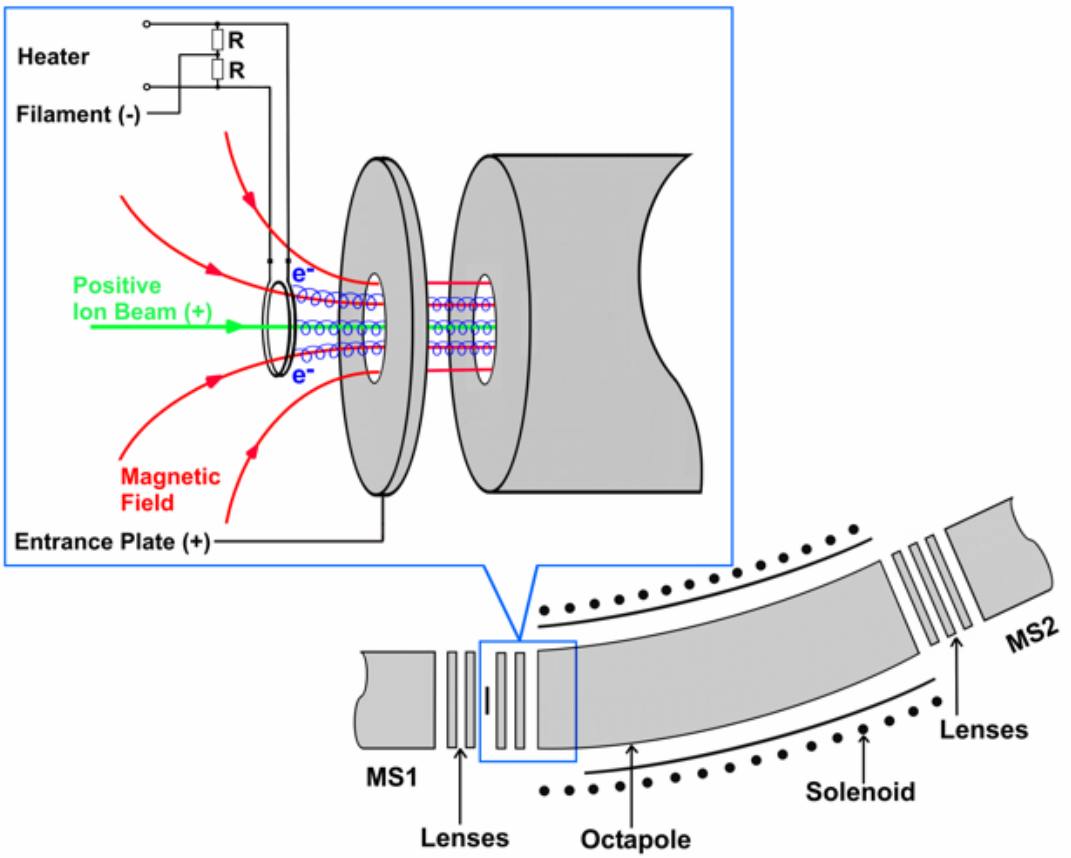

Figure 2.5 ECD chamber in parallel-flow configuration with one solenoid (indicated by the black dots around the octupole).

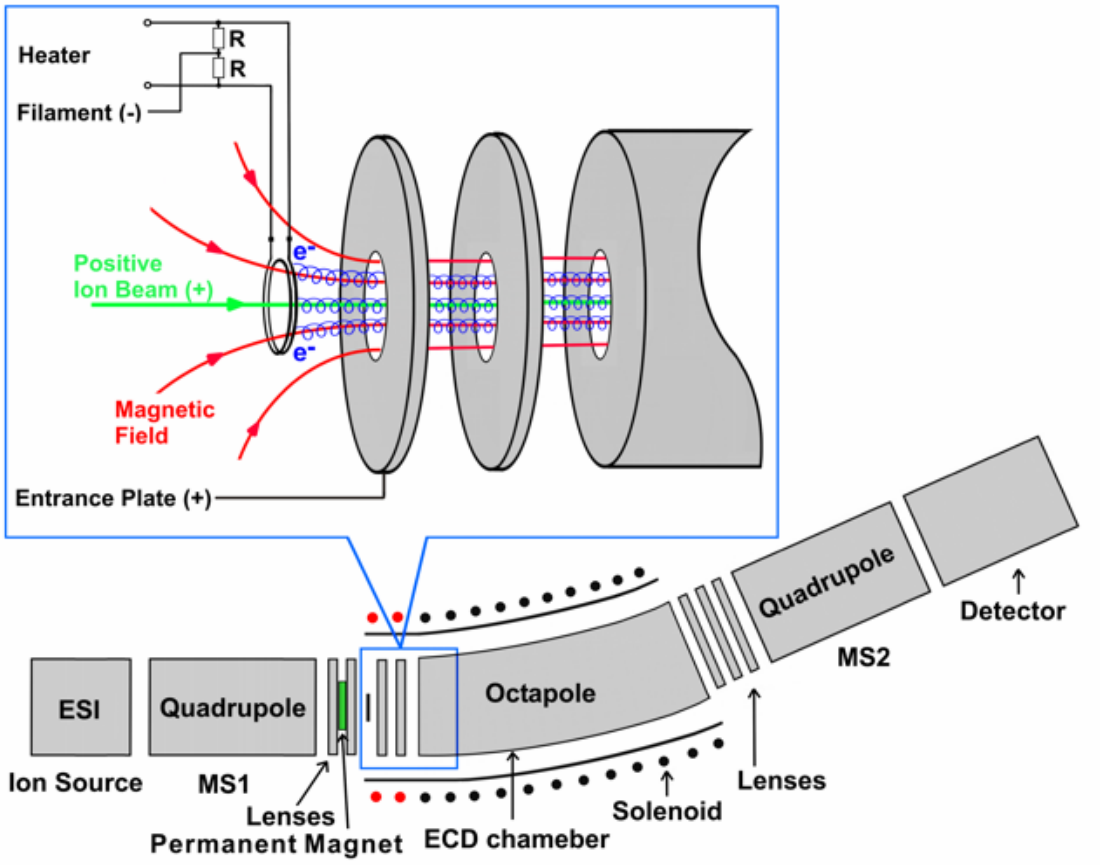

Figure 2.6 ECD chamber in parallel-flow configuration with one big solenoid (indicated by the black dots around the octupole) and one small solenoid (indicated by the red dots).

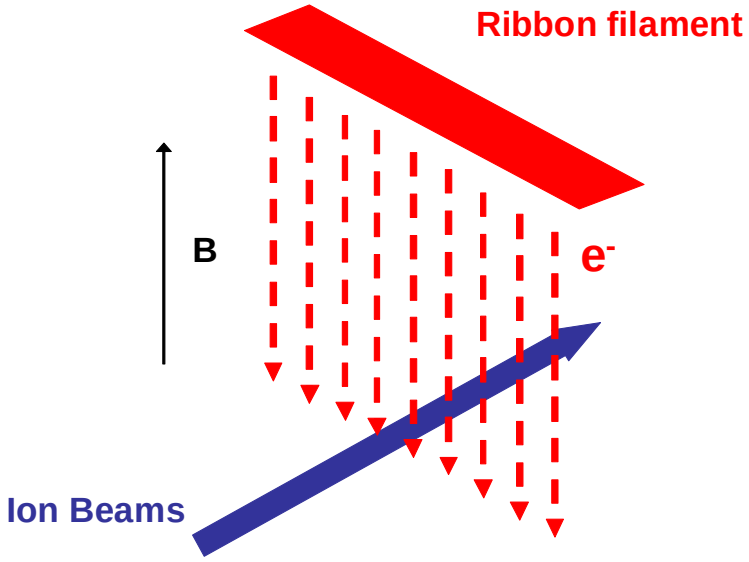

Figure 2.7 Interaction between the electrons and ions in the cross-flow configuration with the wire/ribbon filament.

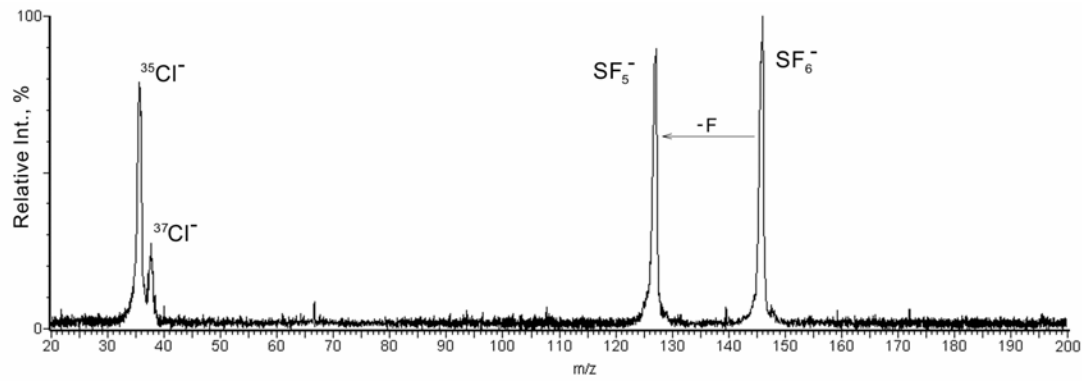

Figure 2.8 REC spectrum of the mixture of CCl_4 and SF_6.

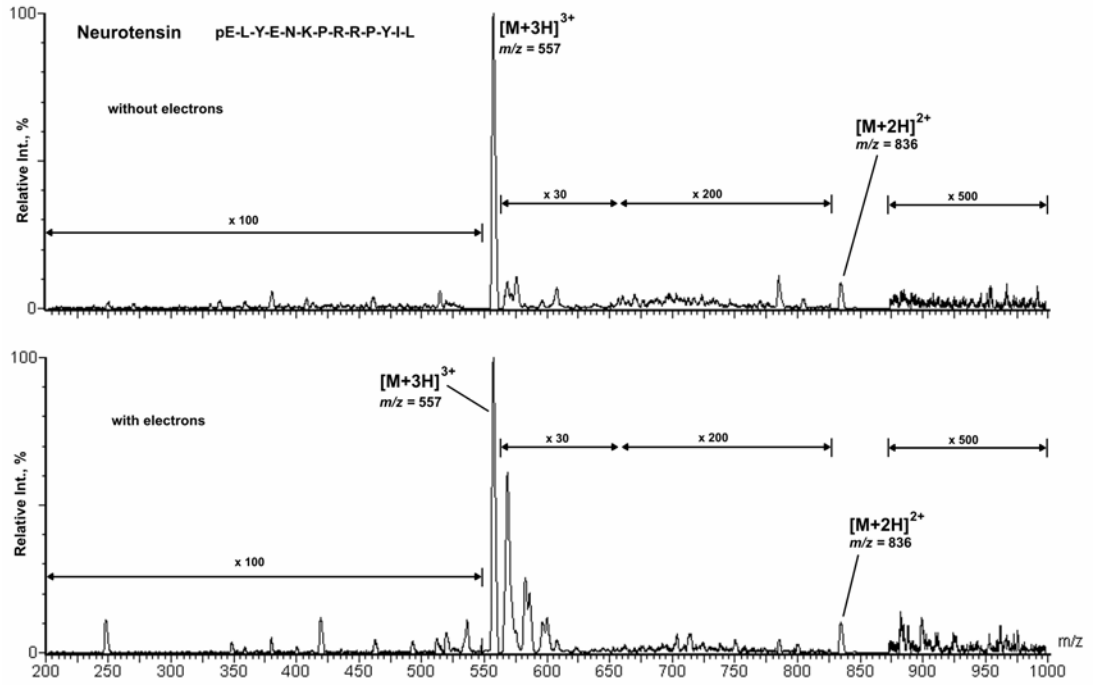

Figure 2.9 The spectra of neurotensin without (top) and with (bottom) crossed electron beams.

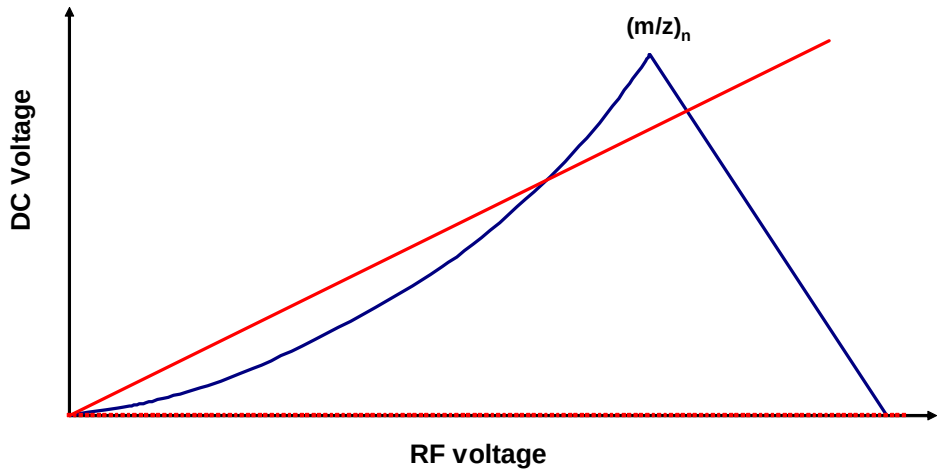

Figure 2.10 Stability diagrams for ions plotted in RF- DC space (figure adapted from 'Mass Spectrometry: Principles and Applications', Edmond De Hoffmann and Vincent Stroobant, Wiley, 2001 **)**, showing a straight scan line (red line) through the origin; as shown, only ions with mass-to-charge ratios within a short range about $(m/z)_n$ would pass through the filter. When the scan line has a slope equals to zero, the device is operated in a transmission mode (red dotted line).

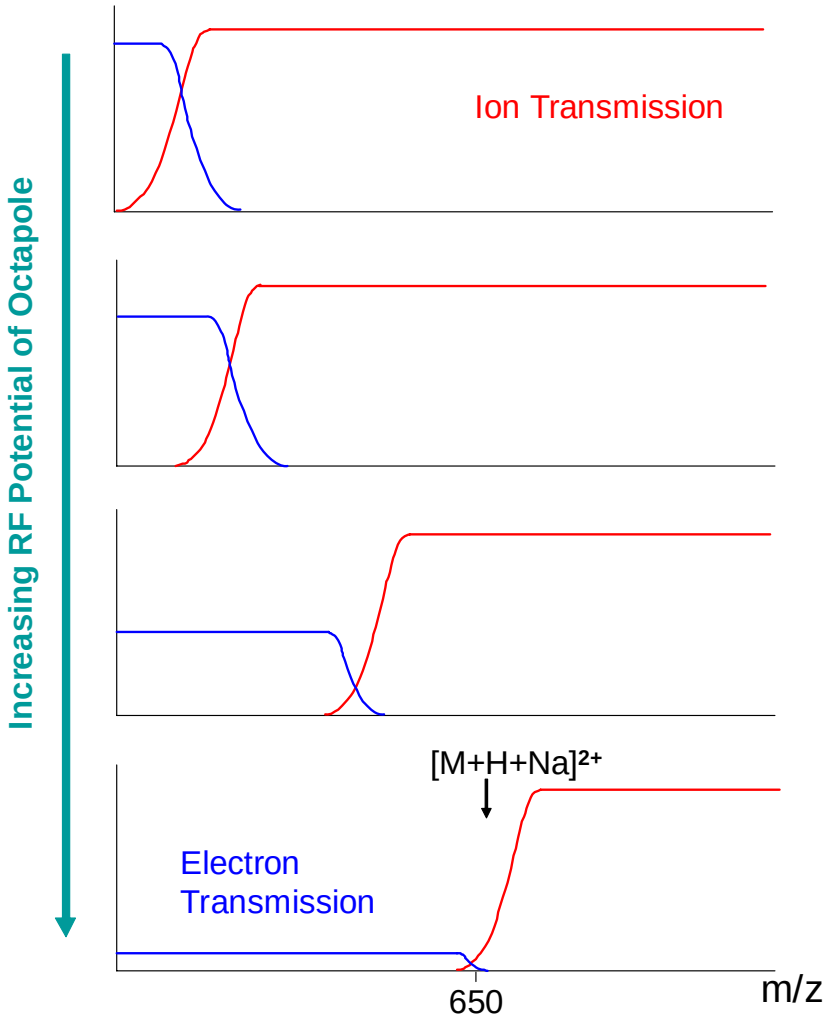

Figure 2.11 Electron and ion transmission with increasing CRFP value of octapole (magnetic field strength and octapole RF frequency kept constant).

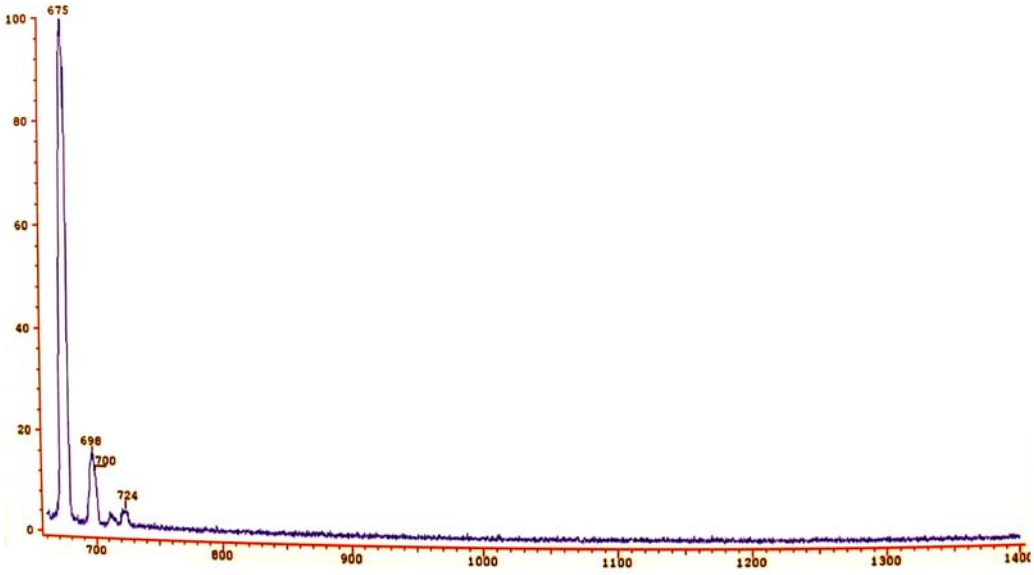

Figure 2.12 Spectrum of substance P without the existence of electron.

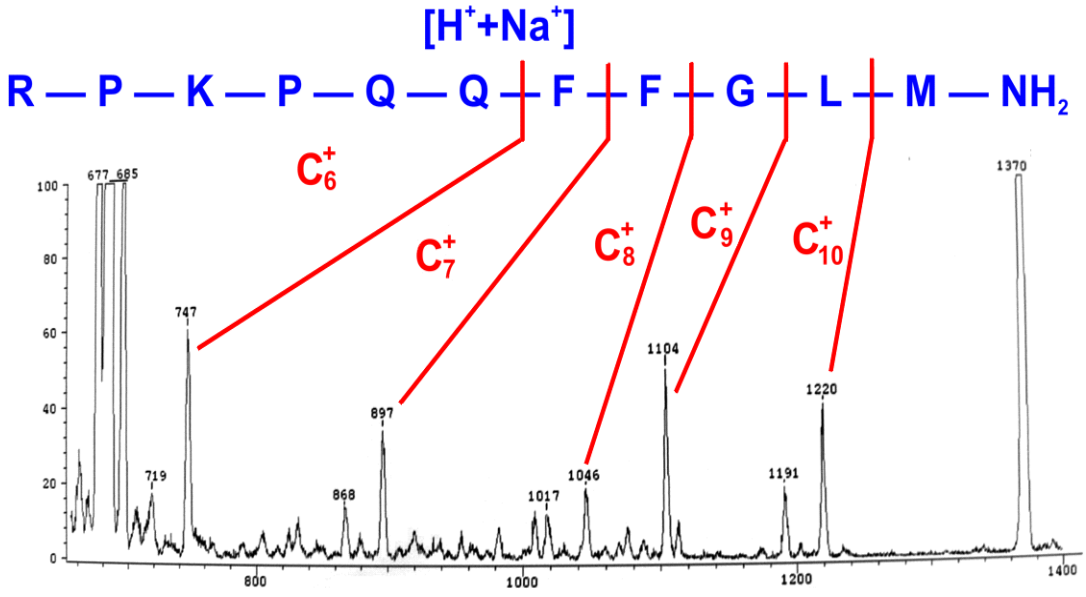

Figure 2.13 ECD spectrum of substance P.

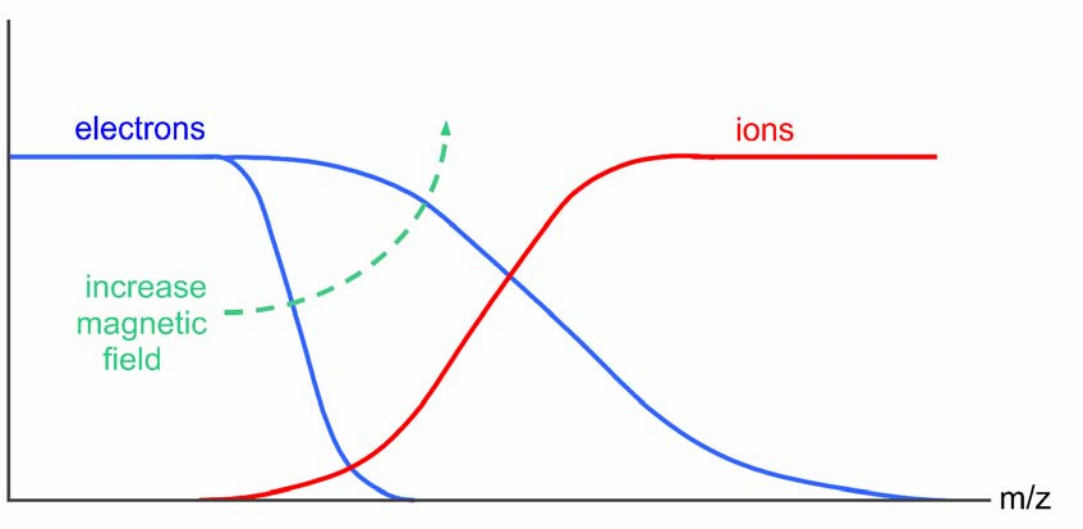

Figure 2.14 When RF frequency and CRFP value kept constant, the affect of magnetic field strength on electron transmission.

Table 2.1 Emission current of various materials and shapes for the filaments.

Filament material and shape	Size (mm)	Working current (A)	Electron energy (eV)	Emission current (uA)
Rhenium wire	D/0.178	2.5	70	60
			10	7
Rhenium ribbon	Thickness/0.051, width/0.64	4.5	70	90
			10	9
2% Thoriated Tungsten Wire	D/0.15	4	70	70
			10	8
Thoriated Tungsten Wire	D/0.203	5	70	80
			10	8

3. Charge-Remote Metastable Ion Decomposition of Free Fatty Acids under FAB MS: Evidence for bi-Radical Ion Structures

Hong Ji,[1] Jeff Morré,[1] Valery G. Voinov,[2] Max L. Deinzer,[1] and Douglas F. Barofsky[1]*

[1]Department of Chemistry, Oregon State University, Corvallis, Oregon 97331

[2]Pacific Institute of Bioorganic Chemistry, Vladivostok, 690022, Russia

Analytical Chemistry, **2007,** *79,* 2882.
American Chemical Society
Columbus, OH 43210, USA

* Corresponding author, email: doug.barofsky@oregonstate.edu, fax: 541-737-2062

3. Charge-Remote Metastable Ion Decomposition of Free Fatty Acids under FAB MS: Evidence for bi-Radical Ion Structures

3.1. Abstract

Classical charge-remote fragmentation (CRF) of a series of long-chain saturated and monounsaturated fatty acid anions, a well-known phenomenon under collisional activation conditions, is observed for the first time during fast atom bombardment of the analyte-matrix mixture without collisional activation. The process is efficient enough to allow collision induced dissociation (CID) and metastable ion decomposition MS/MS spectra of any charge-remote $[M\text{-}H_2\text{-}(CH_2)_n]^-$ fragments as well as spectra of neutral losses to be recorded. The results obtained are in contradiction with the generally accepted theory that CRF results exclusively in terminally unsaturated carboxylate anions. The new results indicate that a multi-step radical mechanism is involved in CRF ion formation. The first step of the process appears to be accompanied by hydrogen elimination that occurs randomly throughout the molecule. The primary fragment radical ions formed can decompose further with the formation of the next generation of CRF ions.

3.2. Introduction

Charge-remote fragmentation (CRF), as an analytically useful and fundamentally interesting gas-phase reaction, was first observed in high energy collision induced dissociation (CID) mass-analyzed ion kinetic energy (MIKE) spectra of fatty acid carboxylate anions and their methyl esters.[1,2] Since that time several groups have carried out investigations of this phenomenon using experimental approaches that include different functionalities and isotope labeling,[3] changing the internal energy content of precursor ions[4], and analysis including quantum chemical calculations.[5] This list is far from comprehensive; the interested reader is referred to recent review articles for further detail.[6] These past efforts have lead to the conclusion that high-energy collisions are generally necessary for CRF to occur; however, no consensus about the mechanism of CRF has been reached, and investigation of this phenomenon continues.

The instrumental configuration for collisional activation, which assumes the use of multi-analyzer instruments, imposes limitations on studying CRF. There are, however, three instances in which CRF reactions have been observed under regular FAB conditions without CID. Boyd and coworkers[3b, c] noted that FAB or, more appropriately, liquid secondary ion mass spectrometry (LSIMS) positive ion mass spectra of quaternary ammonium ions contained complete sets of CRF ions, in which the most intense fragment ion's abundance was 4-5% relative to the parent quaternary ammonium ion. P.Traldi and co-workers[3h, 7] observed that alkyl-trimethylammonium

halides apparently undergo CRF during positive ion FAB just as they do when subjected to CID and, furthermore, that alkyl-trimethylammonium halides can be characterized by FAB analysis without tandem mass spectrometry. In attempting to locate epoxides in acetogenin, Laprévote et al.[8] found that the linked scan FAB spectrum of lithium-cationized long-chain acetogenin exhibited the same fragment-ion peaks in the absence of a collision gas as in the presence of gas, although with appreciably lower intensity.

As far as fatty acids (FA) are concerned, it has been observed in experiments with ESI,[9] negative ion chemical ionization (NICI),[10] and resonance electron capture (REC)[11] that carboxylate anions are stable species and do not dissociate without collisional activation. Furthermore, CRF of carboxylate anions has not been observed under FAB[1, 6b] or static SIMS[12] conditions. In contrast to these previous findings, it is demonstrated in the present report that FA carboxylate anions formed under FAB desorption/ionization conditions can undergo CRF reactions without activation in a collision cell. The occurrence of CRF under regular FAB conditions provides an opportunity to study these reactions on double sector instruments operating in linked scan modes.[3h, b] Although the high chemical background usually present in FAB spectra poses a potential problem, the present results show that interference from the matrix is to a large degree suppressed.[13]

Although there is currently no agreed upon mechanism for CRF, it seems commonly accepted that these reactions result in terminally unsaturated fragment

ions.[14] In the present work, this concept was tested by monitoring the various CRF ions generated in the source of a double focusing, sector (Nier-Johnson *E, B* geometry) mass spectrometer in a straight scanning mode, i.e. scanning the magnetic field (*B*), or in linked scanning[15] mode, i.e. simultaneously scanning the electric (*E*) and magnetic fields according to one of the following mathematical relationships: *B/E* = constant (to obtain product ion spectra) or $(B/E)\cdot\sqrt{1-E}$ = constant (to obtain neutral loss spectra). The results from the experiments unambiguously indicate that carboxylate anions can form not only as terminally unsaturated species but also as bi-radical fragments.

3.3. Experimental

The fatty acids, octadecanoic (stearic) $C_{18:0}$ (>99%), cis-9-octadecenoic (oleic) $C_{18:1}$ (99%), cis-13-docosenoic (erucic) $C_{22:1}$ (≥99%), trans - 13-docosenoic (brassidic) $C_{22:1}$ (99%), and 10-undecenoic $C_{11:1}$ (98%), and the compounds, triethanolamine (TEA) (≥99%), diethanolamine(DEA) (≥98%), nitrobenzyl alcohol (NBA) (98%), and glycerol (>99.5%) were purchased from Sigma-Aldrich chemical company (St. Louis, MO) and used as received.

All the experiments were performed on a JEOL 600H mass spectrometer equipped with a FAB source. The energy of the Xe atoms was 4 keV, and the Xe flux was equivalent to 5 mA. TEA, DEA, NBA, and glycerol were used as matrices. Small amounts of fatty acid samples were mixed with matrix on the tip of the stainless steel FAB-probe. The ion accelerating voltage was 3kV. The temperature of the ionization

chamber was maintained below 50 °C. Negative ion (NI) spectra of ions produced by unimolecular decompositions in the ion source were recorded in the normal magnetic scan mode. Product-ion spectra of ions originating in the first field free region (FFR) located between the ion source and the electric sector, whether by metastable decomposition or CID, were recorded by linked scanning[15] with *B/E* held constant, and neutral losses spectra were recorded by linked scanning[15] with $(B/E)\cdot\sqrt{1-E}$ held constant. Helium was used as collision gas, and the pressure of the helium was adjusted until the intensity of the precursor ion signal was reduced by 50%.

3.4. Results

3.4.1. FAB of fatty acids in the negative ion mode, magnet scanning

The NI FAB spectrum of stearic acid (Fig.1a), a typical representative of saturated long-chain hydrocarbon compounds, closely resembles a standard CID spectrum (Fig.1b) except for the presence of three peaks in the former (marked with asterisks) that originate from the matrix. The intensities of the CRF ions in both spectra are about the same and are generally equal to 1% of the precursor ion intensity, which is the normal efficiency for CID of carboxylate-anions.[16] Oleic $C_{18:1}$ and erucic $C_{22:1}$ acids, representatives of monounsaturated compounds, yield spectra (Fig.2) that are practically the same as those produced by standard CID[16,17] and, therefore, allow the positions of double bonds to be easily determined. The same CRF patterns were observed for all matrices used without noticeable effect on CRF efficiency.

3.4.2. FAB of fatty acids in the negative ion mode, *B/E*-linked scanning (product ion spectra).

The spectrum of the decomposition products of the metastable ion $[M\text{-}H]^-$ for stearic acid in the first FFR (Fig.1c) consists of a full set of CRF-ion peaks and differs from its CID counterpart (Fig.1b) by a shift in the envelope maximum to a higher mass range, in accordance with the amount of internal energy deposited. Downstream in the second FFR (between the electric and magnetic sectors), no ion peaks corresponding to metastable ion decomposition were observed, neither with (Fig.1b) nor without (Fig. 1c) collisional activation in the first FFR.

The fact that free fatty acids experience CRF reactions in the ion source makes it possible to investigate the structure of CRF ions with a double-sector instrument using *B/E*-linked scanning. The CID mass spectrum of the stearic acid fragment ion *m/z* 183 (Fig. 3a) and that of the $[M\text{-}H]^-$ of 10-hendecenoic acid (Fig.3b), which is terminally unsaturated counterpart of stearic acid's CRF ion *m/z* 183, clearly show different fragmentation patterns. Both spectra contain numerous CRF-ion peaks, but only the spectrum of 10-hendecenoic acid has a gap between precursor and *m/z* 141; this gap is known from previously reported results to be characteristic of a terminal double bond.[18] By contrast, no double–bond gap can be seen in the spectra of stearic acid's CRF *m/z*-183 ion (Fig. 3a and 3c), instead peaks corresponding to $[M_P\text{-}CH_2]^-$ and $[M_P\text{-}C_2H_4]^-$ at *m/z* 169 and 155 respectively are distinctly present where the gap would be if this structure terminated in a double bond.

Spectra obtained from the metastable ion decomposition of stearic acid's *m/z*-183 fragment (Fig. 3c) and of $[M-H]^-$ of 10-hendecenoic acid's exhibit the same fragmentation patterns seen in the CID spectrum. Specifically, the latter spectrum (not shown because it is identical to the CID spectrum) has the same gap as seen in its CID spectrum (Fig. 3b). The spectrum of metastable ion decomposition of stearic acid's fragment ion at *m/z* 183 again consists of a full set of CRF ions including ones with *m/z* 155 and 169 (Fig.3c). In comparison with the CID spectrum, the relative abundances of the ions at *m/z* 155 and 169 are much higher in the metastable ion spectrum. This difference in intensity distribution of CRF ions between CID and metastable ion spectra was further studied by varying the collision gas pressure. The abundances of these particular ions gradually decrease with pressure and ultimately disappear at a pressure that suppresses 90% of the precursor ion signal. The same patterns, namely the presence of peaks that should be absent were the terminal double bond present, were observed for different CRF ions for all the fatty acids studied (see the appendix).

In order to rule out the possibility that the linked scan mode might not be sensitive to the presence of double bonds in CRF fragment ions, a CRF fragment ion of brassidic acid with *m/z* 279 was selected as a precursor ion, and its CID spectrum was recorded (Fig. 4). There is clearly a gap between the peaks at *m/z* 183 and 237 corresponding to the native double bond at the C-13 position, but there is no gap

corresponding to a terminal double bond. Signals at *m/z* 265 and 255, corresponding respectively to $[M_P\text{-}CH_2]^-$ and $[M_P\text{-}C_2H_4]^-$, are both clearly present.

3.4.3. FAB-MS of fatty acids in negative ion mode, (*B/E*)• $\sqrt{1-E}$ -linked scanning (neutral loss).

Spectra due to neutral losses in the first FFR were recorded to follow metastable ion decay and collision induced decomposition. No significant difference in the pattern of peaks was observed between the spectra obtained with and without collision gas, but adding gas did result in higher dissociation efficiency and better *S/N*. The mass window created by the JEOL 600H in a (*B/E*)• $\sqrt{1-E}$ -linked scan mode extends broadly (up to ±5 Th in separate tests) about the selected neutral loss rather than narrowly as it would in a true tandem mass spectrometer. The results are a series of spectra similar to those shown in Figure 5. The CID spectra for neutral losses of 14 and 42 Th from stearic acid, in addition to a series of CRF ion peaks corresponding to losses from the termini of the precursor CRF ions, contain the ions formed by elimination of the terminal units 16 and 44 Th from the precursor $[M\text{-}H]^-$. The mass assignments in these spectra were confirmed by increased absolute and relative intensities of these signals in the spectra of losses of 16 and 44 Th.[19] The appearance of these series of ions is further evidence that CRF anions of fatty acids are unstable structures that dissociate into second generation CRF ions.

3.5. Discussion

Although FAB is a soft ionization technique that provides information mainly about molecular mass, there are many instances in which FAB spectra exhibit structurally significant metastable ion fragmentation. The observations of CRF reactions under FAB conditions cited in the Introduction[3b, c, h, 7, 8] are excellent cases in point. The present finding that anions of fatty acids produced by FAB undergo extensive CRF would appear to be just one more such example were it not for the fact that it was demonstrated several years ago that CRF[1,6b] and metastable ion decomposition[20] of carboxylate anions does not occur under FAB conditions – the latter studies were conducted on a Kratos mass spectrometer. At least one other situation of this sort exists in the literature – in an earlier study of alkyl-trimethylammonium halides using a Kratos instrument,[21] no CRF ions were observed, but in a later study using a ZAB-2F instrument,[7] CRF ions of the same compounds were found. Unfortunately, the disparity in such instances cannot be readily resolved by experimental means. In a Kratos source, such as was used in the earlier studies in question, the axis of the atom-gun is perpendicular to the direction of ion extraction, whereas in the JEOL source used in the present study, the atom-gun's axis is at an angle of ~75^{o} relative to the direction of ion extraction. Experimentally, it would be impractical to determine whether this difference of 15^{o} in incidence has a significant effect on CRF reactions of carboxylate-anions by changing the FAB gun's position because the JEOL's ion source is rigidly constructed and its use is shared. Regardless of the reason for the disparity, the unexpected phenomenon found in the present study that carboxylate anions undergo extensive metastable ion decomposition helps to

explain discrepancies between data reported by different laboratories and also makes the determination of CRF kinetics of FAB formed ions tricky.

The results of the present study provide both indirect and direct evidence that CRF produces, in addition to terminally unsaturated species, radical fragment ions. The spontaneous decomposition of CRF ions in the first FFR of the mass spectrometer provides the indirect evidence in favor of radical fragment ions. If the CRF ions were unsaturated at the termini of the carboxylate-anions, they would require extra excitation energy for decomposition; however, the spectra of metastable ion decomposition (Fig. 3c) and neutral losses (Fig. 5) clearly show that CRF ions are not stable species. These spectra indicate a chain of events in which metastable radical ions, resulting from CRF ions formed by FAB, are in turn stabilized by subsequent decomposition into second generation, stable carboxylate-anions. Though the formation of the second-generation CRF ions is of itself a relatively minor process, the effect integrated over all fragments produced by long chain molecules can be considerable in terms of data interpretation. The presence of peaks corresponding to $[M_p\text{-}CH_2]^-$ and $[M_p\text{-}C_2H_4]^-$ in the CID (Fig. 3a) and metastable (Fig. 3c) spectra of CRF ions is direct evidence for a radical structure. If the product ions of CRF terminated in double bonds, their CID and metastable spectra should exhibit characteristic double-bond gaps as does the CID spectrum of $[M\text{-}H]^-$ of 10-undecenoic acid (Fig. 3b). The formation of terminally unsaturated ions by the 1,4-elimination of H_2 and neutral alkenes was validated by Adams and Gross with the results they obtained from a study of lithiated fatty acids.[18] In that work, the MS/MS spectra of

pairs of ions with *m/z* 141, of which one was a fragment of lithiated 10-undecenoic acid and the other was its terminally unsaturated counterpart $[M+2Li-H]^+$ of 6-heptenoic acid, were compared and found identical. The CRF precursor ion in that comparison was so short, however, that it must be regarded as a special case that does not necessarily rule out the formation of radical CRF ions. In a study by Dua et al., it was clearly demonstrated that the short CRF ions are special cases.[22] By systematically analyzing nona-8-enoic acid with deuterium and carbon-13 labeling, those investigators showed that the fragment ion with *m/z* 113, which can be formally assigned to terminally unsaturated CRF ions as $CH_2=CH(CH_2)_3CO_2^-$ hex-1-enoic carboxylate anion, is in fact the cyclopentyl carboxylate anion. In the study by Adams and Gross, the lithiated CRF ion with *m/z* 141, which corresponds to *m/z* 127 for the nonlithiated fatty acid carboxylate anion, only has seven carbon atoms in its chain, i.e. it is even shorter than the structure analyzed by Dua et al. If formation of radical ions is initiated through random elimination of a H-atom from the chain, there can be no other fragment ions except those that were observed by Adams and Gross.[17] Hence, the use of a short precursor ion by Adams and Gross demonstrated formation of the terminal unsaturated ion, but did not rule out formation of radical fragment ions. In the present study, starting from the next CRF ion of *m/z* 141, peaks corresponding to $[M_p - CH_2]^-$ and $[M_p - C_2H_4]^-$ are always present.

Radical mechanisms have been proposed by Wysocki and Ross[23] and extensively studied later by Claeys.[24] The evidence found in the present work that the CRF ions do not lead exclusively to terminally unsaturated carboxylate anions clearly

supports a radical mechanism with hydrogen atom elimination along the carbon chain, very likely with the same probability distribution as the one that takes place under REC conditions.[11, 25] Similar evidence for a radical mechanism was obtained by Wysocki and Ross,[23, 26] who found that a series of second generation fragment ions corresponding to the loss of C_nH_{2n} was produced when CRF ions with *m/z* 218 and 219 generated from protonated 2-pentadecylpyridine by collisions with Ar were allowed to collide with Xe target gas. In the present case, the second generation CRF ions are observed without collisional activation; this is the result of both different compound type and different experimental approach. Specifically in the latter case, the primary CRF ions were formed in source and, therefore, required about one tenth of the time to arrive in the first FFR that those CRF ions formed in the first FFR required to arrive in the second FFR.[27] As a result, not only terminally unsaturated but also radical CRF ions arrive in the first FFR. Hence both the CID and spontaneous decomposition spectra recorded consist of $[M_p\text{-}CH_2]^-$ and $[M_p\text{-}C_2H_4]^-$ ions. The fact that metastable ion decomposition is observed in the first FFR and not at all in second FFR shows how critically CRF reactions depend on instrumental time scale.

3.6. Conclusion

It is found that fatty acid carboxylate anions experience CRF reactions under regular FAB conditions, without collisional activation. The efficiency of CRF is sufficiently high to allow analysis of the resulting $[M\text{-}H_2\text{-}(CH_2)_n]^-$ fragments by linked scanning in conjunction with CID and metastable ion decomposition.

Results obtained in the present work clearly indicate that CRF of fatty acid anions must involve formation of radical anions in addition to terminally unsaturated fragment ions, i.e. those having stable carboxylate anion structures. The latter are unique in the sense that they are the last to be formed in the decomposition process. If radical ions are formed, they further stabilized by decomposition to the second generation CRF ions, which in their turn, can be radical ions and decompose to the third generation and so on until stable carboxylate anions are finally produced. Distinguishing between the first and subsequent generations of CRF ions in CID spectra is not a trivial task, because all have the same mass and eventually the same structure. Additional experiments with different standards, including deuterium labeled compounds, need to be performed in order to clarify the mechanism of CRF reactions.

3.7. Acknowledgement

The research reported in this paper was supported directly by a grant from the W.M. Keck Foundation and indirectly by an Environmental Health Sciences Center Grant (ES00210) from the National Institute of Environmental Health Science.

3.8. References

1. Tomer, K. B.; Crow, F. W.; Gross, M.L. *J. Am .Chem. Soc.* **1983,** *105*, 5487.

2. M.Bambagiotti A., M.; Coran, S. A.; Giannellini, V.; Vincieri, F. F.; Daolio, S.; P.Traldi *Org. Mass Spectrom.* **1983,** *18*, 133.

3. (a) Bowie, J. H. *Int. J. Mass Spectrom. And Ion Phys.* **2001**, *212*, 249. (b) Seto, C.; Grossert, J. S.; Waddle, D.S.; Curtis, J.M.; Boyd, R.K. *Int. J. Mass Spectrom. And Ion Phys.* **1999**, *188*, 27. (c) Seto, C.; Grossert, J.S.; Waddle, D.S.; Curtis, J.M.; Boyd, R.K. *J. Am. Soc. Mass Spectrom.* **2001**, *12*, 571. (d) Contado, M.J.; Adams, J.; Jensen, N.J.; Gross, M.L. *J. Am. Soc. Mass Spectrom.* **1991**, *2*, 180. (e) Jensen, N.J.; Tomer, K.B.; Gross, M.L. *J. Am .Chem. Soc.* **1985**, *107*, 1863. (f) Huysmans, L.; Nizigiyimana, L.; Van den Heuvel, H.; Claeys, M. *Int. J. Mass Spectrom.*, **1999**, *188*, 39. (g) Denekamp, C.; Van den Heuvel, H.; Voinov, V.G.; Claeys, M.; Seto, C.; Grossert, J.S.; Waddell, D.S.; Curtis, J.M.; Boyd, R.K. *Rapid Commun. Mass Spectrom.* **2000**, *14*, 1035. (h) Bambagiotti-Alberti, M.; Coran, S.A.; Benvenuti, F.; LoNosto, P.; Catinella, S.; Favretto, D.; Traldi, P. *J. Mass Spectrom.* **1995**, *30*, 1742.

4. Griffiths, W.J.; Brown, A.; Reimendal, R.; Yang, Y.; Zhang, J.; Sjövall, J. *Rapid Commun. Mass Spectrom.*, **1996**,*10*, 1169.

5. Siegel, M.M.; Colthup, N.B. *Appl. Specrosc.* **1988**, *42*, 1214.

6. (a) Cheng, C.; Gross, M.L. *Mass Spectrom. Rev.* **2000**, *19*, 398. (b) Gross, M.L. *Int. J. Mass Spectrom.* **2000**, *200*, 611.

7. Bambagiotti-Alberti, M.; Coran, S.; Giannellini, V.; Favretto, D.; Traldi, P. *Rapid Commun. Mass Spectrom.* **1994**, *8*, 439.

8. Laprévote, O.; Girard, C.; Das, B.; Laugel, T.; Roblot, F.; Leboeuf, M.; Cavé, A. *Rapid Commun. Mass Spectrom.* **1992**, *6*, 352.

9. Griffiths, W.J.; Yang, Y.; Lindgren, J.Å.; Sjövall, J. *Rapid Commun. Mass Spectrom*. **1996**, *10*, 21.

10. Bambagiotti-Alberti, M.; Coran, S.; Vincieri, F.F.; Petrucciani, T.; Traldi, P. *Org. Mass Spectrom.* **1986**, *21*, 485.

11. Voinov, V.G.; Claeys, M. *Int. J. Mass Spectrom.* **2000**, *198*, 23.

12. Stapel, D.; Brox, O.; Benninghoven, A. *Applied Surface Science* **1999**, *140*, 156.

13. Shiea, J.; Sunner, J. *Int. J. Mass Spectrom. And Ion Phys.* **1991**, *109*, 265.

14. In a recent review, a new "charge-assisted" mechanism is suggested that leads to terminally unsaturated CRF ions with resonance stabilized structures [Harvey, D.J. *J. Am. Soc. Mass Spectrom.* **2005,** *16*, 280].

15. Boyd, R.K. *Mass Spectrom. Rev.* **1994**, *13*, 359 and references wherein.

16. Jensen, N.J.; Tomer, K.B.; Gross, M.L. *Anal. Chem.* **1985**, *57*, 2018.

17. Voinov, V.G.; Claeys, M. *Int. J. Mass Spectrom.* **2001**, *205*, 57.

18. Adams, J.; Gross, M.L. *J. Am .Chem. Soc.* **1989**, *111*, 435.

19. Haddon, W.F. *Org. Mass Spectrom.***1980**, *15*, 539-543.

20. Adams, J.; Gross, M.L. *J. Am .Chem. Soc.* **1986**, *108*, 6915.

21. Lyon, P.A.; Crow, F.W.; Tomer, K.B.; Gross, M.L. *Anal. Chem.* **1984**, *56*, 2278.

22. Dua, S.; Bowie, J.H.; Cerda, B.A.; Wesdemiotis, C.; Raftery, M.J.; Kelly, J.F.; Taylor, M.S.; Blanksby, S.J.; Buntine, M.A. *J. Chem. Soc. Perkin Trans.2*, **1997**, *4*, 695.

23. Wysocki, V.H.; and Ross, M.M. *Int. J. Mass Spectrom. And Ion Phys.* **1991**, *104*, 179.

24. (a) Clayes, M.; Nizigiyimana, L.; Van den Heuvel, H.; Derrick, P.J. *Rapid Commun. Mas Spectrom.* **1996**, *10*, 770. (b) Nizigiyimana, L.; Rajan, P.K.; Haemers, A.; Claeys, M.; Derrick, P.J. *Rapid Commun. Mas Spectrom.* **1997**, *11*, 1808. (c) Clayes, M.; Nizigiyimana, L; Van den Heuvel, H.; Vedernikova, I.; Haemers, A. *J. Mass Spectrom*. **1998**, *33*, 631. (d) Huysmans, L.; Nizigiyimana, L.; Van den Heuvel, H.; Claeys, M. *Int. J. Mass Spectrom*. **1999**, *188*, 39.

25. Voinov, V.G.; Van den Heuvel, H.; Claeys, M. *J. of Mass Spectrom.* **2002**, *37*, 313.

26. Wysocki, V.H.; Ross, M.M.; Horning, S.R.; Cooks, R.G. *Rapid Commun. Mass Spectrom.* **1988**, *2*, 214.

27. Holmes, J.L. *Org. Mass Spectrom.***1985**, *20*, 169.

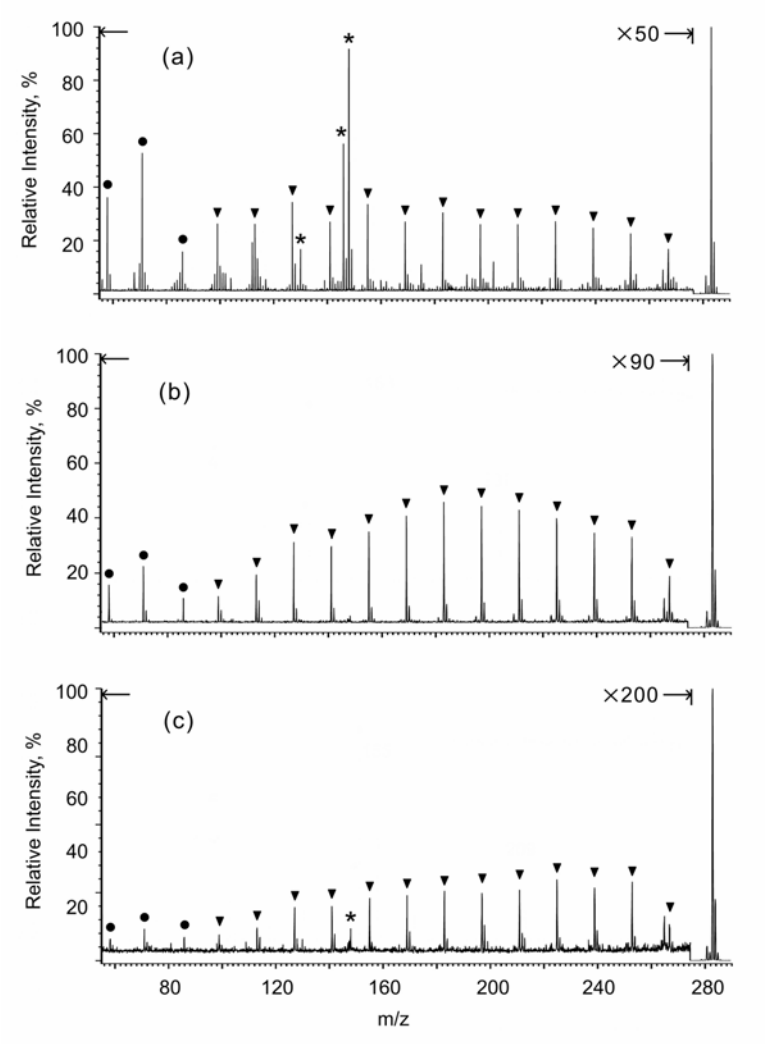

Figure 3.1 NI FAB mass spectrum of stearic acid (**a**); NI FAB-CID product spectrum of $[M-H]^-$ ion of stearic acid (**b**); and NI FAB mass spectrum of metastable ion decomposition of $[M-H]^-$ ion of stearic acid (**c**). TEA was used as matrix. The peaks marked with asterisks are originated from matrix. The peaks marked with triangles are CRF ions.

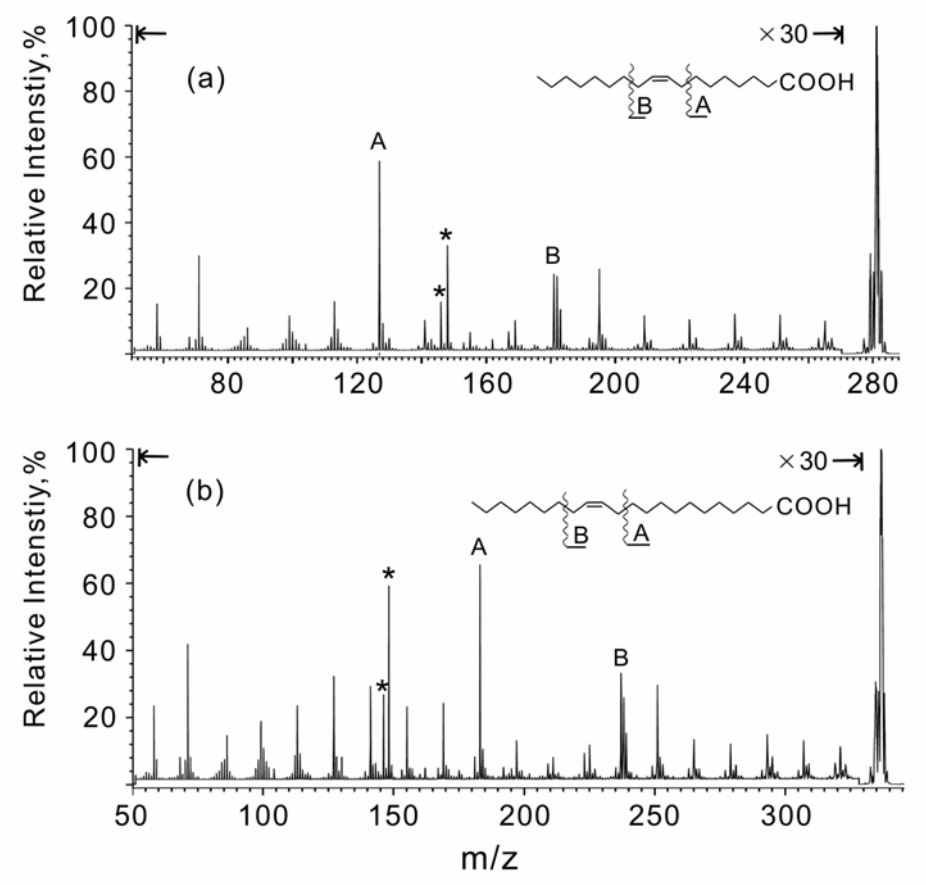

Figure 3.2 NI FAB mass spectra of oleic acid (**a**); and erucic acid (**b**). TEA was used as matrix. The peaks marked with asterisk are originated from matrix.

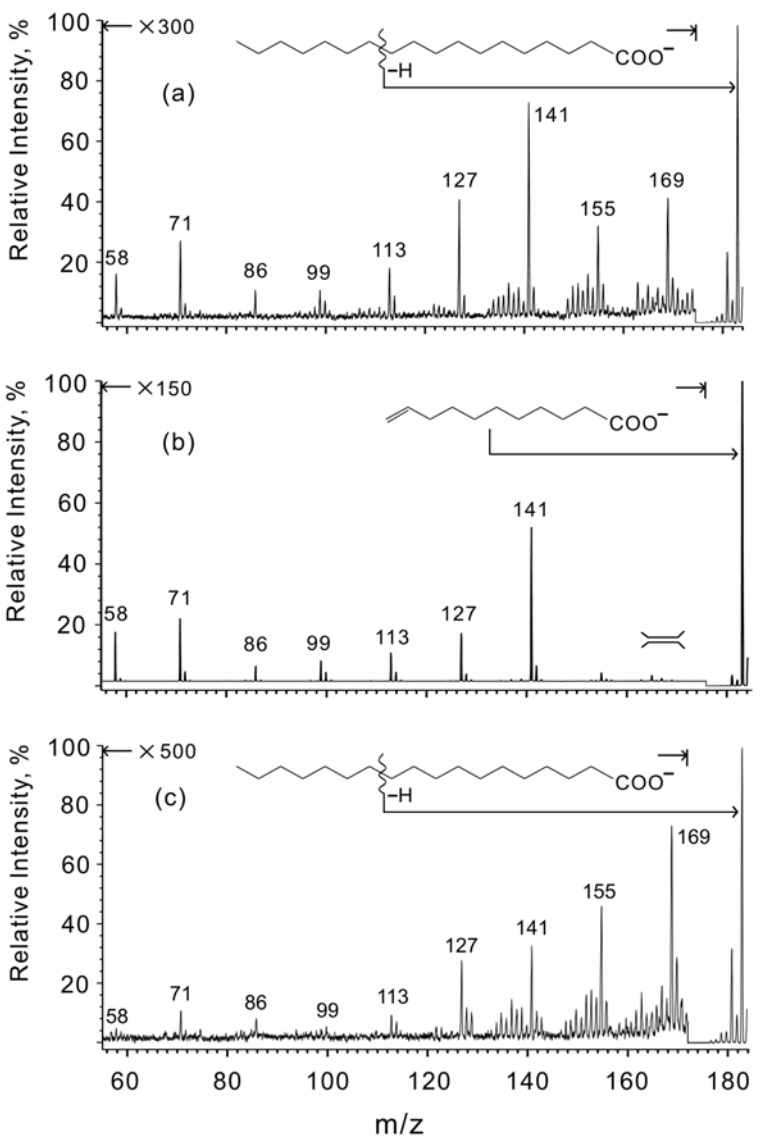

Figure 3.3 Linked scan CID (**a**) and metastable ion decomposition (**c**) spectra of CRF fragment ion at *m/z* 183 of the stearic acid and linked scan CID mass spectrum of $[M-H]^-$ ion of 10-undecenoic acid (**b**). DEA was used as matrix. Symbol for double bond is shown at location where fragment ion formed by cleavage at double bond would be seen.

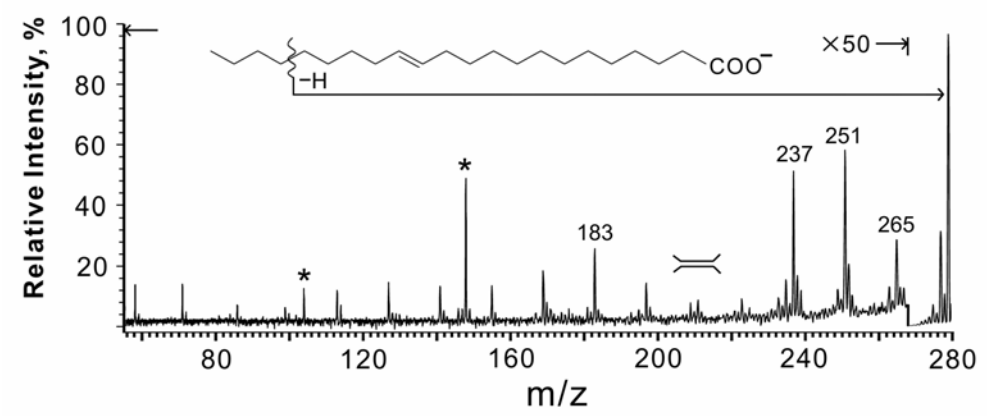

Figure 3.4 Linked scan CID MS/MS spectrum of CRF fragment ion at *m/z* 279 of brassidic acid. DEA was used as matrix. The peaks marked with asterisk are originated from matrix. Symbol for double bond is shown at location where fragment ion formed by cleavage at double bond would be seen.

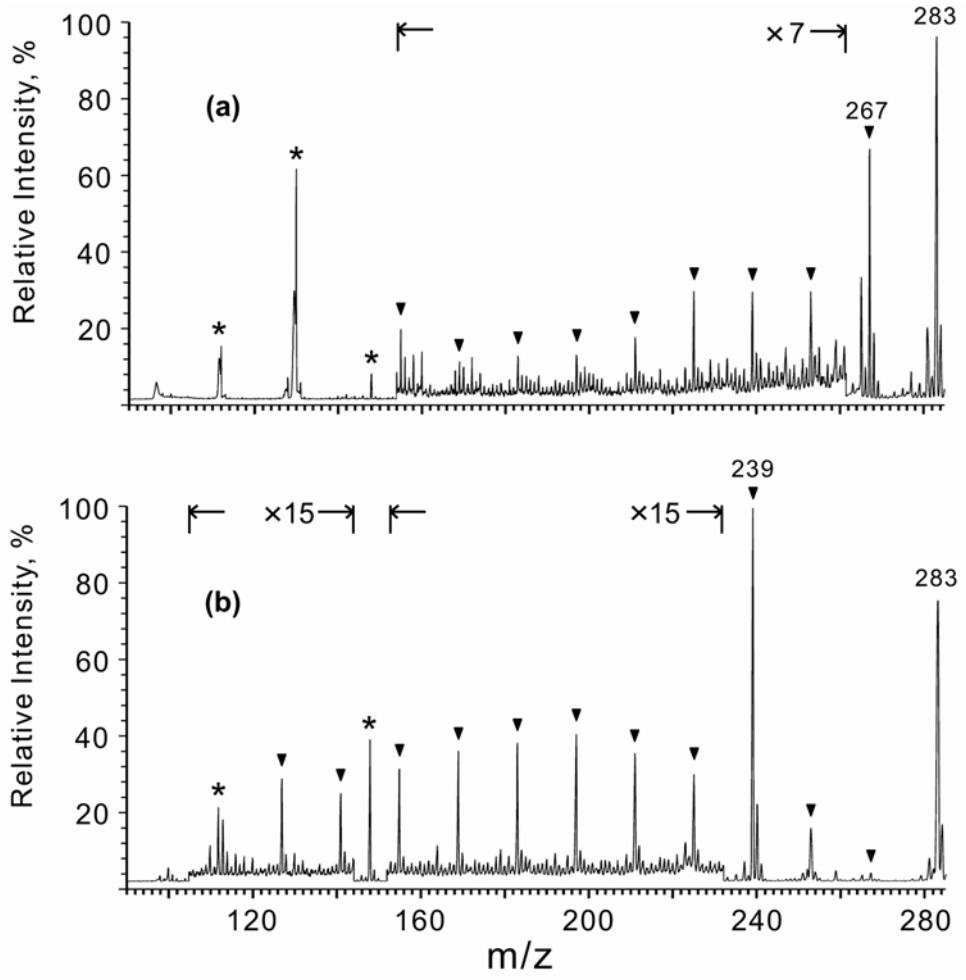

Figure 3.5 Constant neutral loss linked scan CID spectra of stearic acid for m_n = 16 (**a**) and 44 (**b**). TEA was used as matrix. The peaks marked with asterisk are originated from matrix.

4. Distinguishing between *cis*-/*trans*- Isomers of Monounsaturated Fatty Acids by FAB MS

Hong Ji,[𝄞] Valery G. Voinov, [𝄞,♪] Max L. Deinzer, [𝄞] Doug F. Barofsky[𝄞,*]

[𝄞] *Department of Chemistry, Oregon State University, Corvallis, Oregon 97331*

[♪] *Pacific Institute of Bioorganic Chemistry, Vladivostok, 690022, Russia*

Analytical Chemistry, **2007,** *79,* 1519.
American Chemical Society
Columbus, OH 43210, USA

* Corresponding author, email: doug.barofsky@oregonstate.edu, fax: 541-737-2062

4. Charge-Remote Metastable Ion Decomposition of Free Fatty Acids under FAB MS: Evidence for bi-Radical Ion Structures

4.1. Abstract

Fast-atom bombardment (FAB) mass spectrometry in the negative ion mode can be used to unambiguously distinguish between *cis*- and *trans*- isomers of monounsaturated fatty acids by the relative signal strengths of an intense doublet. Under normal FAB ionization/desorption conditions, the deprotonated molecules $[M-H]^-$ of six fatty acids underwent charge remote fragmentation (CRF). A characteristic fragmentation pattern of two intense peak-clusters with three weak intervening peak-clusters are used in each case to identify the position of the double bond. The possibility of resonance electron capture (REC) occurring during the FAB process is discussed.

4.2. Introduction

Owing to their biological importance, the identification and structural determination of unsaturated fatty acids have attracted attention for decades. Early mass spectrometric efforts using electron impact or chemical ionization, either in the positive or negative ion mode, failed to provide useful structural information. Both of these ionization techniques required derivatization of the fatty acids prior to analysis; thus, the structural information obtained from these studies was indirect.

Tomer *et al.* were the first to apply negative fast atom bombardment (FAB) MS/MS to the structural determination of unsaturated fatty acids.[1] In this seminal study, they demonstrated that structural information could be obtained from the intensity distribution of a series of product ions induced by charge remote fragmentation (CRF) of the deprotonated ion $[M\text{-}H]^-$ (for reviews, see [2, 3]). Specifically, the position of a double bond in an unsaturated fatty acid is indicated by a characteristic pattern of two intense peaks, corresponding to cleavage of an allylic bond, and three very much lower intensity peaks in the mass spectrum.[1]

In spite of being able to locate the position of double bonds in unsaturated fatty acids, use of mass spectrometry (MS) to distinguish *cis*- and *trans*- isomers of these compounds has remained challenging and thus little used. To date, relatively little effort has been directed towards improving the utility of the method. Jensen *et al.* [4], using FAB ionization/desorption coupled in conjunction with high energy collision-

induced dissociation (CID) on a four sector mass spectrometer, found that *cis*- and *trans*- isomers could be distinguished by analyzing the relative intensities of two adjacent peaks resulting from cleavage of the allylic bond on the side distal to the double bond. Unfortunately due most likely to the four sector's relatively rapid obsolescence, work on distinguishing *cis/trans* geometric isomers was not pursued further, and its principle finding was largely forgotten. In a more recent study on unsaturated fatty acids using resonance electron capture (REC) at 7.2 eV electron energy, Voinov and Claeys [5] reported an ion peak that is formed by a radical-induced fragmentation that shows different abundances for *cis*- and *trans*- isomers. In principle, this diagnostic ion peak could be used as an indicator of unsaturated fatty acid geometric isomerism; however, the requirement for controlling the electron energy seems thus far to have hindered general application of this method.

CRF of fatty acid carboxylate anions on a commercial double sector (E/B) mass spectrometer operated under normal FAB conditions has recently been observed.[6] In the present study, it is shown how this phenomenon can be exploited to produce spectra under normal FAB conditions that can be used for locating the double bond position and for differentiating between geometric isomers of long-chain monounsaturated fatty acids.

4.3. Experimental

The fatty acids, *cis*-9-octadecenoic acid (oleic acid, > 99%), *trans*-9-octadecenoic acid (elaidic acid, > 99%), *cis*-11-octadecenoic acid (*cis*-vaccenic acid, ≥ 97%), *trans*-11-octadecenoic acid (trans-vaccenic acid, > 99%), *cis*-13-docosenoic acid (erucic acid, ≥ 99%), *trans*-13-docosenoic acid (brassidic acid, > 98%) and triethanolamine (≥ 99%) were purchased from Sigma-Aldrich chemical company (St. Louis, MO) and used without further purification.

The FAB spectra were obtained with a JEOL MS Route JMS 600H mass spectrometer. Triethanolamine was used as matrix. A small amount of fatty acid sample was mixed with matrix on the stainless steel tip of the FAB probe before being introduced into the ionization chamber. Xe atoms were used as primary particles; their energy was 4 keV, and their flux-equivalent was 5 mA. The secondary ions were accelerated to 3 keV. The temperature of the ionization chamber was kept below 50 °C. The magnetic sector was scanned at 5 s/decade, and each spectrum comprised 5 to 10 scans averaged together. Matrix background was subtracted before assessing the relative intensities of peaks for diagnostic purposes.

4.4. Results and discussion

Structural analysis of unsaturated fatty acids by mass spectrometry was first attempted on a three-sector instrument using CID.[1] The resolving power (ca 100-200) of this instrument was insufficient to distinguish the product-ion peaks within the cluster that located the position of the double bond. A doublet peak that made it

possible to distinguish the geometrical isomers of unsaturated fatty acids was later observed on a four-sector mass spectrometer [4], but this form of instrument disappeared quickly when more practical configurations for MS/MS analyses became available in the early nineteen nineties, and the potentially useful analytical approach for *cis/trans* isomerism was neglected and soon forgotten.

In a previous study, CRF of fatty acids was observed under regular negative FAB operating conditions [6]. This discovery makes it possible in principle to conduct structural analysis of long-chain compounds with good sensitivity and resolution on a commercial, double-focusing, E/B-sector instrument. The resolving power of the instrument used in the present study was set at 700, which was more than sufficient to distinguish peak-clusters in the mass spectra of the monounsaturated fatty acids (M_r < 500) while maintaining high sensitivity. Fragment-ion peaks were readily apparent in the mass spectra even without averaging (spectra not shown).

The dominant $[M\text{-}H]^-$ signal in each of the negative ion FAB mass spectra of the three *cis*-isomers of the monounsaturated fatty acids (Figure 1) is accompanied by a series of CRF peaks. The yield of fragment ions is 1 - 2.5 % of the corresponding $[M\text{-}H]^-$ species, depending on the compound. Within each series of fragments, a characteristic pattern, comprising two intense peak-clusters separated by three weak intervening ones, is evident. No noticeable differences in this general pattern were observed between the *cis*- and *trans*- isomers (latter spectra not shown). This observation agrees well with that of Tomer *et al.*[4], who determined that the more

massive of the two intense peak-clusters is due to cleavage of the allylic carbon-carbon bond on the -CH_3 terminal side of the chain whereas the less massive of the two clusters results from allylic cleavage on the carboxyl side of the double bond. Thus, this characteristic pattern enabled the positions of the double bonds to be readily located in all three unsaturated fatty acids analyzed. Specifically, the CRF peaks with *m/z* 127 and 181 could be used to locate the double bond position at C_9 in oleic (Figure 1a) and elaidic acids. Similarly, the peaks with *m/z* 155 and 209 for *cis*- (Figure 1b) and *trans*- vaccenic acid and with *m/z* 181 and 237 for erucic (Figure 1c) and brassidic acids indicated a double bond at C_{11} and C_{13} respectively.

Examination of the more massive of the two intense peak-clusters in the mass spectral pattern described in the preceding paragraph reveals an interesting doublet feature (Figure 2) that was first observed by Jensen *et al.*[4] in their studies with a four sector instrument. According to our latest study [6], the smaller *m/z*-peak of the doublet is due to a diradical ion (odd *m/z*) which can be attributed to a H loss followed by a loss of a C_nH_{2n+1} species. Jensen *et al.* proposed that the larger *m/z*-peak of the doublet is due to the odd-electron radical ion (even *m/z*), which may be formed by an alkyl cleavage of losing a C_nH_{2n+1} species.[4] Of particular interest here, is the fact that the relative intensity of the two peaks in the doublet differs systematically for the *cis*- and *trans*- isomers. Specifically, the mass peak with lower *m/z* in the doublet is more intense than the mass peak with the higher *m/z* for all of the *cis*- isomers (Figures 2a, c, and e). By contrast, the mass peak with lower *m/z* in the doublet is weaker than the mass peak at the higher *m/z* value for all *trans*- isomers (Figures 2b, d, and f). This

mass spectral pattern is reproducible; thus, it should be possible to use it to distinguish the *cis*- and *trans*- isomers of monounsaturated fatty acids.

A third relatively intense peak appears on the high mass side of the *cis*-/*trans*-doublet in each spectrum (Figures 2). This peak is intriguing because it was barely observable in Jensen *et al.*'s study, in which CID was used to fragment the $[M - H]^-$ precursor. One possible explanation for formation of the third ion, is that it results from a molecular radical anion through resonance electron capture (REC) during FAB. It is known that neutrals compose a major part of the sputtered material under FAB conditions [7, 8] whereas ions compose only a fraction ($\sim 10^{-6} - 10^{-1}$) of the total ejecta. In the present study, the existence of free electrons in the ion source was confirmed by loading the sample probe with matrix only, introducing chloroform through the standard sample inlet, and monitoring Cl^- ion in the negative ion FAB mode. The appearance of Cl^- in this experiment indicated that a fraction of the electrons released by FAB of the matrix matched the resonance capture energy of the chloroform that leads to the formation of Cl^-. Evidence for electron capture by oligonucleotides in the negative ion FAB mode has been reported [9], and more recently, REC by unsaturated fatty acids was observed by Voinov and Claeys [5]. At an electron energy of 7.2 eV, these investigators recorded the REC mass spectra of three pairs of monounsaturated fatty acid isomers and observed ions with *m/z* 183 for oleic acid and elaidic acid, *m/z* 211 for *cis*- and *trans*-vaccenic acid, and *m/z* 239 for erucic acid and brassidic acid that were much less abundant in the regular CID spectra of $[M - H]^-$. It was proposed that, rather than being caused by regular CRF, these ions were formed directly by an

alkyl radical loss from excited molecular anions produced by REC. Since both of these ions are presented in the corresponding FAB spectra recorded in the present study (Figures 2) and the availability of low-energy electrons for REC is established by the presence of Cl^- when chloroform was introduced into the ion source, it seems likely that the ion signal adjacent on the high *m/z*-side of the *cis*- /*trans*- doublet is due to a REC product ion. Since the resonant electron energy cannot be measured in this instance however, this argument remains speculative and further study is needed to elucidate the mechanism by which these ions are formed.

In summary, three pairs of *cis*/*trans* fatty acid isomers under regular negative ion FAB ionization/desorption conditions, showed that the $[M-H]^-$ precursors of these compounds underwent charge remote fragmentation to produce a pattern in their mass spectra comprised of two intense peak-clusters with three intervening weak ones. As previously demonstrated [1], this characteristic pattern enabled the double bond position in these compounds to be unambiguously located. The *cis*- and *trans*- isomers of the fatty acids could be readily distinguished by observing the relative intensities of a doublet feature in their mass spectra. This doublet was reported in a study by Jensen *et al.*[4], in which the double bond in all four of the monounsaturated fatty acids analyzed was located at C_9. In the presented study, the trials were extended to compounds that had double bonds at carbons 9, 11, and 13. The mass spectral differences between the *cis*- and *trans*- isomers remained the same regardless of the position of the double bond strongly suggesting that negative ion FAB mass spectra can be used to unambiguously identify the *cis/trans* isomerism of monounsaturated fatty acids.

4.5. Acknowledgements

The research reported in this paper was supported directly by a grant from the W.M. Keck Foundation and indirectly by an Environmental Health Sciences Center Grant (ES00210) from the National Institute of Environmental Health Science.

4.6. References

1 Tomer, K.B.; Crow, F.W.; Gross, M.L. *J. Am. Chem. Soc.* 1983, 105, 5487-5488.

2 Cheng, C.; Gross, M. L. *Mass Spectrom. Rev*. 2000, 19(6), 398-420.

3 Harvey, D.J. *J. Am. Soc. Mass Spectrom.* 2005, *16*, 280-290.

4 Jensen, N.; Lam, K.; Cody, R.B.; Tamura, J. *Rapid Commun. Mass Spectrom.* 1990, *4*, 239-241.

5 Voinov, V.G.; Claeys, M. *Int. J. Mass Spectrom.* 2001, *205*, 57-64.

6 Ji, H.; Voinov, V. G.; Morré, J.; Deinzer, M. L. ; Barofsky, D. F. *Anal. Chem.* 2006, submitted

7 Wong, S.S.; Rölgen, F.W.; Manz, I.; Przybylski M. *Biomed.Mass Spectrom*. 1985, 12, 43-47

8 Benninghoven, A.; Hagenhoff, B.; Niehuis E. *Anal. Chem.* 1993, 65, 630A-640A

9 Laramée, J.A.; Arbogast, B.; Deinzer, M.L. *Anal. Chem.* 1989, 61, 2154-2160

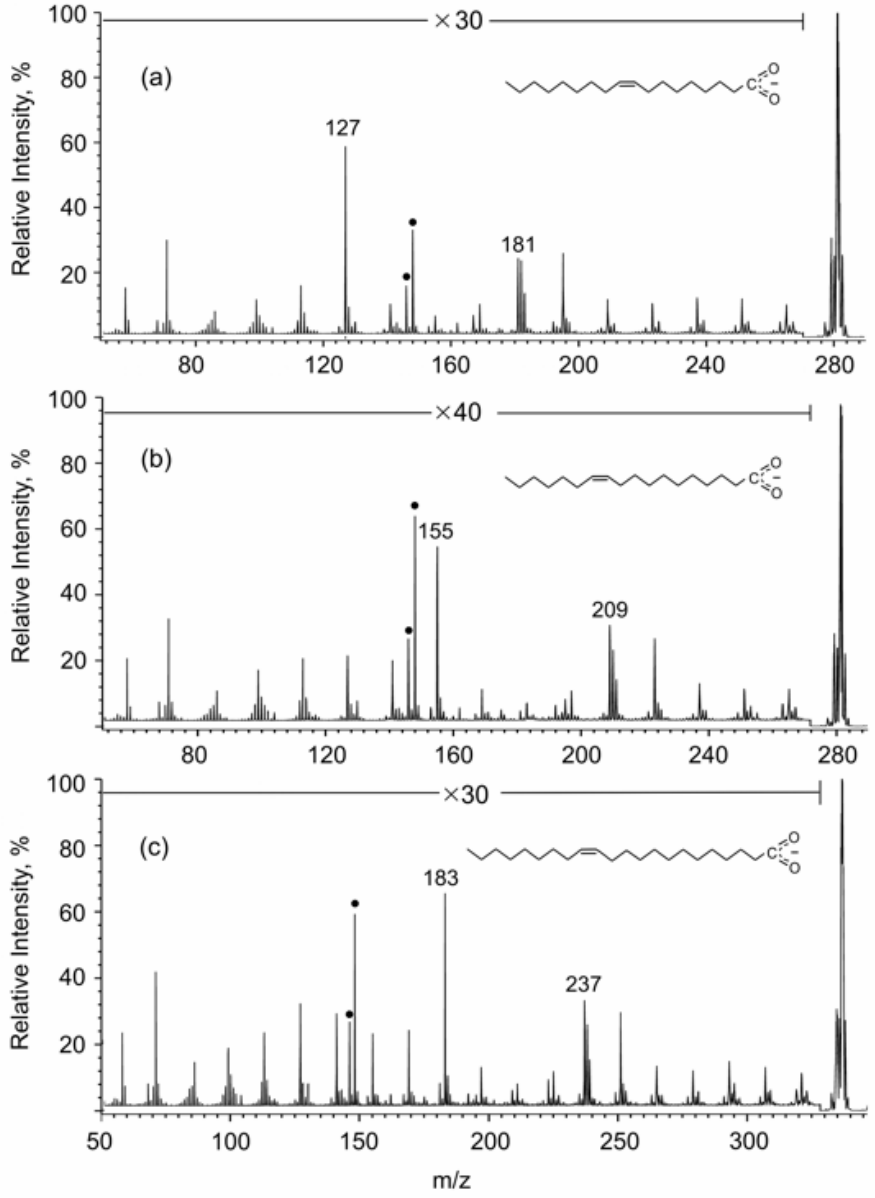

Figure 4.1 Negative ion FAB spectra of (a) oleic (*cis*-9-octadecenoic) acid, (b) *cis*-vaccenic (*cis*-11-octadecenoic) acid , and (c) erucic (*cis*-13-docosenoic) acid. Matrix peaks are marked with •.

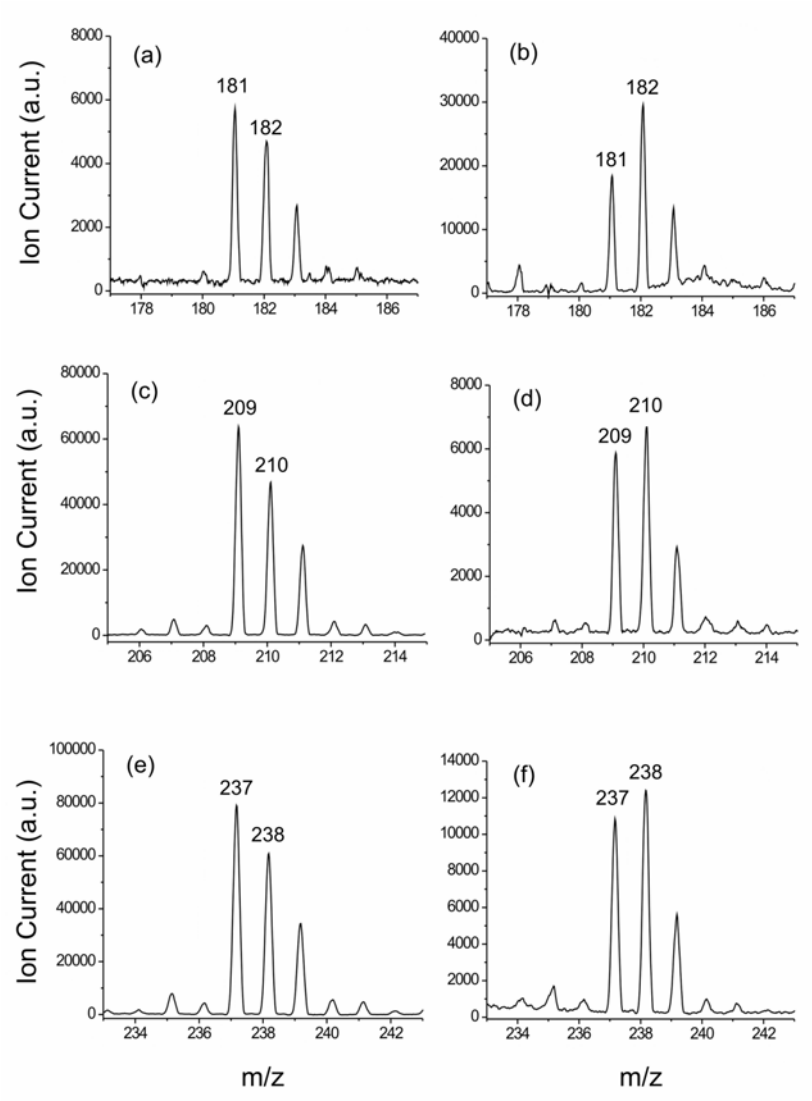

Figure 4.2 Expanded negative ion FAB spectra showing the more massive of the two intense peak-clusters associated with the double bond of (a) oleic (*cis*-9-octadecenoic) acid, (b) elaidic (*trans*-9-octadecenoic) acid, (c) *cis*-vaccenic (*cis*-11-octadecenoic) acid , (d) *trans*-vaccenic (*trans*-11-octadecenoic) acid , (e) erucic (*cis*-13-docosenoic) acid, and (f) brassidic (*trans*-13-docosenoic) acid.

5. Concluding Remarks and Future Work

5.1. Summary

In this thesis I have presented our recent results in the developing of more efficient and economical techniques for fragmenting large bio-molecules. By modifying a triple quadrupole (Q-q-Q) mass spectrometer into a quadrupole-electron capture dissociation-quadrupole (Q-ECD-Q) mass spectrometer， we proved the feasibility of achieving ECD without FTICR instrument. With the cross-flow design, we demonstrated that zero-energy electrons can be transmitted into the reaction volume of the ECD chamber in numbers sufficient to produce detectable resonance electron capture reactions while maintaining ion transmission at a high enough level to perform cross-beam experiments. With the parallel-flow design, we demonstrated that the cross section for ECD could be successfully increased by increasing both the interaction time and effective volume for interaction. Using these new techniques, ECD spectra of polypeptides neurotensin and substance P have been obtained. Comparison of the new methods with previous approaches using traps has been discussed.

In the study of charge-remote fragmentation (CRF)， our results show that the fatty acid carboxylate anions experience CRF reactions under regular FAB conditions,

without collisional activation. The efficiency of CRF is sufficiently high to allow analysis of the resulting $[M\text{-}H_2\text{-}(CH_2)_n]^-$ fragments by CID and metastable ion decomposition. The new results indicate that a multi-step radical mechanism is involved in CRF ion formation. When radical ions are formed, they further stabilized by decomposition to the second generation CRF ions, which in their turn, can be radical ions and decompose to the third generation and so on until stable terminal unsaturated carboxylate anions are finally produced. Our further investigation on three pairs of *cis*/*trans* fatty acid isomers under regular negative ion FAB ionization/desorption conditions, showed that the $[M\text{-}H]^-$ precursors of these compounds underwent charge remote fragmentation to produce a pattern in their mass spectra comprised of two intense peak-clusters with three intervening weak ones. This characteristic pattern enabled the double bond position in these compounds to be unambiguously located. The *cis*- and *trans*- isomers of the fatty acids could also be readily distinguished by observing the relative intensities of a doublet feature in their mass spectra. In the presented study, the trials were extended to compounds that had double bonds at carbons 9, 11, and 13. The mass spectral differences between the *cis*- and *trans*- isomers remained the same regardless of the position of the double bond strongly suggesting that negative ion FAB mass spectra can be used to unambiguously identify the *cis/trans* isomerism of monounsaturated fatty acids.

5.2. Future Work

To turn ECD into a high-throughput tool for applications in proteomics, further improvements, in particular increasing the magnetic field strength by about an order of magnitude (i.e. from ~ 0.05 T to ~ 0.5 T) is needed. For this purpose, we have obtained a new platform, a Q-TOF mass spectrometer from Bruker Daltonics. Preparation for new design and modification has been in its way.

In our study of CRF we have demonstrated that distinguishing between the first and subsequent generations of CRF ions in CID spectra is not a trivial task, because all have the same mass and eventually the same structure. In order to clarify the mechanism of CRF reactions additional experiments with different standards, including deuterium labeled compounds, need to be performed.

Appendix A

Structures of the fatty acids studied in the chapter 3 and 4:

Stearic Acid [Octadecanoic acid, $C_{18}H_{36}O_2$]:

Melissic Acid [Triacontanoic acid, $C_{30}H_{60}O_2$]:

Brassidic Acid [*trans*-13-Docosenoic acid, $C_{22}H_{42}O_2$]:

Erucic Acid [*cis*-13-Docosenoic acid, $C_{22}H_{42}O_2$]:

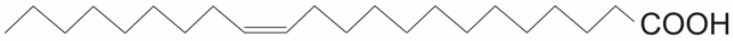

Elaidic Acid [*trans*-9-Octadecenoic acid, $C_{18}H_{34}O_2$]:

Oleic Acid [*cis*-9-Octadecenoic acid, $C_{18}H_{34}O_2$]:

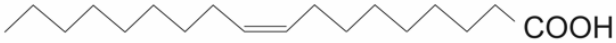

trans-Vaccenic Acid [*trans*-11-Octadecenoic acid, $C_{18}H_{34}O_2$]:

cis-Vaccenic Acid [*cis*-11-Octadecenoic acid, $C_{18}H_{34}O_2$]:

Undecenoic Acid [Undecylenic acid, $C_{11}H_{20}O_2$]:

Appendix B

1. NI FAB mass spectrum of melissic acid. DEA was used as matrix. The peaks marked with asterisks are originated from matrix. The peaks marked with triangles are CRF ions.

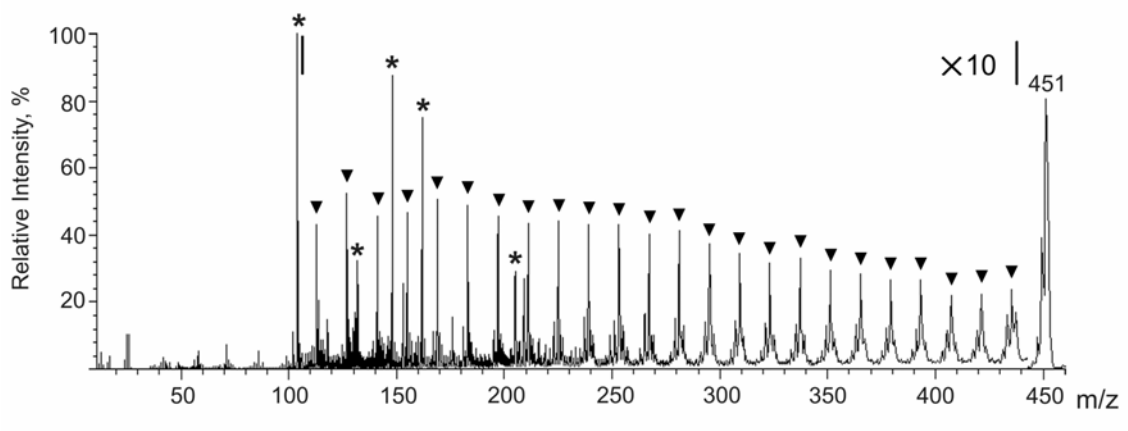

2. Linked scan metastable ion decomposition (**a**), CID with 40% parent peak suppression (**b**) CID with 70% parent peak suppression (**c**) spectra of CRF fragment ion at *m/z* 155 of the Brassidic acid. DEA was used as matrix.

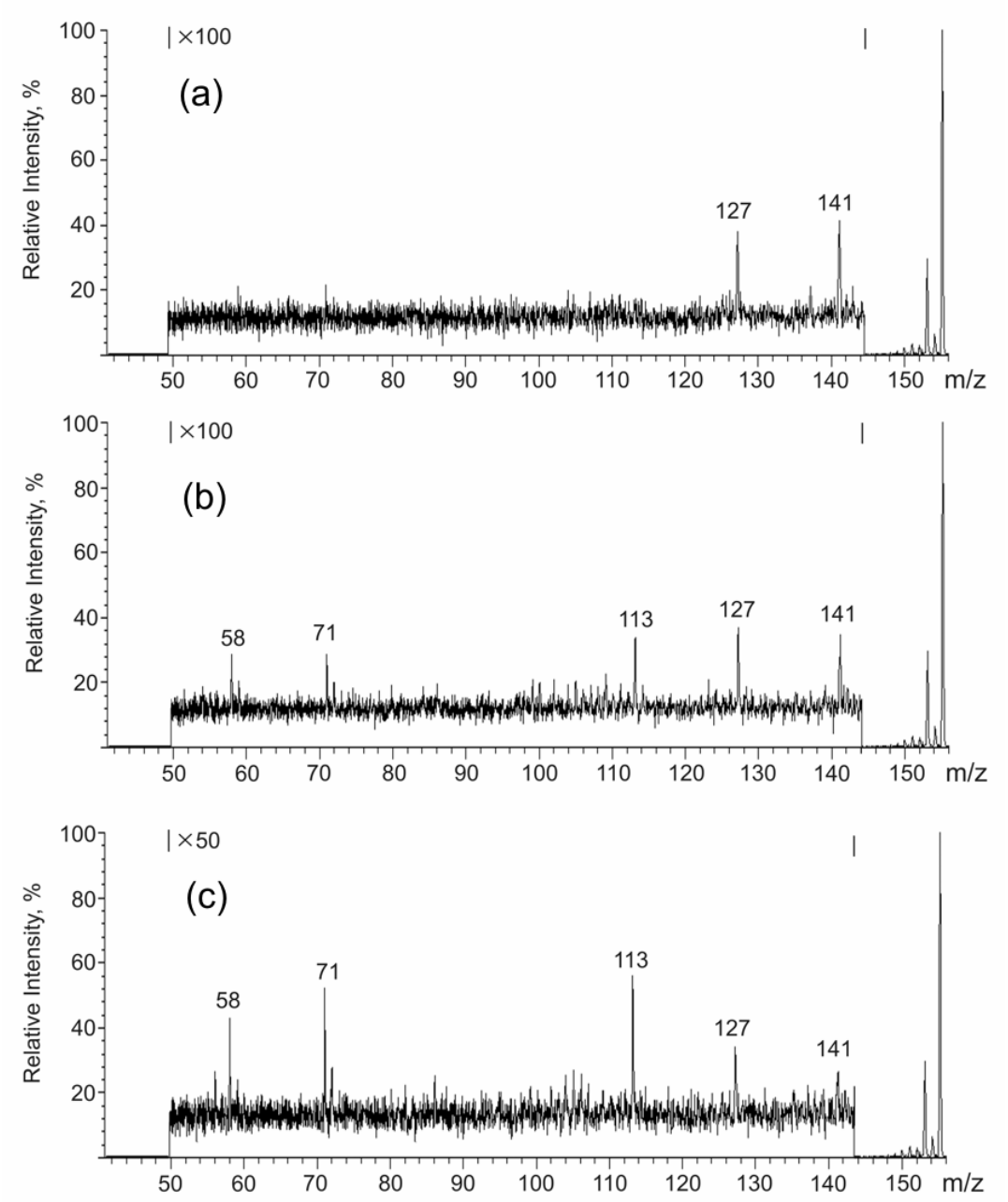

3. Linked scan metastable ion decomposition (**a**), CID with 30% parent peak suppression (**b**) CID with 50% parent peak suppression (**c**) spectra of CRF fragment ion at *m/z* 183 of the Brassidic acid. DEA was used as matrix.

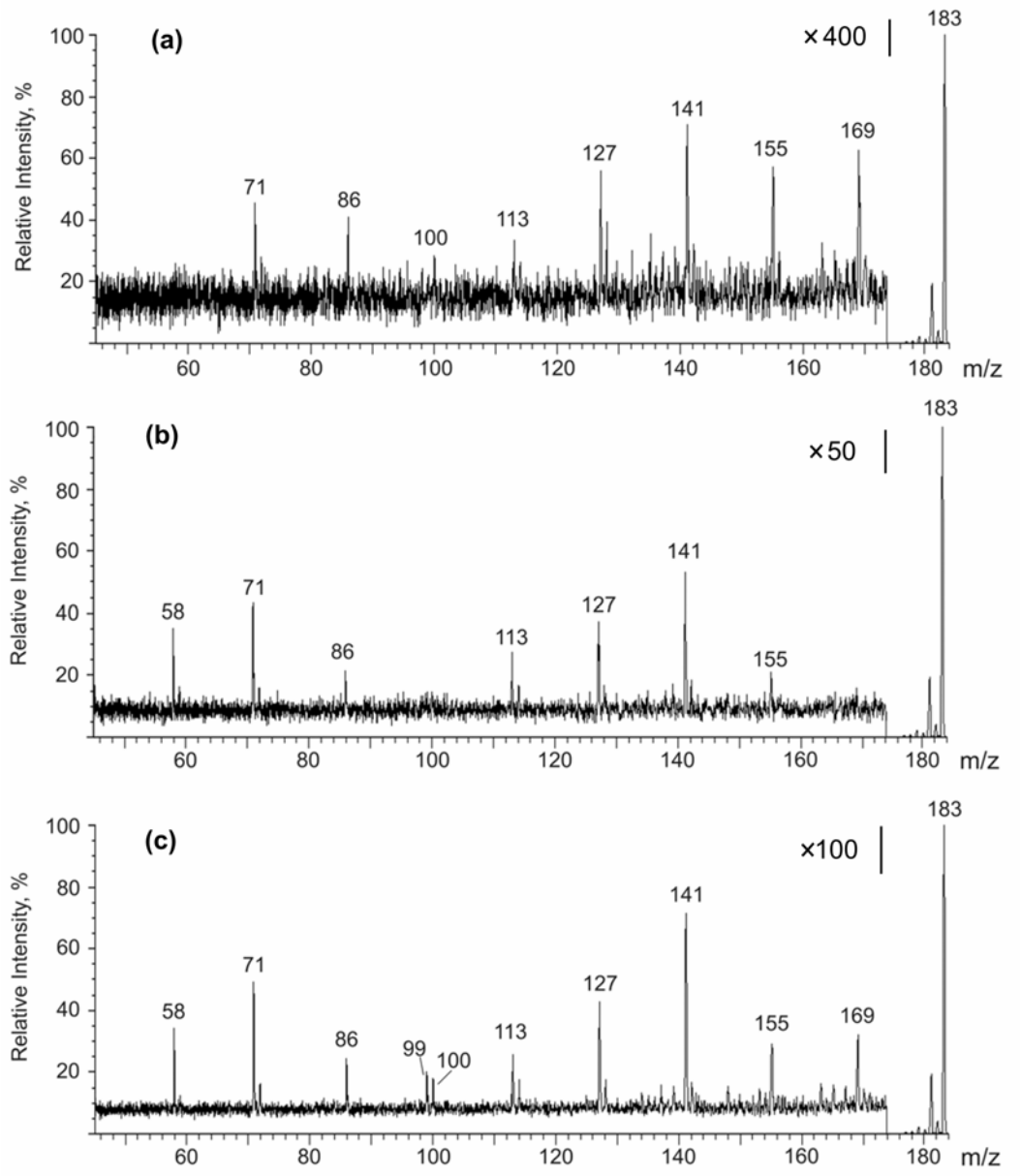

4. Linked scan metastable ion decomposition (**a**), CID with 30% parent peak suppression (**b**) CID with 80% parent peak suppression (**c**) spectra of CRF fragment ion at *m/z* 265 of the Brassidic acid. DEA was used as matrix.

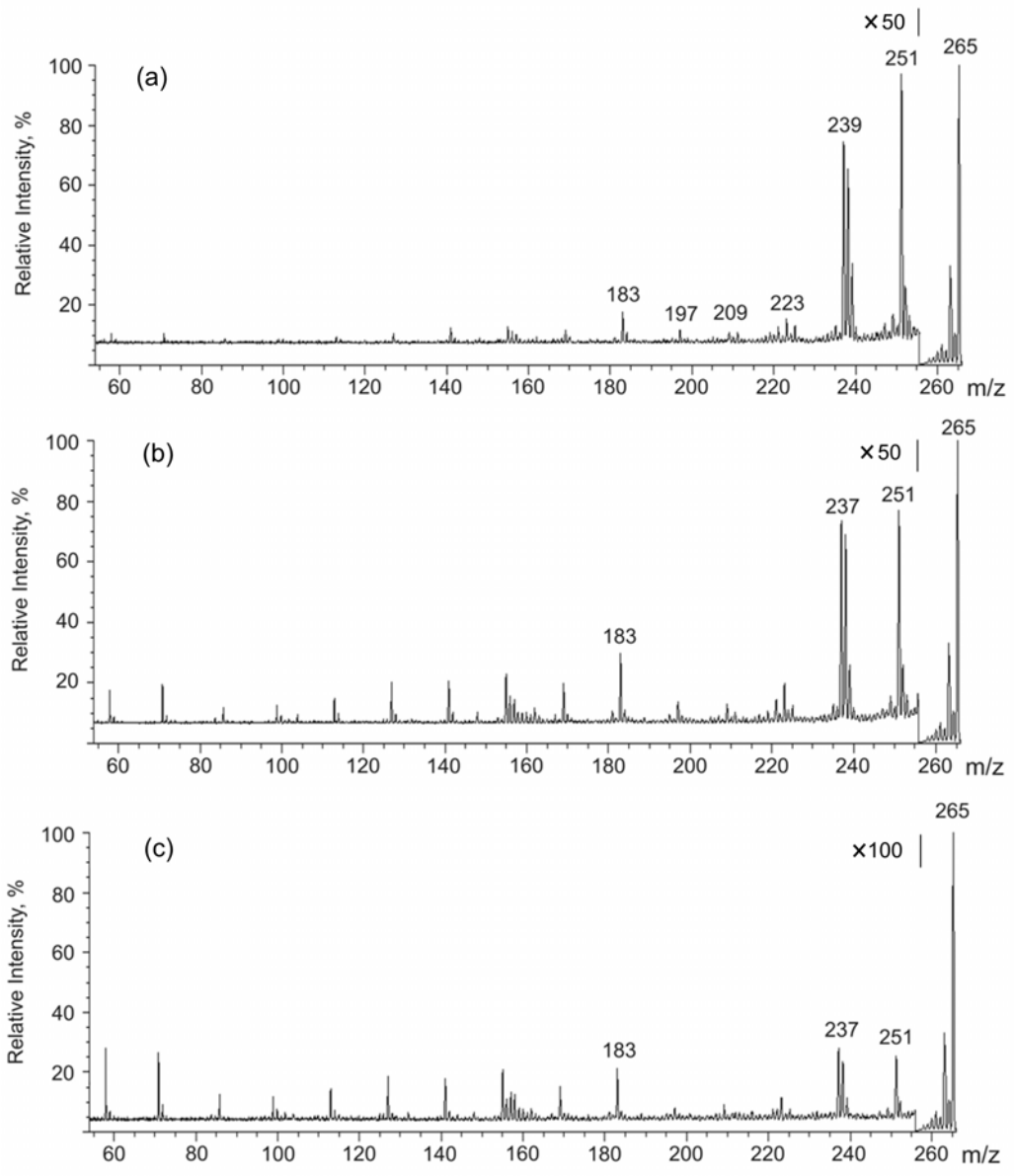

5. Linked scan metastable ion decomposition (**a**), CID with 50% parent peak suppression (**b**) CID with 80% parent peak suppression (**c**) spectra of CRF fragment ion at *m/z* 279 of the Brassidic acid. DEA was used as matrix.

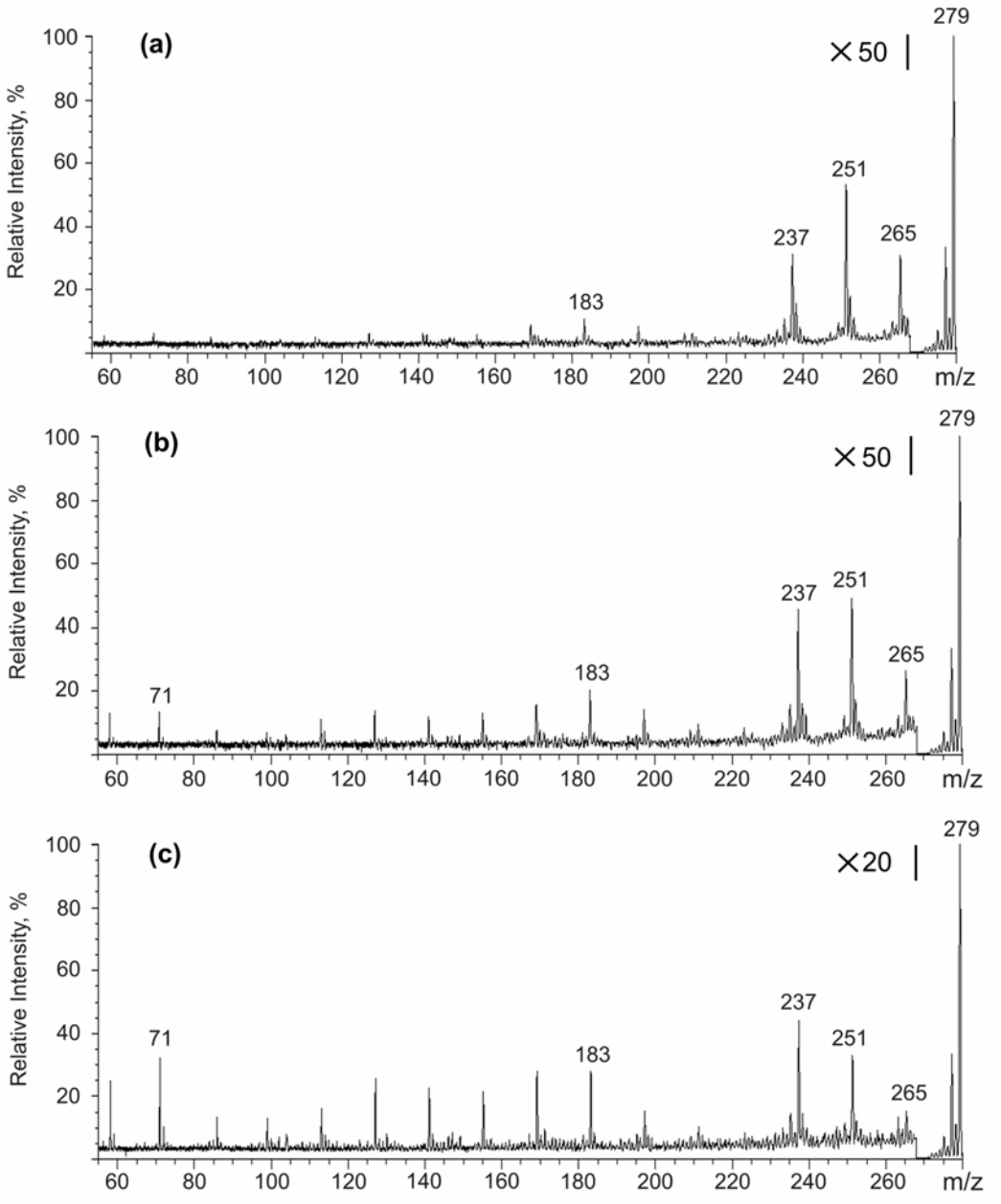

6. Linked scan metastable ion decomposition (**a**), CID with 30% parent peak suppression (**b**) CID with 70% parent peak suppression (**c**) spectra of CRF fragment ion at *m/z* 293 of the melissic acid. DEA was used as matrix.

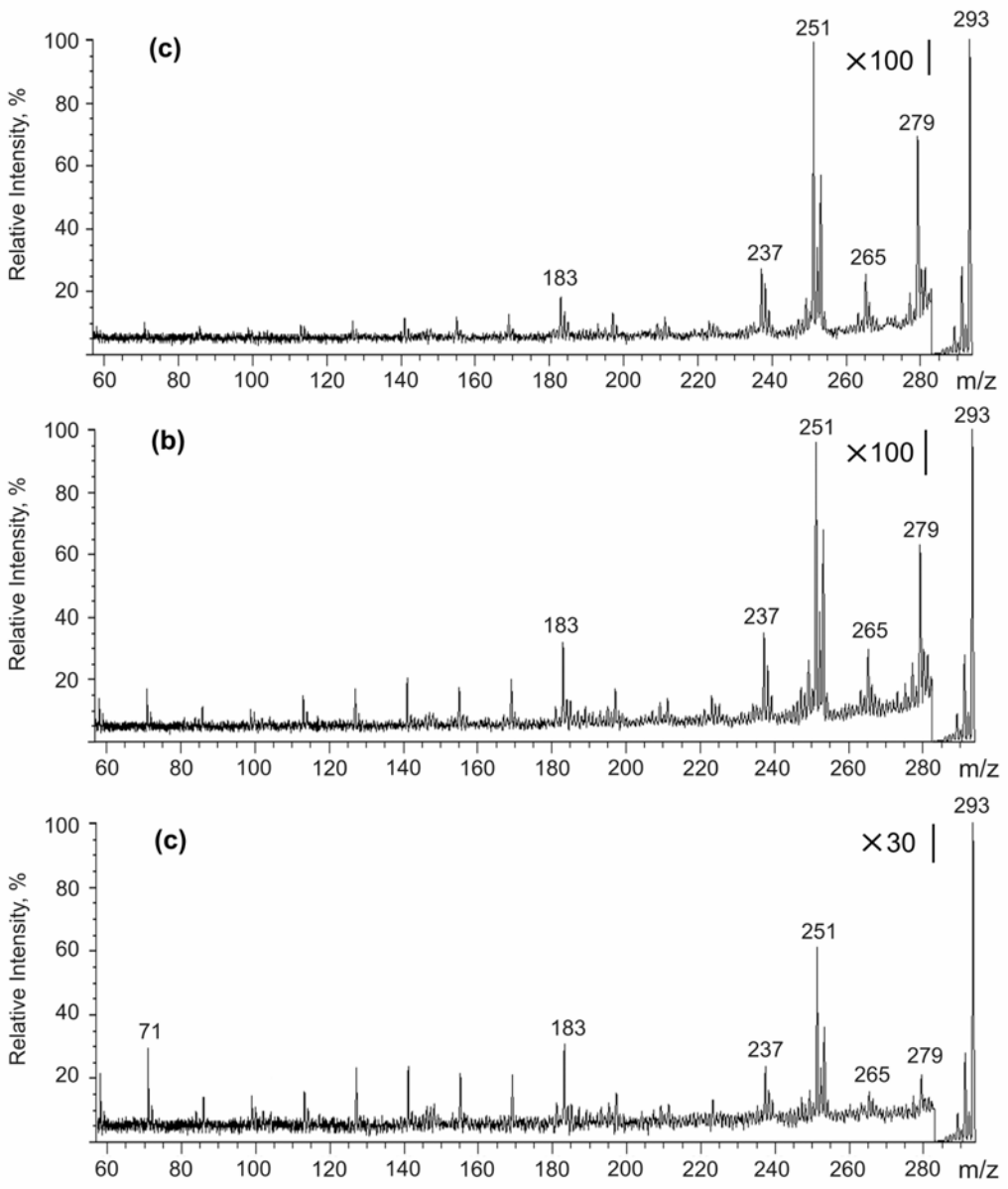

7. Linked scan metastable ion decomposition (**a**), CID with 50% parent peak suppression (**b**) spectra of CRF fragment ion at *m/z* 451 of the melissic acid. DEA was used as matrix.

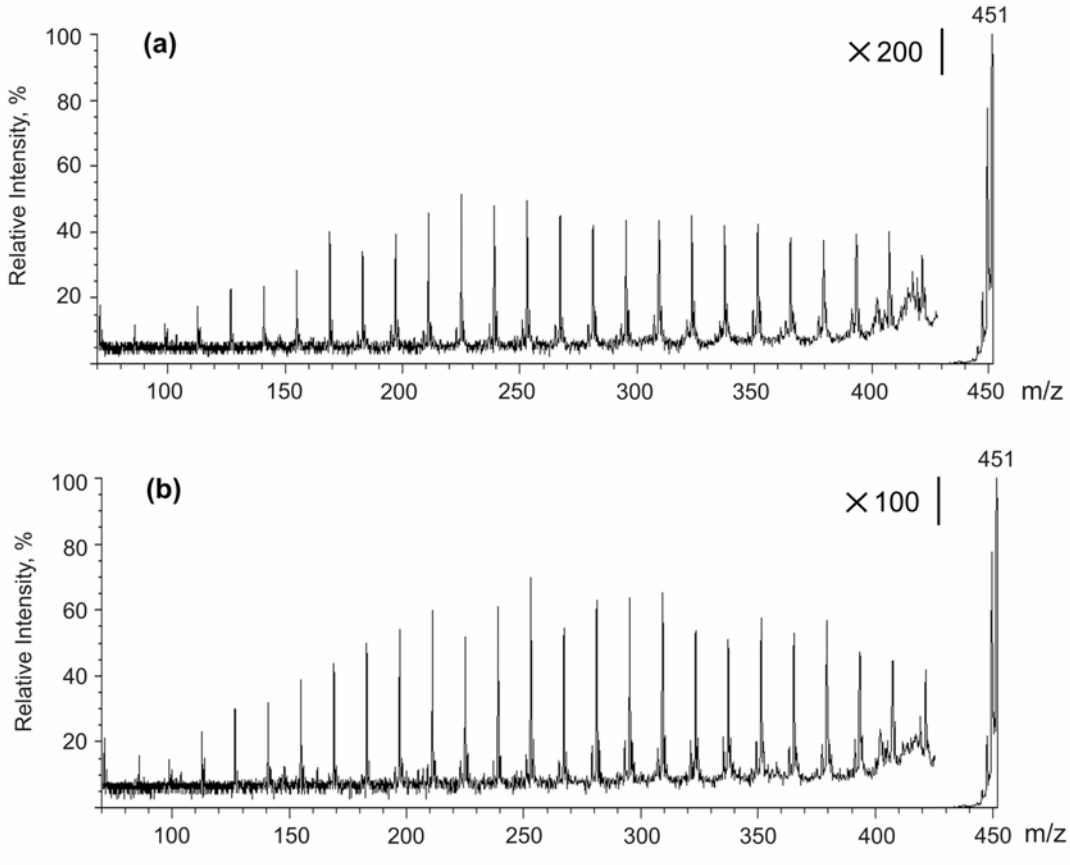

8. Linked scan metastable ion decomposition (**a**), CID with 50% parent peak suppression (**b**) spectra of CRF fragment ion at *m/z* 435 of the Brassidic acid. DEA was used as matrix.

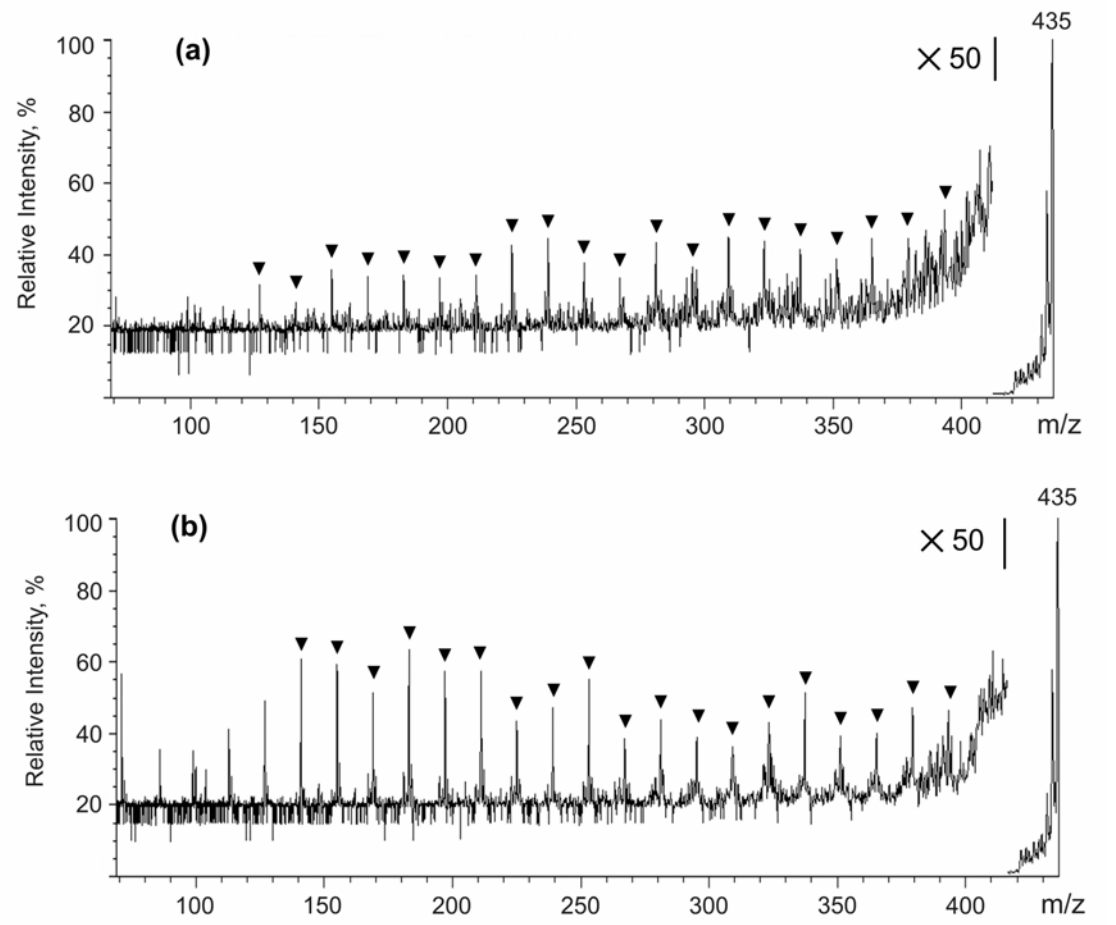

Appendix C

1. The radical initiated mechanism for the formation of the CRF ions.

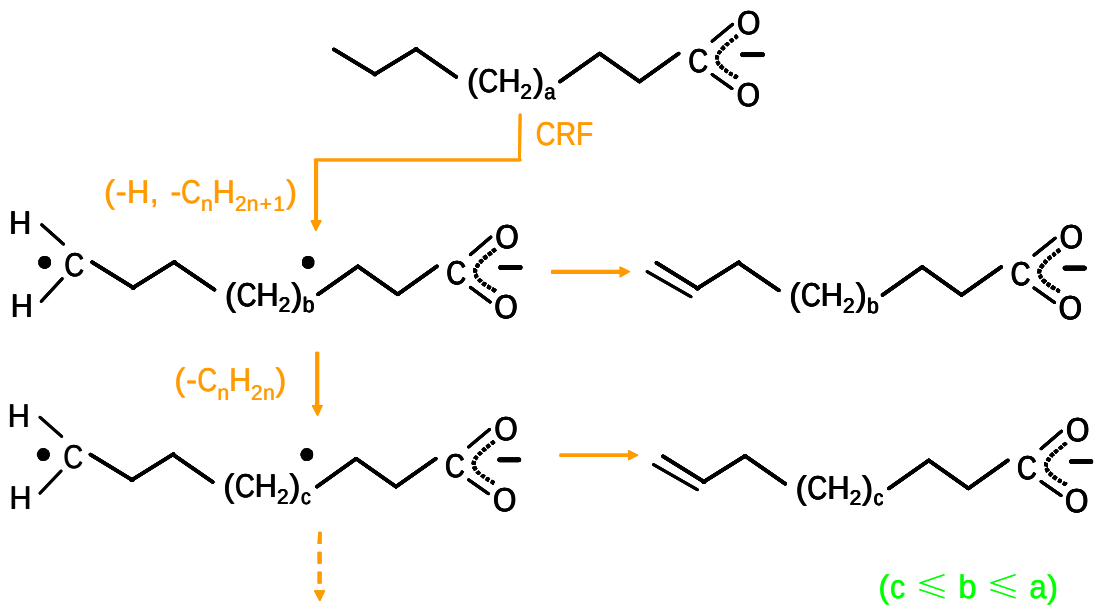

2. The proposal of different mechanisms of the doublet formation (elaidic acid is used as example here).

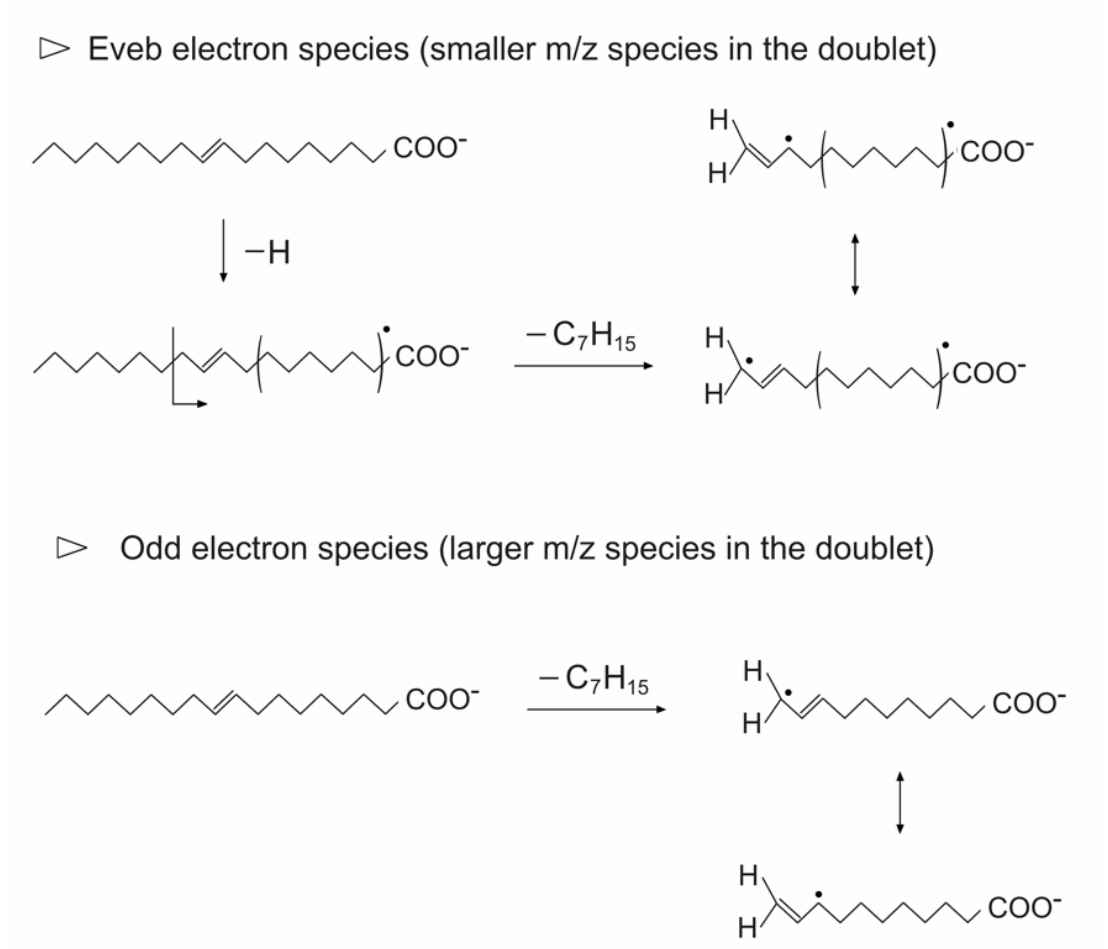

Appendix D

Presented here is the VB interfacing program I wrote for the resonance electron-capture TOF instrument. The program was used for fine tuning of the monochromater unit.

```
Dim Parameter, n, n1, n2, n3 As Integer   'passed to timer routines
Dim Is_List As Boolean          'choose DAC list or Microamp value
Dim DAC_Count(8) As Integer     'holding array for DAC counts
Dim Channel As Integer          'DAC channel value
Dim startTime!, elapsedTime!
Dim num As Integer

Private Sub btnExit_Click()
   btnWrite_Click
   End
End Sub

Private Sub btnRead_Click()

   Dim x As String
   Open "f:\Program Files\Vb\Vb98\Hong\Parameter.txt" For Input As #1
   For n1 = 0 To 8
      Line Input #1, x
      txtOldValue(n1).Text = Format(Val(x), "#0.000")
   Next n1
   Close
End Sub

Private Sub btnLoad_Click()

   For n2 = 0 To 8
   txtParam.Text = txtOldValue(n2).Text
   If n2 <= 6 Then
   n3 = n2
   Else
   n3 = n2 + 1
   End If

   Parameter = n3 + 1
   Channel = Parameter
   MSComm1.Output = "V"
```

```
    num = 0
    startTime = Timer                       'read the system time of day clock
    Do
    DoEvents
    elapsedTime = Timer - startTime
    Loop While elapsedTime < 0.05
    MSComm1.Output = Str(Parameter) + " "

    If Channel < 7 Then
       Parameter = Int((Val(txtParam.Text) + 1.7) * 71.8 * 2)
    End If
    If Channel = 7 Then
       Parameter = Int((Val(txtParam.Text) - Val(txtOldValue(7).Text)) * 329)
    End If
    If Channel = 9 Then
       Parameter = Int((Val(txtParam.Text) + 1.7) * (27.5) / (Val(txtOldValue(8).Text)
+ 1.7) * 148)
    End If
    If Channel = 10 Then
       Parameter = Int((Val(txtParam.Text) + 1.7) * 149)
    End If
    MSComm1.Output = "U"

    startTime = Timer                       'read the system time of day clock
    Do
    DoEvents
    elapsedTime = Timer - startTime
    Loop While elapsedTime < 0.05               'time interval is 50 ms
    MSComm1.Output = Str(Parameter) + " "

    startTime = Timer                       'read the system time of day clock
    Do
    DoEvents
    elapsedTime = Timer - startTime
    Loop While elapsedTime < 0.8            'time interval is 50 ms

here1:
    Next n2

    startTime = Timer                       'read the system time of day clock
    Do
    DoEvents
    elapsedTime = Timer - startTime
    Loop While elapsedTime < 0.8            'time interval is 50 ms
```

```
    btnListFast_Click

End Sub

Private Sub btnWrite_Click()

    Dim x As Single
    Open "f:\Program Files\Vb\Vb98\Hong\Parameter.txt" For Output As #2
    For n = 0 To 8
        x = Val(txtDACVolts(n).Text)
       Print #2, x
    Next n
    Close

End Sub

Private Sub Form_Load()

    'buffer to hold input string
    Dim Instring As String
    'use COM1.
    MSComm1.CommPort = 1
    '9600 baud,no parity,8 data, and 1 stop bit.
    MSComm1.Settings = "9600,N,8,1"
    'tell the control to read entire buffer when input is used
    MSComm1.InputLen = 0
    'open the port.
    MSComm1.PortOpen = True
    opMicroamps(0).Value = True
    opTime(12).Value = True
    opScale(0).Value = True
    Form1.Show
    txtParam.SetFocus

End Sub

Private Sub opVolts_Click(Index As Integer)

    Parameter = Index + 1
    Channel = Parameter
    n = Channel
    MSComm1.Output = "V"
    Timer1.Enabled = True
    num = 0
```

```
End Sub

Private Sub Timer1_Timer()

   Timer1.Enabled = False
   MSComm1.Output = Str(Parameter) + " "

End Sub

Private Sub opMicroamps_Click(Index As Integer)

   Parameter = Index + 1
   MSComm1.Output = "I"
   Timer1.Enabled = True

End Sub

Private Sub opTime_Click(Index As Integer)

   Parameter = Index + 1
   If Parameter = 13 Then Parameter = 0
   MSComm1.Output = "T"
   Timer1.Enabled = True

End Sub

Private Sub opDir_Click(Index As Integer)

   Parameter = Index
   MSComm1.Output = "D"
   Timer1.Enabled = True

End Sub

Private Sub opScale_Click(Index As Integer)

   Parameter = Index + 1
   MSComm1.Output = "S"
   Timer1.Enabled = True

End Sub

Private Sub btnMeter_Click()

   MSComm1.InBufferCount = 0
```

```
   Is_List = False
   MSComm1.Output = "M"
   Timer2.Enabled = True

End Sub

Private Sub btnListFast_Click()

   MSComm1.InBufferCount = 0
   Is_List = True
   MSComm1.Output = "L"
   Timer2.Enabled = True

End Sub

Private Sub Timer2_Timer()
 Timer2.Enabled = False
 Instring = MSComm1.Input



 If Is_List Then
   Comma = -1
   LastComma = 1
   For CountIdx = 0 To 8
      DAC_Count(CountIdx) = Val(Right(Instring, Len(Instring) - Comma - 1))
      If CountIdx < 6 Then
         txtDACVolts(CountIdx).Text = Format((DAC_Count(CountIdx) - 244) / 2 /
71.8, "#0.000")
      End If
      Comma = InStr(LastComma + 1, Instring, ",")
      LastComma = Comma
   Next CountIdx
   txtDACVolts(6).Text = Format((DAC_Count(6) / 329) + (DAC_Count(8) / 149) *
(DAC_Count(7) / 148) / 27.5 - 1.7, "#0.000")
   txtDACVolts(7).Text = Format((DAC_Count(8) / 149) * (DAC_Count(7) / 148) /
27.5 - 1.7, "#0.000")
   txtDACVolts(8).Text = Format((DAC_Count(8) / 149) - 1.7, "#0.000")
 Else
   txtDataIn.Text = Format(Val(Instring) / 17, "#0.00")
 End If

End Sub
```

```
Private Sub btnBump_Click()
   Dim mm%
   num = num + 1
   If Channel < 7 Then
      mm = Channel - 1
      If (num * Val(txtParam.Text) + Val(txtDACVolts(mm).Text)) > 26.6 Then
      MsgBox ("The value exceeds 26.6 eV!" & vbCrLf & "Please click List.")
      GoTo here2
      ElseIf (num * Val(txtParam.Text) + Val(txtDACVolts(mm).Text)) < -1.7 Then
      MsgBox ("The value is lower than -1.7 eV!" & vbCrLf & "Please click List.")
      GoTo here2
      Else
      Parameter = Int(Val(txtParam.Text) * 71.8 * 2)
      End If
   End If
   If Channel = 7 Then
      If (num * Val(txtParam.Text) + Val(txtDACVolts(6).Text)) <
Val(txtDACVolts(7).Text) Then
      MsgBox ("The value of Trap can't be smaller than the value of Energy." &
vbCrLf & "Please click List.")
      GoTo here2
      ElseIf (num * Val(txtParam.Text) + Val(txtDACVolts(6).Text)) > 25 Then
      MsgBox ("The value of Trap exceeds 25 eV!" & vbCrLf & "Please click List.")
      GoTo here2
      Else
      Parameter = Int(Val(txtParam.Text) * 329)
      End If
   End If
   If Channel = 9 Then
      If (num * Val(txtParam.Text) + Val(txtDACVolts(7).Text)) >
Val(txtDACVolts(8).Text) Then
      MsgBox ("The value of Energy can't be larger than the value of MaxSet." &
vbCrLf & "Please click List.")
      GoTo here2
      ElseIf (num * Val(txtParam.Text) + Val(txtDACVolts(7).Text)) < -1.7 Then
      MsgBox ("The value is lower than -1.7 eV!" & vbCrLf & "Please click List.")
      GoTo here2
      Else
      Parameter = Int((Val(txtParam.Text * 25.8) / Val(txtDACVolts(8).Text)) * 148)
      End If
   End If
   If Channel = 10 Then
      MsgBox ("Max Set Can't be Bumped,It only can be updated.")
      GoTo here2
   End If
```

```
   MSComm1.Output = "B"
   Timer1.Enabled = True
here2:
End Sub

Private Sub btnList_Click()
   num = 0
   If n < 7 Then
      Parameter1 = 9                    'can't goto "Fila"
   MSComm1.Output = "V"
   startTime = Timer                    'read the system time of day clock
   Do
   DoEvents
   elapsedTime = Timer - startTime
   Loop While elapsedTime < 0.3

   MSComm1.Output = Str(Parameter1) + " "

   startTime = Timer                    'read the system time of day clock
   Do
   DoEvents
   elapsedTime = Timer - startTime
   Loop While elapsedTime < 1.4

   Else
      Parameter1 = n - 3
   MSComm1.Output = "V"
   startTime = Timer                    'read the system time of day clock
   Do
   DoEvents
   elapsedTime = Timer - startTime
   Loop While elapsedTime < 0.3

   MSComm1.Output = Str(Parameter1) + " "

   startTime = Timer                    'read the system time of day clock
   Do
   DoEvents
   elapsedTime = Timer - startTime
   Loop While elapsedTime < 1.5
   End If

   Parameter2 = n
   MSComm1.Output = "V"
   startTime = Timer                    'read the system time of day clock
```

```
   Do
   DoEvents
   elapsedTime = Timer - startTime
   Loop While elapsedTime < 0.3

   MSComm1.Output = Str(Parameter2) + " "

   startTime = Timer                    'read the system time of day clock
   Do
   DoEvents
   elapsedTime = Timer - startTime
   Loop While elapsedTime < 1.7

   btnListFast_Click
End Sub

Private Sub btnUpdate_Click()
   If Channel < 7 Then
      Parameter = Int((Val(txtParam.Text) + 1.7) * 71.8 * 2)
   End If
   If Channel = 7 Then
      If Val(txtParam.Text) < Val(txtDACVolts(7).Text) Then
      MsgBox ("The value of Trap can't be smaller than the value of Energy.")
      GoTo here1
      Else
      Parameter = Int((Val(txtParam.Text) - Val(txtDACVolts(7).Text)) * 329)
      End If
   End If
   If Channel = 9 Then
      If Val(txtParam.Text) > Val(txtDACVolts(8).Text) Then
      MsgBox ("The value of Energy can't be larger than the value of MaxSet.")
      GoTo here1
      Else
      Parameter = Int((Val(txtParam.Text) + 1.7) * (27.5) / (Val(txtDACVolts(8).Text)
+ 1.7) * 148)
      End If
   End If
   If Channel = 10 Then
      Parameter = Int((Val(txtParam.Text) + 1.7) * 149)
   End If
   MSComm1.Output = "U"

   startTime = Timer                    'read the system time of day clock
   Do
   DoEvents
```

```
    elapsedTime = Timer - startTime
    Loop While elapsedTime < 0.05                    'time interval is 50 ms
    MSComm1.Output = Str(Parameter) + " "

    startTime = Timer                            'read the system time of day clock
    Do
    DoEvents
    elapsedTime = Timer - startTime
    Loop While elapsedTime < 0.8                 'time interval is 50 ms

    btnListFast_Click
here1:
End Sub
```